Thiol Click-Based Polyglycerol Hydrogels for Biosensing and Antiviral Applications

Inaugural Dissertation to obtain the academic degree

Doctor rerum naturalium (Dr. rer. nat.)

Submitted to

the Department of Biology, Chemistry, Pharmacy

of Freie Universität Berlin

by

Boonya Thongrom

2022

The research projects presented in this dissertation were carried out from June 2018 to November 2022 under the supervision of Prof. Dr. Rainer Haag at the Institute of Chemistry and Biochemistry of the Free University of Berlin.

1. Reviewer: Prof. Dr. Rainer Haag, Freie Universität Berlin

2. Reviewer: Prof. Dr. Nan Ma, Helmholtz-Zentrum Hereon, Teltow

Date of defense: 30 November 2022

Declaration of Independence

All of the content in this dissertation is original and has not previously appeared in any form of application for a degree. All the demonstrated figures have been made by me or marked with the related references. The whole work presented herein is the result of my own effort, except where referenced or acknowledged otherwise.

…………………………………

Boonya Thongrom

Berlin, November 2022

Acknowledgement

From the beginning to the end of my dissertation, hardly do I succeed without the support from my beloved people around me. First of all, I would like to express my deep gratitude to Prof. Dr. Rainer Haag for accepting me as a Ph.D. candidate in his group and allowing me to conduct such a wonderful research project. His kindness and great support bring me success in my career path. Furthermore, I truly love the friendly environment in his group and the nice working condition.

I would like to thank Prof. Dr. Nan Ma for being my second supervisor in this dissertation.

I also would like to express thanks to my mentor, Dr. Uwe Schedler for guiding me in the field of polymeric industrial applications and helping me achieve the goal of a biosensing application. I have learned a lot from him and discovered a way to connect research to an industrial one.

I would like to show gratitude toward Dr. Mathias Dimde for being such a terrific consultant and helping me start my hydrogel experiments when I was still inexperienced.

I would also like to acknowledge Dr. Sumati Bhatia for being a good support to my manuscript and for her contribution to my research project.

I would like to thank Dr.Wiebke Fischer for project coordination and management.

Many thanks to our technicians and secretaries in our group for helping me conduct all the work documentarily and experimentally smoothly especially, Anja Stöshel, Eike Ziegler, Marwin Raue, Elisa Quaas, Cathleen Hudziak, Marleen Selent, and Katharina Goltsche.

I would like to thank the Core Facility BioSupraMol for measuring NMR, IR, and Elemental Analysis.

I would like to express my deep appreciation to Dahlem Research School, the Helmholtz MacroBio School, and BMBF research funding for supporting my living in Germany.

I am thankful to Smriti, Peng, Raju, Rui, and Vahid for helping me proofread and giving a useful guide for my thesis.

A deeply special thanks to all my former and current colleagues in AG Haag who are always supportive and helpful. Whenever I am feeling down or unhappy, all my colleagues always come to cheer me up and give me good advice. They all are nice and friendly to me whenever

we meet and have a talk. I always feel really lucky to be part of such a wonderful group with wonderful people. I know myself that I am not smart, so I have learned a lot from them and improved myself more and more.

I would also like to thank all my friends for their good support and for helping me go through all the years during living and studying here in Germany.

Above all, I would like to give all my hearty thankfulness to my family. They always support and encourage me in all situations. Without them, I cannot be successful in my career and my life.

Table of Contents

1. Introduction

Hydrogels as three-dimensional (3D) water-swollen materials have gained great interest due to their high biocompatibility, high water content, ease of use, nontoxicity, and environmentally friendly gelation conditions.[1,2] In nature, many biological hydrogels are an essential part of many organisms. For example, the mucus hydrogels found on the surface of epithelial cells in the lung and intestine in the human body play an important role as a protective barrier against pathogens.[3,4] An animal like a frog builds a mucus hydrogel on its skin surface to retain moisture and to essentially transport oxygen into the body as it breaths through the skin.[5,6] Hydrogels in each leaf of an aloe vera plant function as a storage for not only water but also many bioactive substances such as polysaccharides, vitamins, minerals, and amino acids for its growth.[7,8]

In a field of scientific research and application, many fully synthetic hydrogels such as polyethylene glycol (PEG)-based,[9] gelatin methacrylate (GelMa)-based,[10] polyacrylic acid (PAA)-based,[11] or polyacrylamide (PA)-based hydrogels[12] have been widely used in broad fields of applications[1,13,14] e.g. biomedicine, biochemistry, engineering, agriculture, and biosensing. The emergence of the coronavirus pandemic in 2019 became a hazard to people around the world. Many organizations have realized this global threat and tried to find a way to prevent and protect people against it. To find such a small nanometer-size virus and handle it to prevent further spreading is realized, and one of the powerful methods used to help detect the virus is a biosensing tool.[15] Not only sensing a virus before protection but also killing the virus to cure the symptoms is needed.[16] A 3D biocompatible water-swollen hydrogel could be a good alternative platform to express a high sensitivity toward protein or virus and could even prevent viral infection.

All mentioned hydrogels can be generally fabricated by chemical crosslinking, thereby forming a new covalent bond in between. The design for chemical crosslinking reactions can be varied from enzyme-catalyzed reaction, and photopolymerization, to specific reactions like click chemistry.[17–19] The popularity of using click chemistry in gelation becomes popular due to its simplicity, high specificity, high yield, and no or nontoxic byproduct.[19,20]

In this dissertation, hydrogel formation by using thiol-click chemistry was developed. The use of hydrogels as a biosensing platform was investigated by using streptavidin as a bioprobe. Besides, trapping a virus before infection by using a sulfated hydrogel scaffold was studied.

2. Theoretical Background

2.1 Hydrogels

    2.1.1 Definition

A hydrogel consists of a 3D polymeric crosslinked network which does not dissolve in water, but instead, holds the water content of up to 99% of its weight due to hydrophilic groups such as hydroxy, carboxy, amide, or amine in the polymeric network.[21–23] The hydrophilic network structure of a synthetic hydrogel can be made from one simple small molecular-size hydrophilic type of monomer, for instance, the synthesis of polyacrylamide hydrogels by using acrylamide and bis-acrylamide[12,24] or a macromolecular-size type of monomers such as the hydrogel formed from 4-arm polyethylene glycol (PEG) and a linear PEG crosslinker[25] (see **Figure 1**). By forming sufficient crosslinking points to build a 3D network matrix, a hydrogel can cage the water molecules and start to swell, thereby building a 3D structural form. Hydrogel's morphology can be varied from very soft and slimy like natural human mucus, to hard and rigid like gelatin, depending on its desired application. One of the prime benefits of a typical synthetic hydrogel is its biocompatibility toward biological systems. Owing to the high water content trapped inside its 3D network structure, it can mimic the natural microenvironments, friendly to all micro- and higher organisms. Moreover, synthetic hydrogels can be easily reproduced and upscaled, thus making them attractive, especially for biomedical applications such as wound dressing, contact lenses, cell therapy, tissue engineering, or drug delivery.[1,13,22,26]
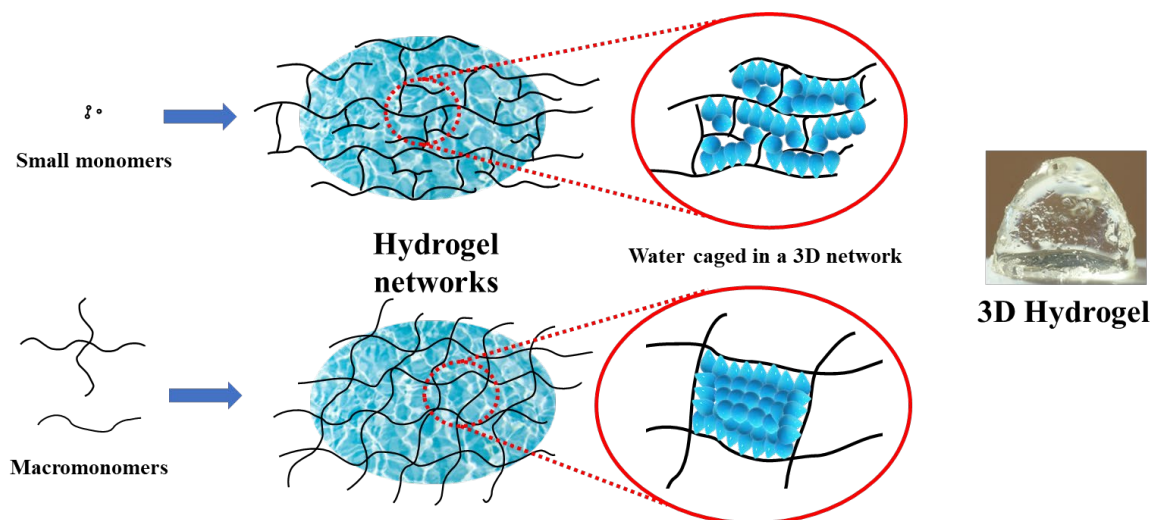
Figure 1. *The hydrogel formed by the polymerization of small monomers (such as PA-based hydrogels) or macromonomers (such as 4-arm PEG-based hydrogels)*

2.1.2 Hydrogel network formation

A Hydrogel network can be formed or crosslinked in 2 classical ways based on the gelation mechanism; physical and chemical crosslinking (**Figure 2**). In the case of the physical crosslinking strategy, gelation is processed by non-covalent interactions, such as chain entanglement, electrostatic interaction, hydrogen bonding, or hydrophobic interaction.[27]

Chain entanglement

To ensure the success of the gelation via chain entanglement, the molecular weight of a linear polymeric precursor usually needs to be at least 35 kDa.[28] In the gelation process, polymer chains start to entangle with each other due to the chain movement in an aqueous solution mixture, until a 3D complex structure is built, which is sufficient to trap the water inside, resulting in a hydrogel. Such hydrogels can express tough and stretchable abilities owing to the great energy dissipation, which comes from the high viscous character of the entangled chains inside a gel matrix.[29,30]

Electrostatic interaction

In terms of a hydrogel crosslinked by electrostatic interaction, one macromonomer precursor must contain positively charged moieties and the other one must contain negatively charged moieties. When mixing precursors in solution, a hydrogel formation takes place by strong ionic interaction between the 2 different types of charges. Examples are the gelation between polyallylamine hydrochloride and tripolyphosphate crosslinker,[31] or the hydrogel formed from polysulfonate and polyquaternary ammonium (**Figure 2**).[32] This type of gel displays high stiffness, strong adhesiveness, and self-healing properties.

Hydrogen bonding

On the other hand, a hydrogel can be simply fabricated by hydrogen bonding. By exploiting an intermolecular hydrogen bonding interaction between many hydrogen atoms and highly electronegative atoms of hydrophilic groups like hydroxyl or amino groups, the gelation is achieved. The most commonly used macromonomer for this type of gelation is polyvinyl alcohol (PVA) which contains many hydroxyl side chain moieties. The conventional technique used to form this type of gel is called freezing-thawing. By making many cycles of freezing and thawing of a PVA solution, the hydrogel matrix starts to appear (**Figure 2**).[33] Hydrogelation between PVA and melamine can also be done using this method.[34] However, it is simpler to form hydrogel with the new alternative gelation method by dissolving PVA in

the solvent mixture of dimethyl formamide (DMF) and dimethyl sulfoxide (DMSO), followed by water exchange.[33]
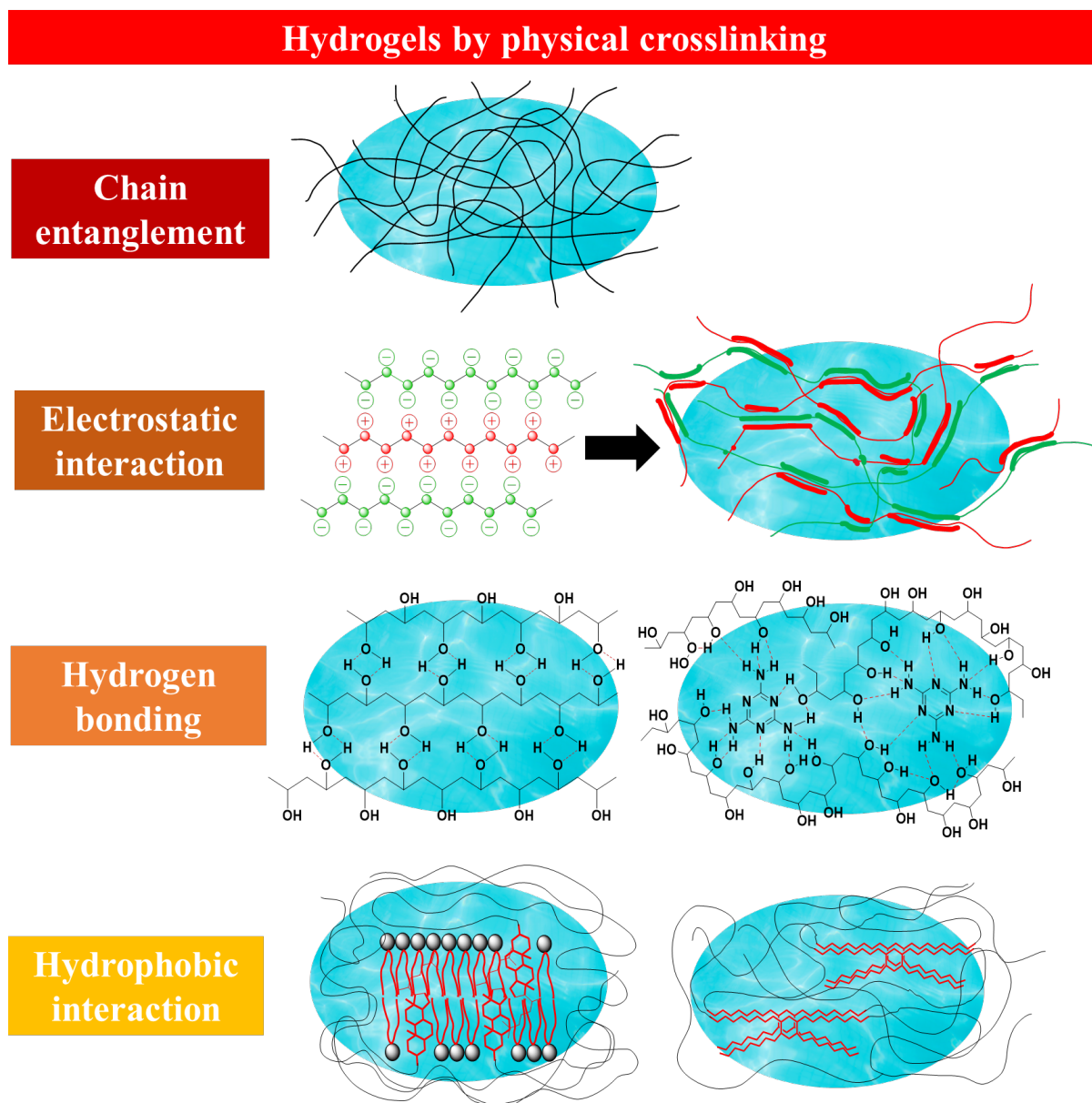
Figure 2. Hydrogel formation by noncovalently physical crosslinking

Hydrophobic interaction

For a hydrogel synthesized by hydrophobic interactions, a polymeric chain must have both hydrophobic (for crosslinking) and hydrophilic parts (for attracting water). A hydrogel can thermodynamically form in aqueous media by the aggregation of hydrophobic domain, serving as crosslink sites. Some good examples of this type of gel, are the gelation between liposome and cholesteryl terminated PEG,[35] or the association of the hydrophobic part of PEG containing hydrophobic dimer fatty acid, which can show self-healing property (**Figure 2**).[36]

<u>Addition reaction</u>
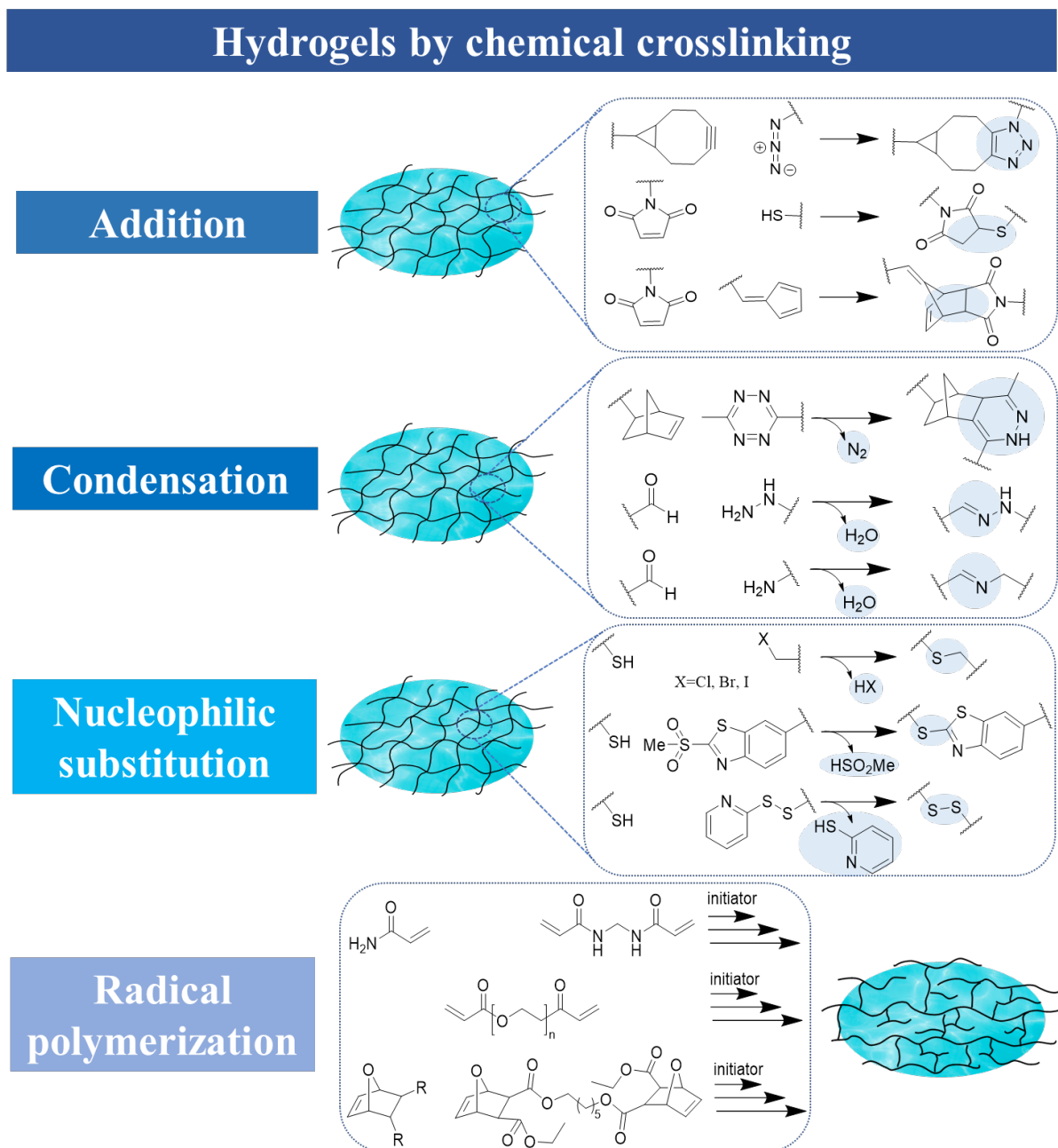
In the case of hydrogel formation by chemical crosslinking,[18] it can be classified into 4 categories; macromonomeric addition, condensation, nucleophilic substitution, and radical polymerization. A hydrogelation by macromonomeric addition is performed when an end group of a macromonomer is functionalized with a group that undergoes an addition reaction, thus building a 3D hydrogel network. The addition reaction in organic chemistry is the reaction where two or more different active molecular sites (functional groups or active molecules having electrophilic or nucleophilic sites) combine to become an adduct without any byproducts generated or any losses of atoms from the active sites.[37]

A common method which is widely used in an addition reaction for gelation is click chemistry. As aforementioned, click reaction gives great benefits including high specificity and simplicity with benign reaction conditions. There are many click reaction additions which have been used. For instance, by using strain-promoted alkyne-azide cycloaddition (SPAAC) between strained cyclooctyne-terminated PEG crosslinker, and azide-functionalized dendritic polyglycerol (dPG) as a hub, a hydrogel could form easily without any catalysts at room temperature (**Figure 3**).[38,39] The key factor to promote the reaction, as the name suggested, is the ring strain from a cycloalkyne which can cyclize with the azide group in a [3+2] dipolar cycloaddition fashion to form a five-membered-ring crosslinking point.[40]

Another example is gelation by thiol-ene click reactions. In this method, one reactant must contain a thiol group and the other reactant contains a double bond. A thiol-ene reaction can be done either by radical reaction where there is an electron-rich double bond acceptor using photoinitiator as a catalyst and UV/Vis light[41] or by nucleophilic addition (thiol-Michael click reaction) in a neat condition where a double bond acceptor is highly electrophilic (electron-poor) which can directly accept free lone pair electrons from a thiol group.[20] An example of a hydrogel that undergoes a thiol-ene click reaction is the PEG hydrogel by thiol-maleimide click reaction[42] or gelatin-based thiol-norbornene click reaction by using lithium phenyl-2,4,6-trimethylbenzoylphosphinate (LAP) as a photoinitiator.[43]

Furthermore, Diels-Alder addition reaction is a certainly useful tool to fabricate a hydrogel. In this method, one macromonomer should have a diene group which is an electron-rich domain to react with an electron-deficient dienophile group of another macromonomer, thereby forming a six-membered-ring product via [4+2] cycloaddition at a crosslinking point of a

hydrogel.[44,45] The example is the PEG-based or Hyaluronic acid (HA)-based hydrogel cooperated by fulvene and maleimide[46] or by methylfuran and maleimide,[47] respectively.

Figure 3. Hydrogel formation by covalently chemical crosslinking

Condensation reaction

A condensation reaction in organic chemistry is a reaction where two different functional groups react with each other to form a new single functional group with a loss of a small molecule like water as a byproduct.[48] In the case of hydrogel formation by condensation, some reactions such as inverse electron-demand Diels–Alder reaction (IEDDA) and Schiff-base reaction by either aldehyde-hydrazine or aldehyde-amino coupling have been commonly used.

An example of IEDDA-based hydrogel is the hyaluronic acid hydrogel formed by the reaction between tetrazine and norbornene moieties in a mild aqueous media, resulting in a dihydropyridazine ring formation with the release of nitrogen gas as a byproduct (**Figure 3**).[49] Unlike normal Diels-Alder reaction, the electron-deficient tetrazine moiety whose diene has a low lowest unoccupied molecular orbital (LUMO) can react readily with an electron-rich ring-strained norbornene whose dienophile has a high highest occupied molecular orbital (HOMO) in a [4+2] cycloaddition way at room temperature. [50,51]

Another example of gelation by condensation reaction is a well-known Schiff-base based hydrogel which is formed by hydrazine- and aldehyde-functionalized macromonomers. A highly nucleophilic hydrazine moiety can react readily with an aldehyde to form hydrazone linkage with a loss of a water molecule.[52] Similarly, a simple amino-aldehyde coupling has been freqeuntly applied in hydrogel formation. The reaction between amine and aldehyde groups yields an imine linkage with a release of a water molecule, as seen from the gelation example between chitosan which naturally contains an amino group, and benzene aldehyde-terminated PEG.[53]

Nucleophilic substitution reaction

A nucleophilic substitution reaction in organic chemistry, on the other hand, is a reaction where an atom or a small molecular part of an electrophilic electron-accepting substrate is substituted by another nucleophilic electron-donating atom or functional group, thereby losing the substituted part as a byproduct which is often called a leaving group. The formed adduct still preserves similar functionality as the electrophilic precursor.[54] In the application of crosslinking chemistry in a hydrogel, a thiol group is mostly chosen since it is a strong nucleophile, and highly selective toward many electrophiles while the substrate must contain an electrophilic site.

The first example is the straightforward thiol-halide click-based hydrogel which is constructed by halogenic-functionalized PEG and thiol-functionalized PEG, leaving stable halide as a leaving group (**Figure 3**).[55] The second example is the hydrogel formed by thiolated PEG and methyl sulfone-functionalized PEG whose methyl sulfone moiety acts as a leaving group.[56] The last example is the gelation from carboxymethyl chitosan and reduced bovine serum albumin (BSA) by a thiol-disulfide exchange between thiol and pyridyl disulfide which contains 2-mercaptopyridine as a good leaving group, forming thus a stable, yet dynamic disulfide crosslinking point.[57]

The last classification of covalently crosslinking chemistry of hydrogel is radical polymerization. In this way, a hydrogel can be formed either from the mixture of a small monomer which often refers to an olefinic monomer, containing a double bond as a polymerization point and a homobifunctional crosslinking monomer, or from a homobifunctional linear polymer by using a radical initiator. Classical examples of this type are the polyacrylamide, polyacrylic acid, or polyacrylate hydrogels by the polymerization of acrylamide-based or acrylate-based monomer and bis-acrylamide or tetra(ethylene glycol) diacrylate, respectively (**Figure 3**).[12,24,58] Another example is the hydrogel crosslinked by the ring-opening metathesis polymerization between oxanorbornene monomer and a bis-oxanorbornene crosslinking agent.[59] The last example is the hydrogel formation from linear PEG diacrylate by using a photoinitiator and UV light.[60]

2.1.3 Polyethylene glycol-based hydrogels

Polyethylene glycol (PEG) or polyethylene oxide (PEO) refers to a linear polyether, synthesized by the polymerization of ethylene oxide by ring-opening polymerization, using ring strain as a driving force. It comprises ethylene oxide as a repeat unit.[61,62] There are many different commercial sizes of PEG or PEO chains ranging from kDa to MDa and the physical properties also vary, dependent on the size; for instance, the melting point of low molecular weight PEG is low and higher with a bigger size.

Typically in the biomedical field, the short name of PEG is preferred when referring to sizes below 30 kDa whereas PEO is preferably called when referring to sizes above 30 kDa.[62] It can be manufactured as a linear chain, three-arm, four-arm, or multi-arm architecture depending on the demand of applications. PEG is a hydrophilic polymer that can be easily dissolved in water due to the high dipole moment of the ether repeating unit, which allows hydrogen bonding to water molecules.[63,64] Not only with water but also with many organic solvents such as dichloromethane (DCM), chloroform, methanol, ethanol, and acetonitrile can solubilize PEG.[65]

Since PEG is inert, nontoxic, and biocompatible with biosystems, [66–69] it is tremendously used in many fields of applications such as bioconjugations, drug-delivery systems, cosmetics, therapeutics, surface sciences, and interestingly, hydrogels.[70,71] In the area of hydrogels, many research studies have used PEG as a hydrophilic base for hydrogel formation due to its high hydrophilicity, biocompatibility, and ease of functionalization processes
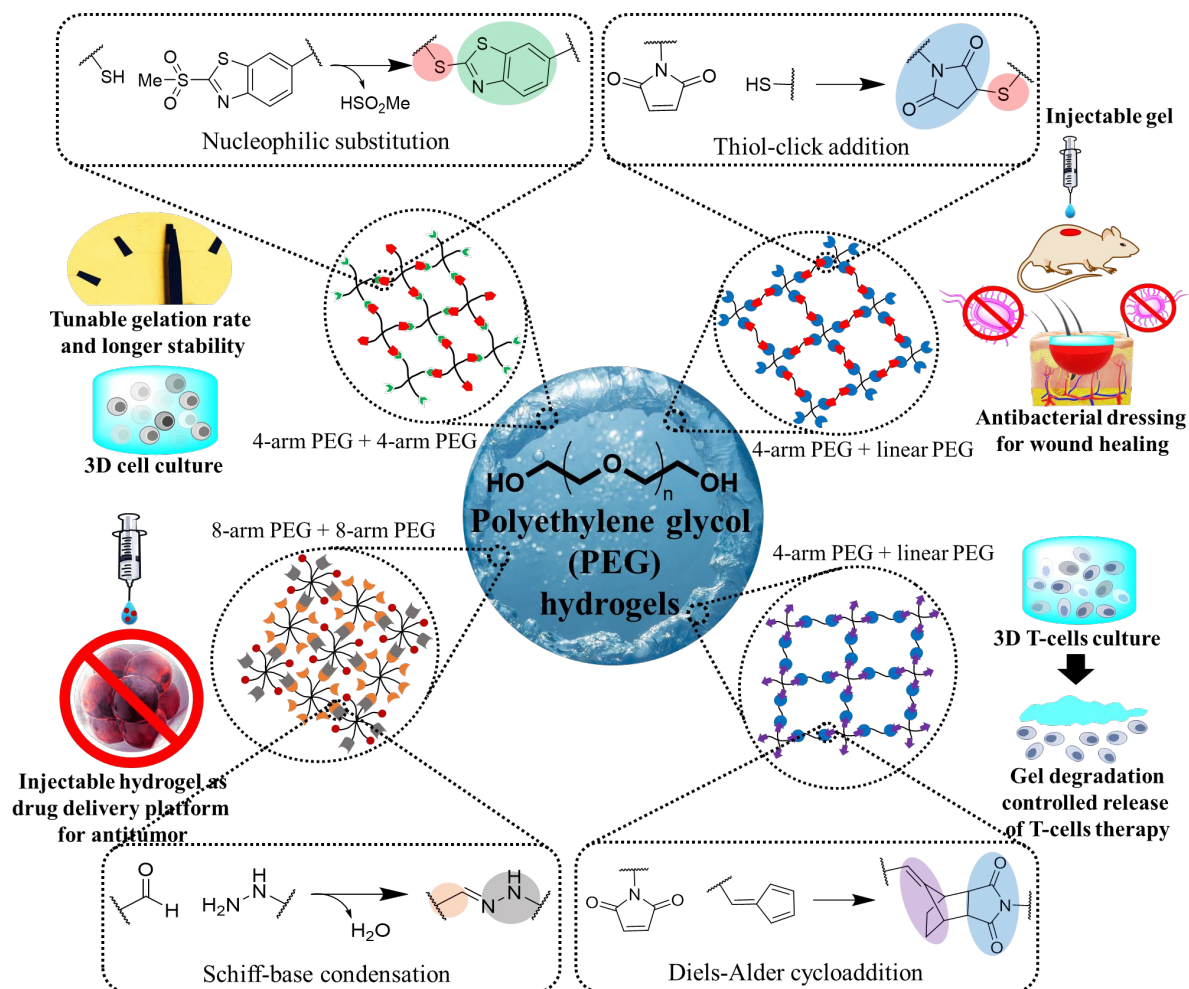
Figure 4. *Examples of PEG hydrogels formed from different PEG architectures by different crosslinking chemistries and their applications. Adopted from Ref.* [46, 52, 56, and 72]

PEG itself has been commonly used to form hydrogels through covalent crosslinking by turning the hydroxyl end group into either specific nucleophiles like thiol, azide, and amino groups or electrophiles like maleimide, carboxylic, aldehyde, halide isothiocyanate, and isocyanate groups. Many crosslinking chemistries such as thiol-click, SPAAC, Diels-Alder, IEDDA, Schiff base, and thiol-disulfide exchange play a big role in it. To fabricate a network hydrogel, when one component is a linear crosslinker, another component must be at least three-arm PEG architecture, unless the radical polymerization of the olefinic homobifunctional linear chain is used.[60] Some use linear and four-arm PEGs, four-arm and four-arm PEGs, or even both eight-arm PEGs in order to build a 3D network scaffold (**Figure 4**).

As a PEG-based hydrogel, it is like a niche for cells to grow due to its biocompatible microenvironment. Therefore, its applications frequently focus on biomedicines. The first example is a hydrogel synthesized from 2 different functionalized four-arm PEGs, one functionalized with a nucleophilic thiol group and another functionalized with a methylsulfone-

based leaving group. This hydrogel is claimed to be noncytotoxic with a tunable gelation rate and improved stability. The application is to encapsulate cells and they could be cultured for more than 2 weeks (**Figure 4**).[56] The second example is the hydrogel based on maleimide-functionalized four-arm PEG as a hub and dithiolated PEG as a linear crosslinker. This hydrogel is injectable and degradable via the hydrolyzable ester linkage which is embedded into the crosslinker. This biocompatible hydrogel was used as an injectable antibacterial dressing to promote the wound-healing process.[72] Another example is the hydrogel prepared from the condensation between hydrazine-functionalized eight-arm PEG and aldehyde-functionalized eight-arm PEG by forming dynamic covalent hydrazone linkage. This self-healing pH-responsive hydrogel is used as a carrier to deliver an anticancer Doxorubicin drug with a control-release ability.[52] Similarly, an injectable hydrogel fabricated from fulvene-terminated four-arm PEG and maleimide-terminated PEG linear crosslinker by Diels-Alder cycloaddition shows the ability of slow releasing the viable encapsulated T-cells for the promising treatment of hematological cancers.[46]

2.1.4 Dendritic polyglycerol-based hydrogels

Dendritic polyglycerol or hyperbranched polyglycerol (dPG or hPG) are polyether polyols with tree-like 3D architectures. It contains multiple hydroxyl groups on the surface of a polymeric molecule.[73,74] dPG is the result of the ring-opening polymerization of glycidol whose ring strain can be released as a driving force.[75,76] Its dendritic structure occurs via the intramolecular ion-exchange reactions between secondary and primary hydroxyl groups of the propagating species since the pKa values of both hydroxyl groups are relatively similar.[73–75] The dPG synthesis can be performed by either using acid catalysis[77] or basic catalysis.[75,76,78] Although the cationic polymerization of glycidol is viable, this method is less popular due to many side reactions, and only low molecular weight polymers (less than 10 kDa) with a broad polydispersity index (PDI) can be achieved.[79] Instead, anionic polymerization can overcome these problems. It has been extensively used and continuously improved to have control over the molecular weight of dPG. Nowadays, a new technology reactor can process dPG synthesis on a big kilogram scale.[80] The reason why this hyperbranched structure is also named dendritic is that its growth is similar to dendrimer synthesis but with incomplete branching due to the random propagation during the polymerization of glycidol.[73,74]

The distinctive characteristic of dPG is its multivalent hydroxyl groups. This makes it well-soluble in water and in other polar solvents such as methanol, ethanol, DMF, and DMSO as

well. Furthermore, they can be modified to many functional groups like amine, carboxyl, aldehyde, azide, thiol, sulfate, or leaving groups with ease. These characteristics make it a greatly versatile template for multipurpose applications, especially in biomedical applications.[73,74,79] dPG macromolecule is, in general, biocompatible and nontoxic to microorganisms. It can be an alternative material to replace or combine with PEG, particularly in hydrogel applications.
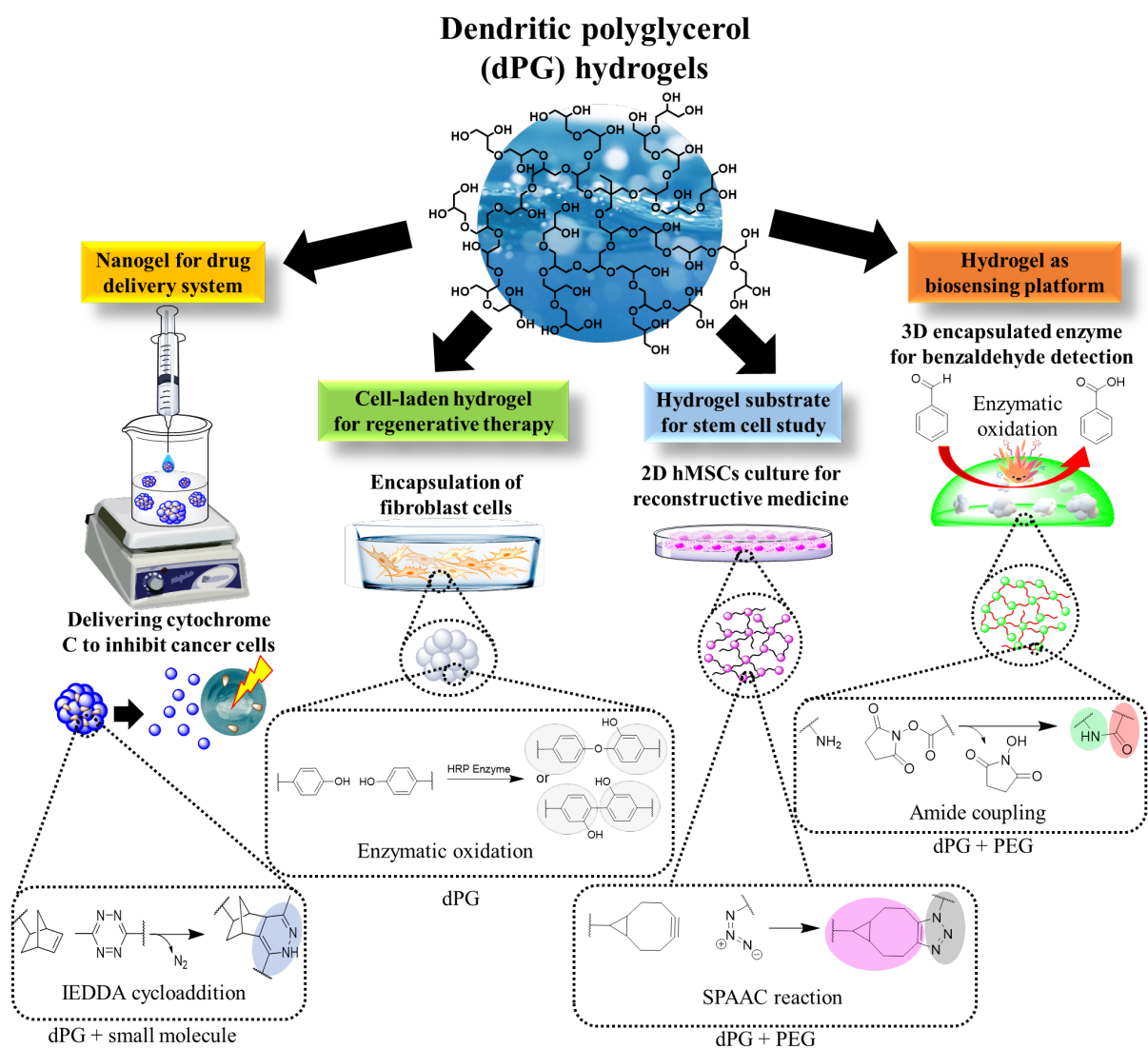
Figure 5. *Examples of dPG-based hydrogels and nanogels with different crosslinking chemistries and their applications. Adopted from Ref.* [38, 82, 83, and 85]

In terms of hydrogel formation, dPG can be used to form hydrogel alone or can be mixed with another biocompatible hydrophilic polymer like PEG in order to improve the mechanical properties of a gel matrix. Since dPG has already a 3D hyperbranched scaffold and ball-like shape, one can promptly build a hydrogel simply when it is functionalized with several desired

crosslinking groups which are randomly distributed all around the macromolecular surface. Similar to PEG hydrogelation, many step-growth polymerization strategies involving covalent crosslinking chemistry have been used to fabricate dPG-based hydrogels. Certainly, click chemistries such as SPAAC, IEDDA, thiol-ene, or Schiff-base, have been screened.[81]

The applications of dPG-based and PEG-based hydrogels are alike as they focus mainly on biochemical, pharmaceutical, and biomedical applications, owing to their biocompatible, noncytotoxic, and bioinert properties.[79,81] When only the dPG component is used to construct a hydrogel, the applications often direct to a nanogel as a carrier for a drug/bioactive substance delivery system.[81] One good example is the dPG-based nanogel synthesis formed by IEEDA between norbornene-functionalized dPG and dimethyl tetrazines via the nanoprecipitation method to obtain a low dispersity index of 0.1 on average. Besides, these nanogels have a redox-responsive effect which comes from the disulfide bond embedded in the crosslinker molecule. The application of these nontoxic stable nanogels is for the delivery of Cytochrome C which is a multifunctional enzyme used as a cancer inhibitor.[82] Another example is the hydrogel fabricated by using only phenol-functionalized dPG. Interestingly, the gelation happens via an enzymatic reaction of horseradish peroxidase by oxidative crosslinking between phenol groups. Since these hydrogels are well cytocompatible, the application is oriented as a cell-laden hydrogel for the encapsulation of living cells for future promising regenerative therapy (**Figure 5**).[83]

When combining dPG and PEG for hydrogel formation, its mechanical properties can be improved due to the elastic nature of the linear crosslinker PEG. A good example of this type of gel is the hydrogel prepared by the SPAAC click reaction between cyclooctyne-functionalized dPG and azide-terminated linear PEG. This soft cytocompatible hydrogel was used as a gel bed for the study of the stemness of human mesenchymal stem cells (hMSCs). The result showed that this gel substrate can mimic the cell environments and is excellent for the two-dimensional culturing of hMSCs by keeping their pluripotency whose potential can be further used in clinical reconstructive medicine.[38] Another example is the hydrogel constructed from amino-functionalized dPG and *N*-hydroxysuccinimide active ester-terminated linear PEG via amide coupling reaction. This hydrogel was applied in a biosensing study by using redox enzyme periplasmatic aldehyde oxidoreductase (PaoABC) which is *in situ* encapsulated in the hydrogel matrix. The general function of this PaoABC is to detoxify aldehyde by changing it to acid in the cell.[84] In this study, the entrapped PaoABC is used for the amperometric detection of benzaldehyde by oxidizing it to benzoic acid.[85]
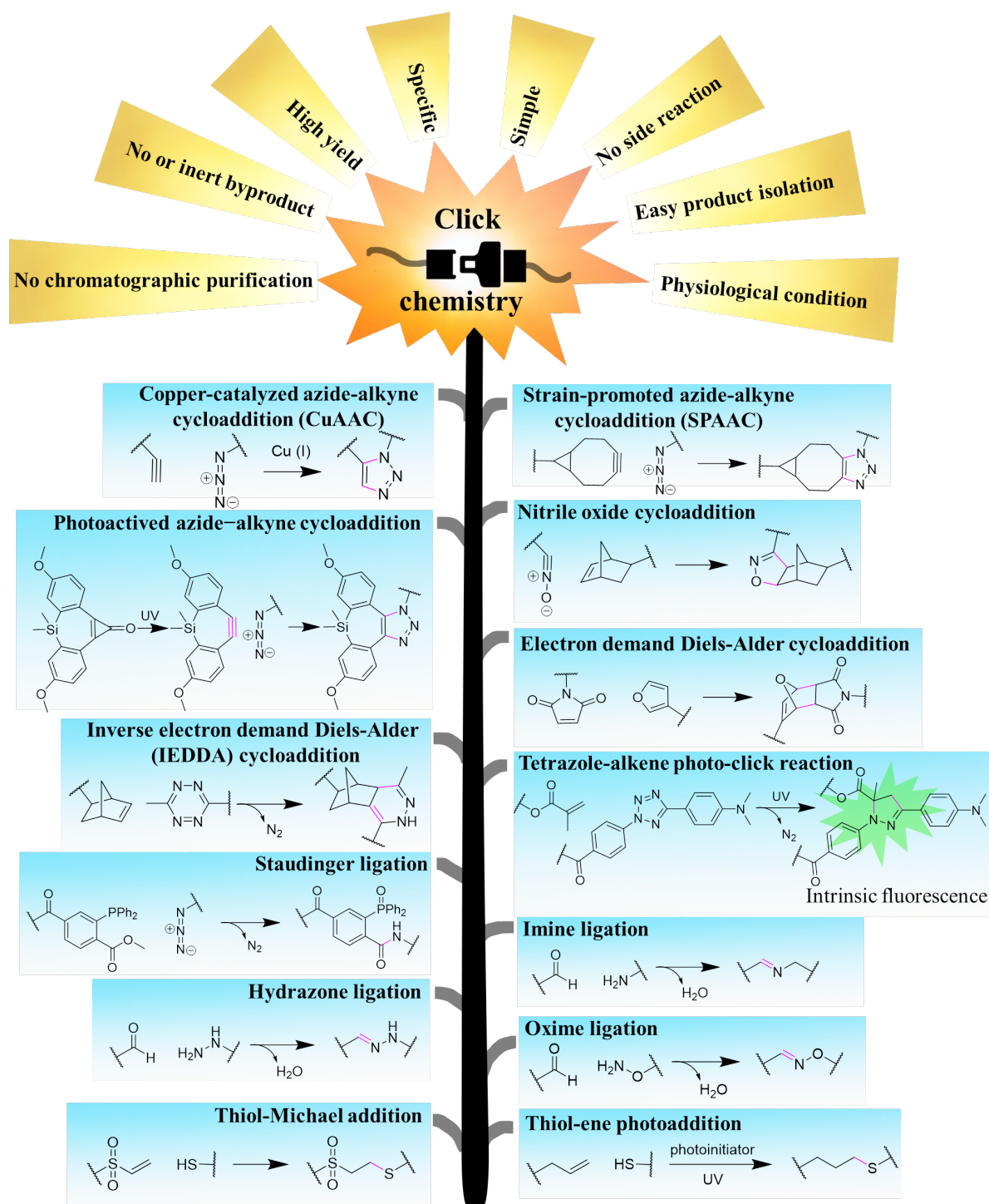
2.2 Click chemistry

2.2.1 Click chemistry overview

Click chemistry, termed by Sharpless in 2001,[19] is a chemical reaction between 2 different functional groups which has high specificity toward each other. The reaction should be, in principle, simple (without any complicated methods) under a benign condition, generally fast, have a very high yield, have no side reactions, insensitive to a physiological condition which contains water and oxygen, and have unreactive byproducts.[86–88] Besides, the purification must be easy without the chromatographic method. In terms of thermodynamics, a click reaction must have a great thermodynamic driving force which is higher than 20 kcal mol^{-1} by having either greatly energetic reactants or an extremely stable final product.[88] In late 2022, Carolyn Bertozzi, Morten Meldal, and Barry Sharpless who start their pioneer work in click chemistry won the Nobel Prize in Chemistry. Their work can turn the difficulty of the conjugation between chemistry and biological substances into a bed of roses with click chemistry, making it immensely beneficial in pharmaceutical and biomedical applications for mankind. Since its simplicity and specificity as the name states, it is convenient to just attach a clickable functional group to any substances or biomaterials which are needed to combine to any desired counterparts and it will readily produce the desired adduct. Click reactions have been employed as a super powerful tool for large areas of applications such as chemistry, biochemistry, bioengineering, bioconjugation, pharmaceuticals, and biomedicine.[87–89]

Many reactions including addition, condensation, or nucleophilic substitution are considered click reactions by the definition. The first highlight is the copper-catalyzed azide-alkyne cycloaddition (CuAAC).[90] It is a concerted 1,3- dipolar cycloaddition between a dipolar azide functionalized group and an alkyne group by forming a new bond at the first and third position of a dipolar molecule, thereby producing five-membered triazole ring (**Figure 5**). Cu (I) acts as a catalyst to accelerate the reaction in such a mild condition like water at room temperature and the triazole heterocycle product is highly stable.[91] Similarly, the strain-promoted azide-alkyne cycloaddition (SPAAC) also involves a concerted 1,3 dipolar cycloaddition between a dipolar azide and not terminal alkyne but a cyclooctyne. The obvious benefit of using these reactants is that there is no need of using Cu (I) as a catalyst and the reaction can spontaneously proceed by exploiting the ring strain of a cyclooctyne as a driving force to form a triazole adduct. There is an even more fancy reaction that ends up in the same result as SPAAC but can have spatial and temporal control ability.[92] A key reaction is a cyclopropenone group

embedded in the eight-membered ring which can be activated by UV light, resulting in a cycloalkyne ring which can further click with azide.[93] Moreover, beside an azide, a nitril oxide which is another active dipolar group can click with a ring-strained alkene namely norbornene to give a five-membered ring adduct (**Figure 6**).[18,94]

Figure 6. *Click chemistry principles and many different types of click reactions*

Normal and Inverse Electron Demand Diels-Alder (DA and IEDDA, respectively) reactions are also considered a click reaction. As aforementioned, the DA is the [4+2] cycloaddition between electron-rich diene which contains 4 π-electrons, and electron-deficient dienophile which contains 2 π-electrons. The concerted reaction happens via the delocalization of these π-bonds to make 2 new sigma-bonds, forming thus a stable six-membered ring adduct.[45] An example is a reaction between maleimide and either furan or fulvene groups (**Figure 6**).[46,89] In contrast, the IEDDA reaction, despite having a similar mechanism, is carried on by combining electron-rich dienophile and electron-poor diene instead.[50] An example is a reaction between tetrazine and norbornene which produces dihydropyridazine adduct and nitrogen gas as a byproduct.[49] Another interesting click reaction which is fairly similar to IEDDA by releasing a nitrogen gas is the Tetrazole-alkene photo-click reaction.[18,89] This reaction involves aromatic-conjugated tetrazole moiety and alkenes such as allyl[95] or methacrylate[96] moieties. The reaction is catalyzed by the UV light and the resulting product is self-fluorescent five-membered ring pyrazoline (**Figure 6**).

Another type of click reactions which employs the azide group as a reactant is a Staudinger ligation. This reaction utilizes the unique characteristics of the Staudinger reaction between triphenylphosphine and azide which produces an iminophosphorane intermediate and releases nitrogen gas as a byproduct. In general, this iminophosphorane is sensitive to hydrolysis and will be hydrolyzed as soon as it contacts water to produce stable phosphine oxide and amine products.[92] To make an adduct of this ligation, an ester group must be functionalized on the ortho-position of one phenyl ring of the triphenylphosphine moiety. The intramolecular reaction between a nucleophilic iminophosphorane and an electrophilic carbonyl ester occurs in water, giving an amide bond which connects both reactants (**Figure 6**).[18,92,97]

A simple condensation reaction such as Schiff-base can be considered a click reaction. As mentioned, the Schiff-base click reaction occurs between the aldehyde functional group and either amine, hydrazine, or hydroxylamine group to condense into imine or hydrazone, or oxime adduct respectively, with the release of a water molecule as a byproduct (**Figure 6**).[18,89]

Last but not least, Thiol-ene click chemistry has been one of the most widely used click methods so far. It can either undergo UV light with a photoinitiator as a catalyst or just base-catalyzed aqueous condition. The former condition can be applied to a non-electrophilic olefinic acceptor such as an allyl group with spatiotemporal control whereas the latter one

happens when using an electrophilic double bond such as maleimide or vinyl sulfone in physiological condition to yield thioether as an adduct (**Figure 6**).[20,41]

### 2.2.2 Thiol-ene click reaction in hydrogel crosslinking

Sulfur is one of many essential elements which has been utilized nowadays in biological and nonbiological research frontiers. The generic functional form of sulfur used in many research studies is a chemical thiol (SH) functional group.[98] Why is it powerful? It is of course thanks to the chemical properties of it being such a strong nucleophile compared to hydroxy group (OH).[99] A sulfur atom is larger than oxygen, has less electronegativity than oxygen, and has vacant *d*-orbitals, making it better charge distribution over the volume surface area, thus better polarizable.[98,100] As a good electron donor, finding a perfect match of a thiol has been reported,[101] to be a double bond. The thiol-double bond (thiol-ene) reaction has been extensively studied and later categorized as click chemistry due to its high specificity, robustness, quantitative yield, no byproduct, efficiency, and various commercial availabilities (**Figure 7**).[41] Typically, there are two types of thiol-click reactions; radical-based thiol-ene and nucleophilic-based thiol-Michael reactions.

Radical-based thiol-ene reaction undergoes photocatalytic reaction by using a photoinitiator as a catalyst. Thiol can easily undergo a hydrogen abstraction to form thiyl radical which can react with ene, resulting in thioether adduct with high conversion.[41,102] Usually, an acceptor should be an electron-rich double bond such as allyl or a strained double bond like norbornene to ensure complete conversion of step-growth thiolation, and avoid a side reaction of chain-growth homopolymerization of a double bond itself, which can happen when using a highly electrophilic double bond e.g. acrylate or acrylamide.[41] In terms of hydrogel formation by using this thiol-ene click reaction, an olefinic and thiol groups will be functionalized on either side chain, or end chain of a synthetic or biological hydrophilic polymer, enabling to crosslink and hence forming a 3D network hydrogel.

The nucleophilic-based thiol-Michael reaction is, on the other hand, catalyzed by gently basic conditions, even at physiological conditions is sufficient to proceed with the reaction. Since a thiol group is quite acidic, having pKa around 7-11 depending on either aromatic or aliphatic neighbor, it can be readily deprotonated in basic condition and becomes a thiolate anion which is much stronger nucleophile than its conjugated acid, thiol.[20] Meanwhile, the double-bond acceptor must be electrophilic enough to react with a thiol nucleophile. Many electron-withdrawing adjacent groups such as carbonyl, nitrile, aromatic, or sulfone help greatly reduce

the activation energy of a LUMO of a double bond by the conjugated system.[20,103] Therefore, it is easy to run this reaction at only room temperature in just an aqueous weak-basic medium without any catalysts.
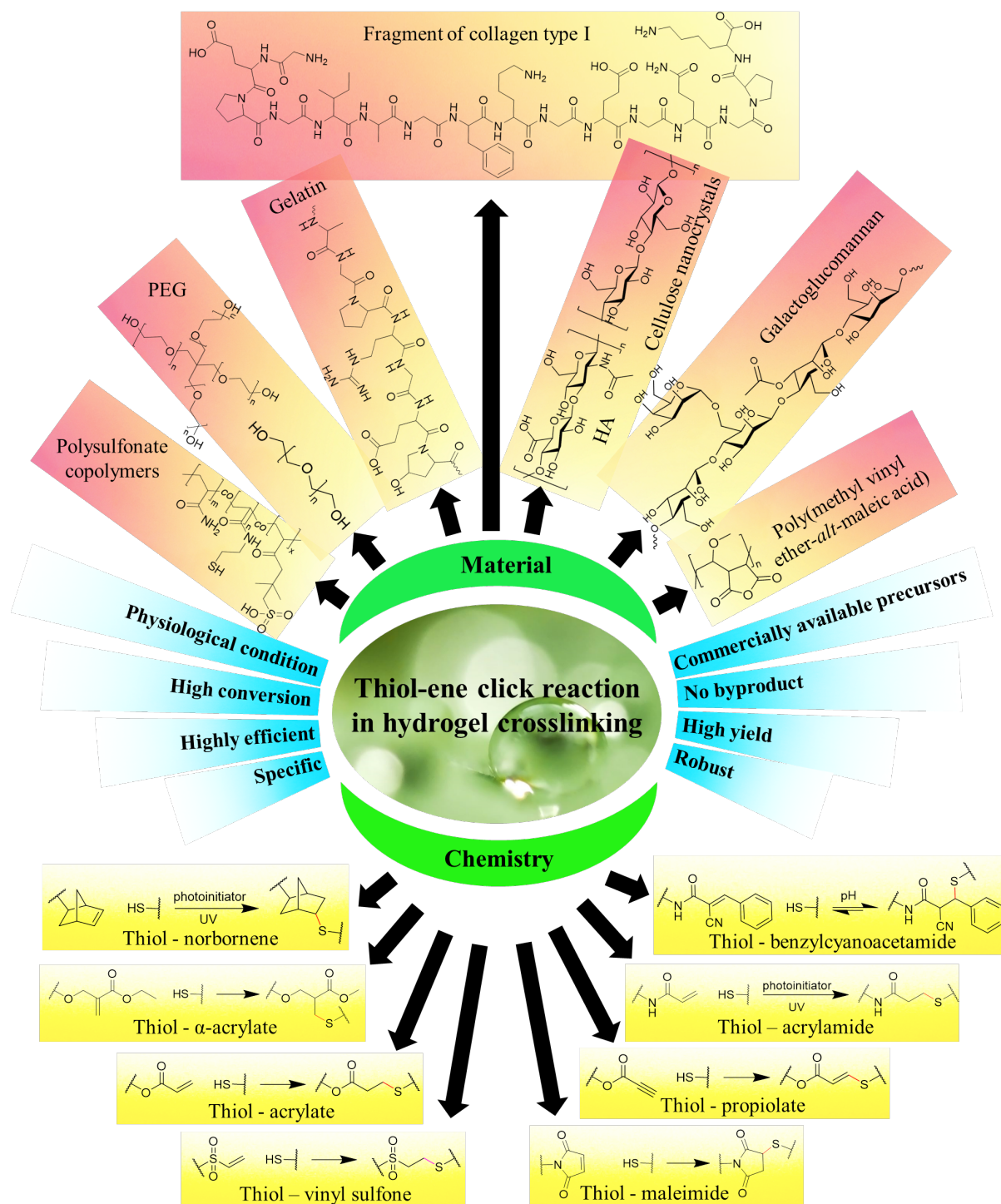
Figure 7*. Different types of thiol-ene click chemistries and gel materials used.*

To functionalize a thiol group onto a material, the simplest and most straightforward method is to convert a hydroxyl group (OH) which can be found in many materials such as PEG, HA, or Gelatin to thiol. The first step is to convert OH to a leaving group which later reacts with thiol-donating compounds such as NaSH, thiourea, or thioacetic acid. After the hydrolysis, a SH group is formed.[104,105] Other methods involve conjugating a thiol-containing compound with a polymer via ester or amide couplings or by reacting Traut's reagent with an amino group on a polymer. On the other hand, a double-bond acceptor could be functionalized onto a polymer via ether, ester, or amide formations from an ene-containing compound.

As they are easy and efficient, Thiol-click reactions have been employed in many hydrogel materials. For instance, gelatin which contains many amino functional groups on the side chain can be functionalized with either norbornene carboxylic acid to have norbornene linked by an amide bond, or with *N*-acetyl, homocysteine thiolactone to form *N*-acetyl homocysteine linked via amide bond with a free SH.[43,106] Similar crosslinking chemistry example is viewed by using thiol-functionalized collagen which is formed by using Traut's reagent and norbornene-terminated eight-arm PEG (**Figure 7**).[107] The next examples are acryloyl-family-based crosslinking chemistry. These acryloyls can be acrylate-, methacrylate-, ethyl methacrylate- (or α-acrylate which is named by substitution at α carbon next to a carbonyl group), acrylamide or propiolate. These can be added onto many materials such as linear PEG, four-arm PEG, galactoglucomannan, or HA. In the meantime, thiol groups can be decorated onto PEG, polysulfonate copolymers, and cellulose nanocrystals (**Figure 7**).[108–111] Other examples are the rapid gelation which comes from a highly electrophilic double bond such as maleimide-functionalized four-arm PEG[42] or HA together with gelatin[112] or vinyl sulfone-functionalized poly(methyl vinyl ether-*alt*- maleic acid).[113] The last noticeable example is the pH-responsive reversible thiol-Michael click hydrogel formed from benzylcyanoacetamide- and thiol-terminated four-arm PEG (**Figure 7**).[114]

2.3 Hydrogel characterization by rheology

2.3.1 Rheology overview

Rheology is the study of the mechanical properties of a material when a certain force is applied and simultaneously exhibited deformation and flow characteristics.[115,116] The technology to measure these mechanical or rheological properties is called rheometry. The rheological study of materials provides information on how materials behave when external force is applied.[116]

All materials have a rheological property. For instance, a solid metal structure has an ideal elastic behavior while a waterfall has an ideal irreversibly viscous-flow character. Some soft materials such as foams, pastes, colloids, cells, crosslink polymers, and hydrogels show both viscous and elastic characteristics after applied mechanical stress.[115] These unique characters are thus called viscoelasticity. Material can be rheologically characterized in 2 simple ways; steady shear and oscillation shear rheometry (**Figure 8**). Steady shear characterization gives information about the viscosity of materials when shear rate is applied, whereas oscillation shear experiment provides data on material stability by elastic and viscous modulus parameters as a function of applied stress, strain, frequency, or time.[116]

In terms of hydrogel characterization by rheology, it is important to know some mechanical properties of hydrogels to ensure a suitable application for which a gel is applied.[117] For example, some hydrogels should be stiff enough to be used as a gel platform for 2D cell growth[38] or soft to some extent for 3D cell encapsulation[46] in order to keep them alive, grow or differentiate. On the other hand, some hydrogels as a delivery vehicle[117] or viscosupplementation[118] should be able to flow like a liquid or be injectable through a syringe and reverse or heal back to their original shape subsequently.

2.3.2 Oscillation shear rheology for hydrogel

As mentioned, hydrogels are a viscoelastic soft solid and one of the best characterization systems used to explain their mechanical properties is oscillation shear rheology.[119] This experiment is to quantify the viscoelasticity of a hydrogel in terms of elastic and viscous moduli at a certain shear strain. A shear strain is a deformation parameter which explains how a material deforms from its original shape when applied shear stress (force). The most common properties which are generated from oscillatory shear are a storage modulus (G´) and loss modulus (G´´) (**Figure 8**).[116,120,121] A storage or elastic modulus (G´) is the quantity parameter which explains how energy gets stored inside a molecular matrix and represents elastic (solid)

behavior while a loss modulus (G´´) explains how energy gets dissipated away during deformation, which therefore represents viscous (flow) behavior.[116,121] In covalently crosslinked hydrogels, the elastic character is typically predominant (G´ > G´´) whereas the viscous response is predominant (G´´ > G´) in noncovalently entangled hydrogels due to high-stress relaxation.[115]
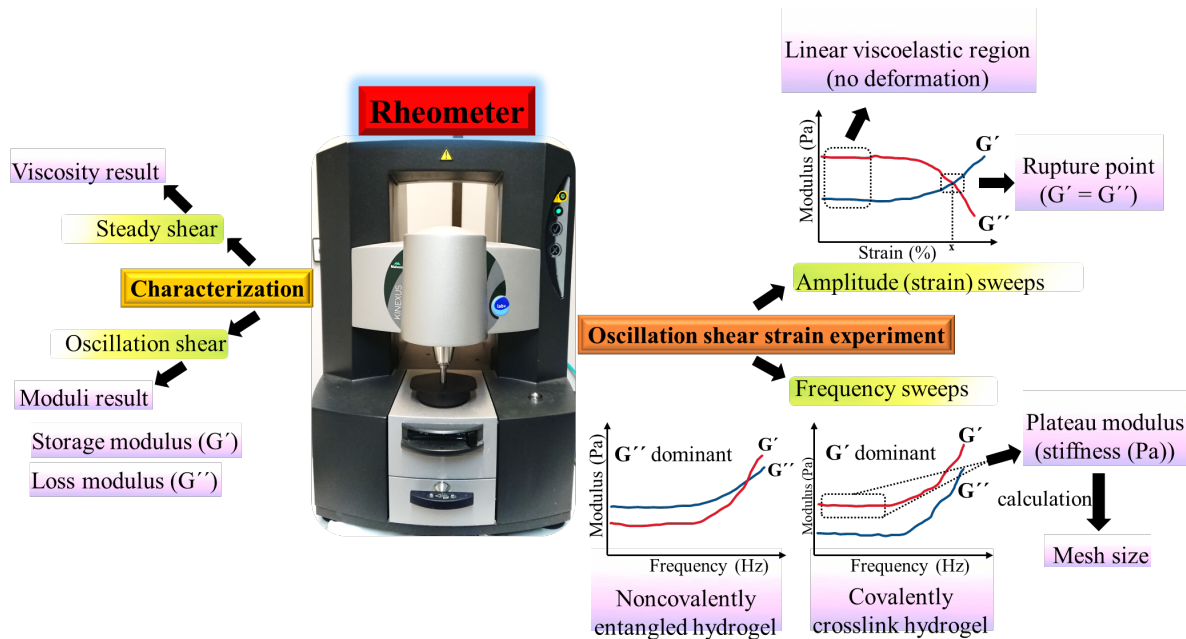

Figure 8. Diagram of rheological characterization by rheometer

To quantify the viscoelasticity of a hydrogel, the first thing to do is to defy the linear viscoelastic region (LVR) in strain (or amplitude) sweeps which are done by monitoring the shear moduli when increasing shear strain at a constant frequency (normally set as 1 Hz).[116] In this region, it supposes to be independent of applied strain (or no deformation happened) at a microstructural level. Any values which fall in this linear range can be picked and further applied to the next step which is frequency sweeps. Amplitude sweeps can also give information on a rupture point at a crossover point between falling G´ and rising G´´ when ramping strains up (**Figure 8**).[122] In this situation, the matrix structure starts to irreversibly deform and stored energy dissipates much more. In the frequency test, the range of frequencies which is a process of a time scale is scanned while a constant value of shear strain from LVR is applied. It can determine the material behavior in a short- or long-time deformation and is very useful in many applications.[121,123] In addition, the plateau G´ where it is independent of frequencies can further refer to the stiffness (directly related) and mesh size (by calculation) of a material (**Figure 8**).[2,124]

2.4 Hydrogel applications

2.4.1 Hydrogels for biosensing applications

Biosensing application is the analytical way to utilize a biosensor which is a sensing tool for the detection of a target analyte.[125] A biosensor is the combination of a biomolecular probe and a transducer which acts as a detector to amplify the sensing result to be cognitively realized. A 3D network hydrogel can provide high biocompatibility toward microenvironments and serve as a good platform for a biological probe.[14] To have a clear image of hydrogel-based biosensing applications, some cases are illustrated. The first example is the *in situ* encapsulated streptavidin probe in dPG-PEG based 3D hydrogel as a biosensing platform to target biotin by using a fluorescence dye as a transducer to display a sensing performance (**Figure 9**).[39]
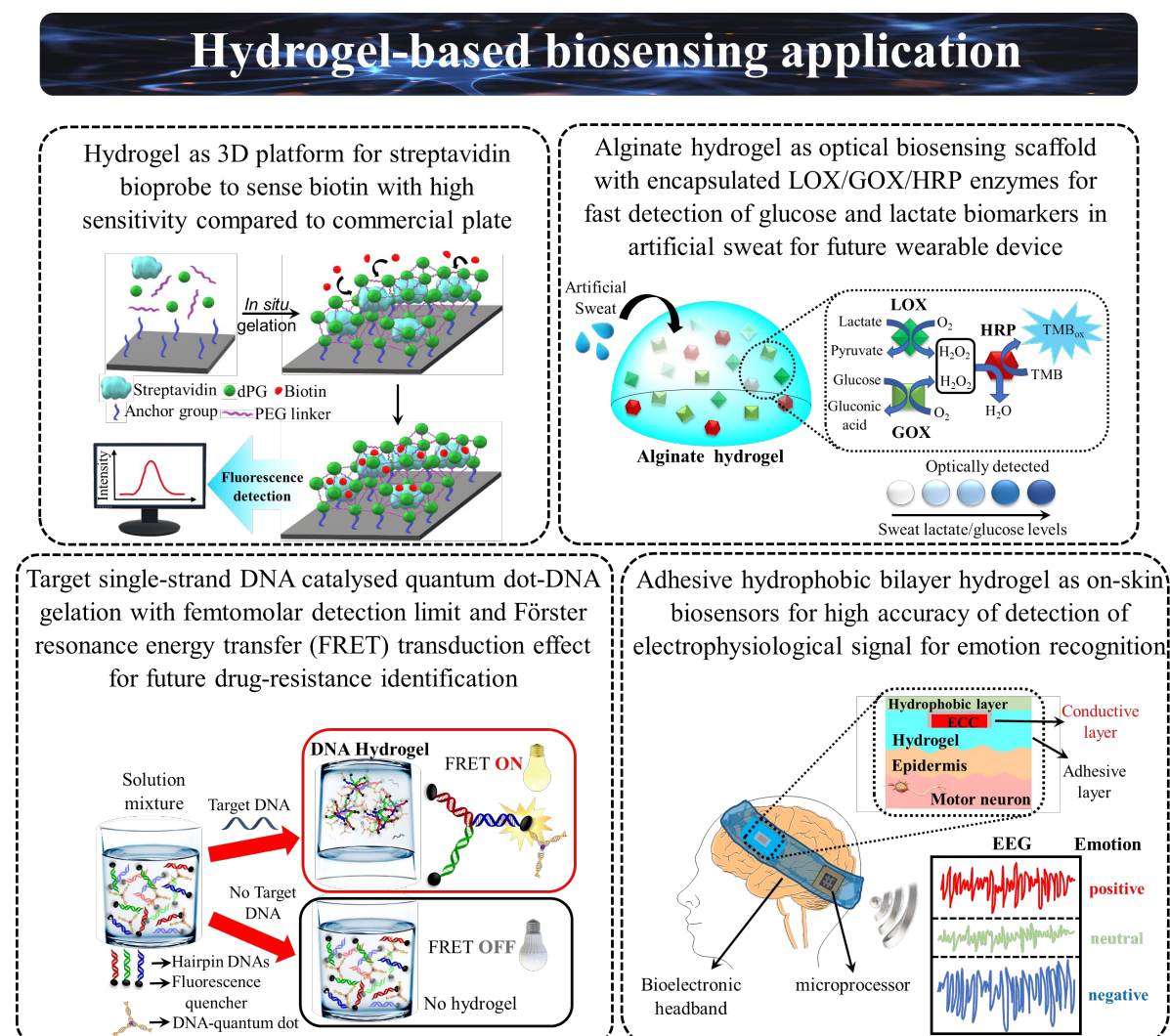

Figure 9. *Illustrations of different biosensing applications based on hydrogel platforms. Adopted from Ref.* [39, 125, 126, 127 and 128]

Other examples, lactate/glucose oxidase (LOX/GOX) and horseradish peroxidase (HRP) enzymes as a bioprobe as well as tetramethylbenzidine (TMB) as a colorimetric transducer are encapsulated inside the alginate-based hydrogel as an optical biosensing platform for the detection of lactate/glucose target in artificial sweat.[125,126] Another interesting example is a wearable hydrophobic-bilayer hydrogel sandwiched with electrodes as a biosensing probe to target electrical signal which directly relates to human emotion.[127] In the last case, the target DNA catalyzes the gelation of the mixture of ssDNA-quantum dot and hairpin DNAs. These hairpin DNAs act as a probe to sense the target DNA with high detection of femtomolar range by Förster resonance energy transfer (FRET) as a transduction method.[128]

2.4.2 Sulfated polymers for virus binding

Since the rise of the coronavirus pandemic in late 2019, people have learned that virus infection can invade our lives. Many studies have focused on understanding the virus infection mechanism and the way to prevent its infection.[129]
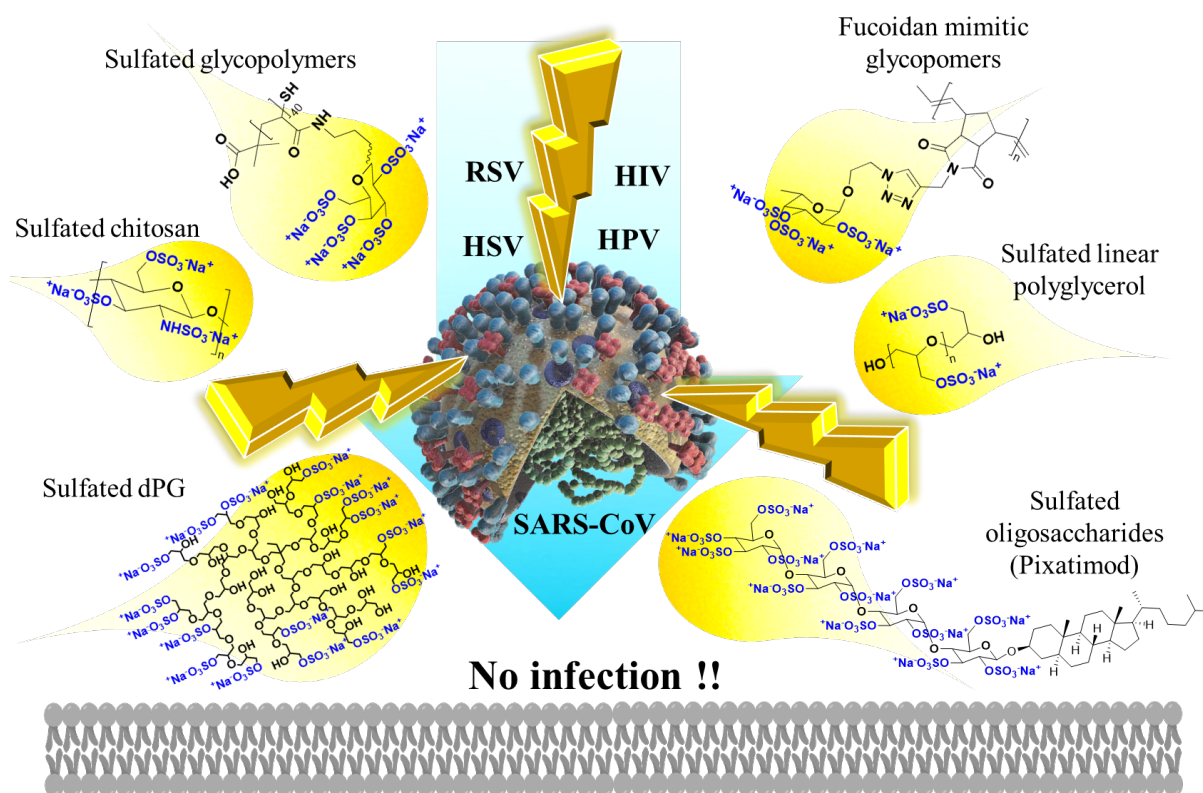
Figure 10. *Exemplary sulfated polymers able to inhibit viruses via electrostatic interaction*

Heparan sulfate (HS), the natural polysaccharides found on the cell surface of higher organisms, plays a crucial role in inhibiting viruses before they intrude into the cell.[130] A negatively charged sulfate group which is decorated on HS is found to be the key active point to block a virus at its positively binding domain by strong electrostatic interaction. It is not only a sulfate group but also its number in one molecule and the polymeric architecture are also important.[130] Since then, HS or polysulfate mimetics as alternative prophylactic agents or antiviral drugs have been studied intensively.[131] Many polymers such as linear polyglycerol, dPG, glycopolymers, chitosan, or oligosaccharides were sulfated and investigated for their potential against viruses (**Figure 10**).[132–136] Many virus species e.g. human immunodeficiency virus (HIV), herpes simplex virus (HSV), human papillomavirus (HPV), respiratory syncytial virus (RSV), and severe acute respiratory syndrome-associated coronavirus (SARS-CoV) contain the positively charged binding domain and can bind strongly to sulfated polymers, thus blocking it.[130,131,134]

3. Scientific Goals

The objective of this thesis is to develop the 3D hydrogel as a versatile platform by using dPG and PEG, crosslinked by thiol-ene click chemistry. dPG and PEG are the perfect water-soluble combine since they are biocompatible and friendly to biological systems, allowing their use for biosensing and biomedical applications.

In the first project, dPG is functionalized with different types of double-bond acceptors such as acrylate, allyl, acrylamide and reacts with PEG whose end group is terminated with a nucleophilic thiol group. Streptavidin (a biosensing probe) together with the functionalized dPG and PEG are mixed *in situ* to form a hydrogel. This project aims to employ hydrogels as a platform for the study of biosensing applications by exploiting streptavidin to characterize them. Moreover, these gel platforms are characterized in terms of stability and degradability for further applications (**Figure 11**).

In the second project, the hydrogel which is made from sulfated-dPG and PEG is used as an antiviral agent for the study of virus-binding ability. dPG is functionalized with maleimide as a crosslinking group and additional sulfate as a virus inhibitor, while linear PEG end groups are thiolated. The flexibility of the sulfated hydrogels is varied by a dilution method to have the stiffness ranging from stiff to soft slimy characters. They are subjected to test with herpes simplex virus (HSV) type 1 by plaque reduction assay and later investigated, compared to the result of their nonsulfated version (**Figure 11**).
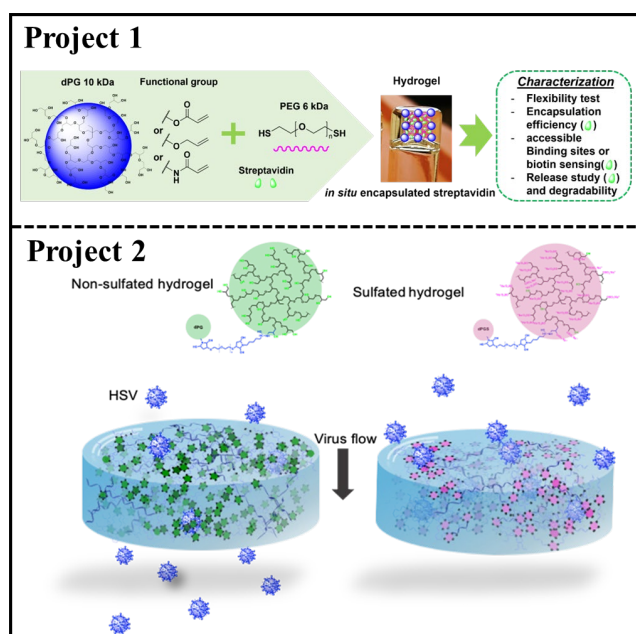
***Figure 11**. Overview of the two projects in this dissertation.*

4. Publications

In this part, the published articles are listed and the author contributions are specified.

4.1 Thiol-Click Based Polyglycerol Hydrogels as Biosensing Platform with *in situ* Encapsulated Streptavidin Probes

Boonya Thongrom, Mathias Dimde, Uwe Schedler*, and Rainer Haag*

Macromolecular Chemistry and Physics **2022**, 2200271

https://doi.org/10.1002/macp.202200271

https://creativecommons.org/licenses/by-nc/4.0/

Figure 12. *Graphical Synopsis. Reprinted with permission from Ref.*[137] *Copyright © 2022 John Wiley & Sons.*

Contributions of authors

Boonya Thongrom performed all experiments and characterizations as well as wrote the manuscript. Mathias Dimde helped initiate the project, designed the project idea, proofread the manuscript and revise some parts. Uwe Schedler and Rainer Haag contributed to the supervision of this project, provided clear scientific guidelines, and corrected the manuscript.
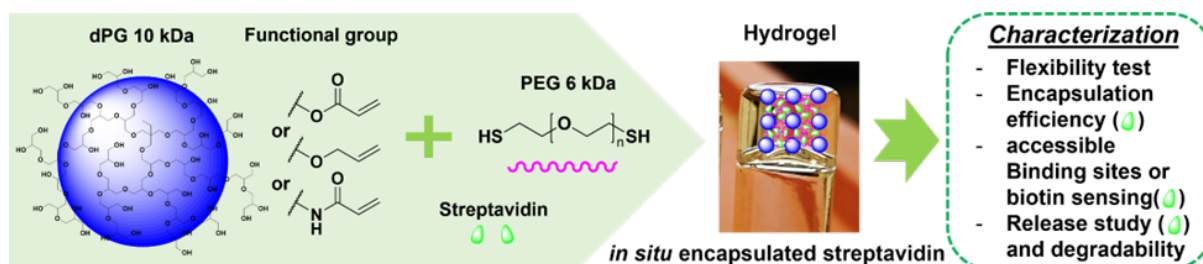
Thiol-Click Based Polyglycerol Hydrogels as Biosensing Platform with In Situ Encapsulated Streptavidin Probes

Boonya Thongrom, Mathias Dimde, Uwe Schedler,* and Rainer Haag*

An in situ streptavidin-encapsulated hydrogel based on dendritic polyglycerol (dPG) which is functionalized with either an acrylate, allyl or acrylamide group and dithiolated polyethylene glycol (PEG) is constructed via a thiol-click chemistry approach and is investigated for biosensing applications. The hydrogel platform is screened for the encapsulation and release efficiencies of the model protein streptavidin under varying physicochemical conditions, for example, crosslinking chemistry reactions, the molar ratio between the two gel components, macromonomer concentrations or pH-values. By that, tailor-made hydrogels can be developed, which are able to encapsulate or release the model protein for several days based on its modality. Furthermore, the accessible binding site of encapsulated streptavidin or in other words, the biotin-binding performance is quantified, and the stability of the various hydrogel types is studied by rheology measurements, ^{1}H NMR, gel permeation chromatography (GPC), and mass loss experiments.

1. Introduction

Streptavidin is a homo-tetramer-type protein with a weight of roughly 55 kDa comprised of 4 binding sites.[1,2] It has been used as a biomolecular probe to sense or detect biotin since it binds strongly and specifically to streptavidin. The binding interaction between them is recognized as one of a strongest non-covalent interaction in nature so far.[3–5] Many modern biosensors exploit the high-affinity streptavidin-biotin interaction and thus provide access to a variety of assays based on it. Biomolecules, including proteins and nucleic acids, can be biotinylated using established protocols and immobilized on a streptavidin biosensor surface for diverse assays. However, streptavidin when fluorescently labeled is also used on the detection side of biosensors. The high sensitivity and stability of streptavidin-based biosensors enable both kinetic and quantification experiments.

In the field of immunoassays, streptavidin is also used both as a capture molecule for biotinylated species and as a detector molecule in sandwich assays.[6] Streptavidin-coated microtiter plates or beads allow an immobilization of any biotinylated molecule and thus provide flexibility for the solid phase assays compared to the antibody- or antigen-coated solid phase.[7] Streptavidin-coated materials, for example, glass slide,[2] silicon wafer,[2,8] gold-coated surface,[9,10] magnetic particle,[11] Teflon[12] or polymeric nanocarrier[13] are widely used in clinical diagnostics and there are numbers of manufacturers. However, there is still a sensitivity limit of detection for biotinylated compounds due to the limited streptavidin loading on the surface, its poor accessibility, and the low stability of immobilized streptavidin.

To improve its sensitivity for biotin detection, a 3D surface coating such as a polymeric brush[14,15] or hydrogels has been developed to cage it inside the 3D matrix.[1,2,16] Herrmann et al. have previously demonstrated the improvement of the sensitivity of biotin detection, compared to a commercially available streptavidin slides, by using an in situ streptavidin-immobilized hydrogel as a 3D sensing platform.[2] By using a hydrogel, the loading of streptavidin, and stability and accessibility of its binding site can be improved due to a water-based nature of the hydrogel, its high permeability inside the 3D network and its biocompatible gel material which can mimic the naturally environmental condition.

The use of immobilized streptavidin as a bioactive sensor on a coated surface has been extensively studied. Besides the quantification of the binding site,[2,17,18] the immobilized efficiency, or in other words an encapsulation efficiency in case of a streptavidin encapsulated inside a 3D matrix has been measured and is an essential factor for the validation of the material. This parameter can identify a streptavidin amount loaded inside and later imply directly the sensitivity of the detection. However, no systematic studies on the quantification of an encapsulation efficiency have been reported.

Click chemistry, a reaction which has high specificity, quantitative yield, benign condition and produces no or nontoxic

B. Thongrom, M. Dimde, R. Haag
Institut für Chemie und Biochemie
Freie Universität Berlin
Takustraße 3, 14195 Berlin, Germany
E-mail: haag@zedat.fu-berlin.de
U. Schedler
PolyAn GmbH
Schkopauer Ring 6, 12681 Berlin, Germany
E-mail: u.schedler@poly-an.de

**ADVANCED
SCIENCE NEWS**

www.advancedsciencenews.com

**Macro-
molecular
Chemistry and Physics**

www.mcp-journal.de

byproducts which can be easily removed without chromatographic technique, can be applied to a hydrogel crosslinking chemistry. Our group has used strain-promoted azide alkyne click (SPAAC) which is fast and bioorthogonal for the construction of a gel network.[2,19–21] However, the process to obtain its function on a gel precursor, especially cyclooctyne moiety is very costly and needs many synthetic and purification steps. Inverse electron demand Diels Alder reaction (iEDDA) is also of interest due to its even better bioorthogonality than strain-promoted azide alkyne click (SPAAC). A byproduct N_2 gas releasing inside the gel matrix might nevertheless interfere some optical analysis and not suitable for isolated space application.[22,23] To tackle these problems, a thiol-click chemistry crosslinking approach is proposed. Here, a high reaction specificity, a quantitative reaction, and easy purification step with high yields in terms of the synthesis of the gel precursors and remarkably good cost-effectiveness are given. The reaction between a thiol and a double bond acceptor is also fast and produces no byproduct.[24–27]

In this study, we introduce a hydrogel constructed by dendritic polyglycerol (dPG) and polyethylene glycol (PEG) building blocks via thiol-click reaction as a sensing platform to detect a biotin. Streptavidin is noncovalently encapsulated in situ during gel formation and its stability in different crosslink types of the hydrogel was analyzed.

2. Results and Discussion

2.1. Synthesis and Characterization of the Macromonomers for Hydrogel Preparation

The hydrogels developed in this study were based on multivalent dendritic polyglycerol (dPG), and polyethylene glycol (PEG) as a linear bifunctional crosslinker. To create a biocompatible 3D hydrogel network, dPG and PEG components were functionalized accordingly. For the crosslinking chemistry, thiol-Michael and a thiol-ene reaction were preferred due to their high yield, ease of preparation, high specification, straightforward, and inexpensive precursor preparation. For this purpose, a thiol group on a chain of the linear crosslinker PEG is linked to an olefinic acceptor group of the spherical dPG. The corresponding "thiol-click based" dPG-PEG hydrogels were investigated as a biosensing platform based on the concept of in situ encapsulation of a model protein streptavidin. The PEG dithiol crosslinker was synthesized according to the procedure from Mahadevegowda et al.[28] PEG(OH)$_2$ 1 was first mesylated at the chain end, then thiolated with thiourea and hydrolyzed. Two intact thiol groups were detected at the end chain of PEG-dithiol 3 by ^{1}H NMR (Figure S10, Supporting Information). A multivalent dPG hub 4 was functionalized with different functionalities to investigate the chemical and mechanical properties of the corresponding hydrogels. For this purpose, the multivalent hydroxyl groups of the dPG were functionalized with different olefinic acceptor groups for further crosslinking.
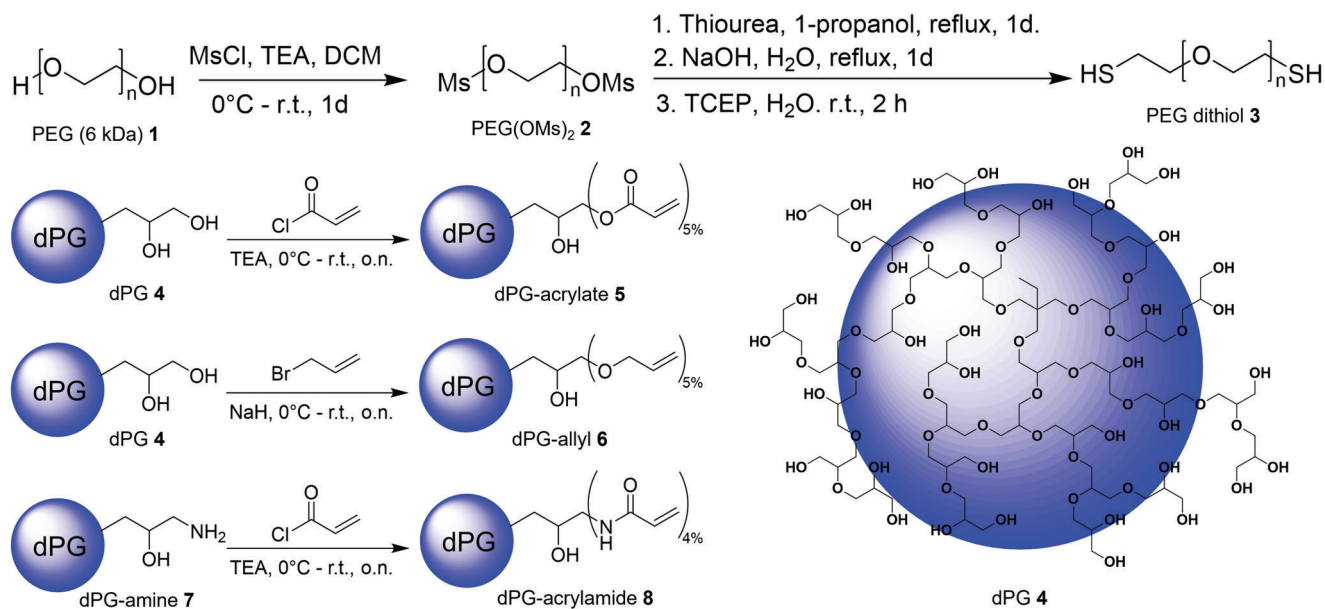
In the case of the dPG-acrylate 5, ≈5% functional groups were introduced by an acrylation reaction and characterized by ^{1}H NMR end group analysis (Figure S12, Supporting Information). The dPG-allyl 6 was prepared by allylation with allyl bromide, here 5% functional groups were introduced (Figure S12, Supporting Information). The dPG-acrylamide 8 was synthesized by an

acrylation reaction starting from dPG-amine (synthesized according to the procedure from Sebastian et al.[29]) whose number of amino groups were confirmed by ^{1}H NMR of dPG-NHBoc (Figures S13–S15, Supporting Information). A functionalization of 4% of acrylamide groups was calculated by ^{1}H NMR (Figure S16, Supporting Information). All reaction schemes of the individual gel components are shown in **Scheme 1**.
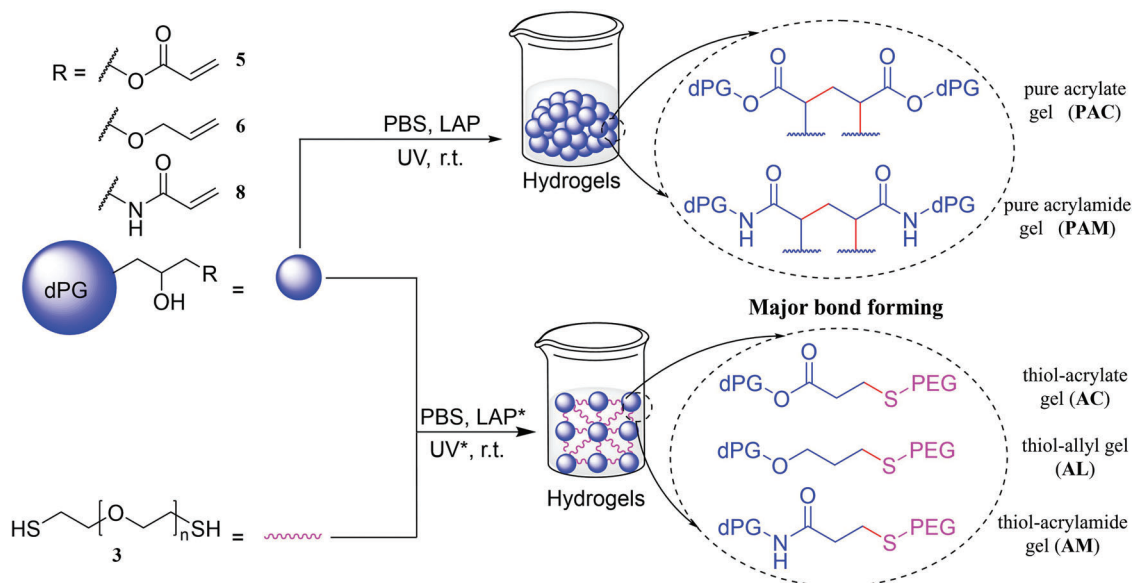
2.2. Hydrogel Formation and Flexibility Test

In this study, acrylate, allyl or acrylamide Michael acceptor groups on the dPG surface were used to verify their properties to form tailor-made hydrogels in terms of gel stability, flexibility and degradability. Furthermore, acrylate- and acrylamide-based hydrogels can be formed with PEG-dithiol by mixing both precursors, whereas allyl-based hydrogel formations need to be initiated via additional photo initiators and UV light. For the latter one, time-dependent start points, and defined reaction times favor the application in tissue engineering[30] and protein encapsulation.[31] All hydrogel samples in all experiments were measured in triplicate and each reported value is the mean value plus its standard deviation. Before investigating a biosensor application, the hydrogels with different crosslinking chemistry were rheologically characterized to determine the gel strength in terms of storage modulus (which directly refers to stiffness) and elasticity. Here, no biomolecule was yet added during gelation. A general procedure for the formation of thiol-acrylate hydrogel was to simply mix the 2 components (dPG-acrylate 5 and PEG-dithiol 3) under physiological pH. After successful crosslinking via thiol-Michael reaction, a solid hydrogel was formed. In case of thiol-allyl and thiol-acrylamide hydrogel preparations, a radical photoinitiator lithium phenyl-2,4,6-trimethylbenzoyl phosphinate (LAP) and UV light were required for a thiol-ene based reaction. After mixing the gel components (dPG-allyl 6 or dPG-acrylamide 8 with PEG-dithiol 3) with LAP, the mixing vessel was irradiated with monochromatic UV light of 365 nm for 10 min at the lateral side of a vessel. The UV light intensity was ≈190 μW cm^{-2} (**Figure 1**). Moreover, the gelation of pure dPG-acrylate 5, pure dPG-allyl 6, and pure dPG-acrylamide 8 were studied in a similar approach to thiol-allyl and thiol-acrylamide gelation. The solution of pure dPG-allyl 6 was, however, unable to turn to a rigid hydrogel. The reason is probably that the side reaction of chain transfer to another allylic group inhibits the bond formation between two allylic groups.[32–34] On the other hand, the new bond formation on thiol-acrylamide hydrogel could come from both thioether bond (major) and C–C bond between the two double bonds (minor).[35,36]

In the gelation study, thiol-acrylate gel types were used because they are easy to prepare, and no catalyst or initiator was needed. Gelation screening based on the molar ratio of PEG to dPG component (PEG:dPG) was performed under similar conditions and the invert test tube method, in which the vessel of the gel mixture is inverted after the reaction time elapsed to see whether the mixture flows or not, was used to determine the gelation point. At higher ratio of dPG, there was no gel forming while starting from 1:1 ratio to higher PEG ratio, rigid gel emerges (Table S1, Supporting Information). Increasing the PEG ratio helps to build a 3D network structure and to form a solid hydrogel.

**ADVANCED
SCIENCE NEWS**

www.advancedsciencenews.com

[M] **acro-
olecular**
Chemistry and **Physics**

www.mcp-journal.de

Scheme 1. Synthetic route for the functionalization of PEG-dithiol 3, dPG-acrylate 5, dPG-allyl 6, and dPG-acrylamide 8 and an idealized fragment structure of dendritic polyglycerol (dPG) 4.

Figure 1. Hydrogel formation procedure of thiol-acrylate, thiol-allyl, thiol-acrylamide, pure acrylate, and pure acrylamide hydrogels. (*) LAP and UV light were applied only to thiol-allyl and thiol-acrylamide gelation types.

The flexibility of each hydrogel type was determined using a rheometer with an 8 mm parallel plate geometry. The oscillation frequency sweep test at a constant strain of 1% and 25 °C was used to measure the storage modulus, which directly reflects the stiffness of a hydrogel. Thiol-acrylate hydrogels were prepared at different ratio and concentrations with designation as AC1, AC2, AC3 and AC4 while thiol-allyl gel AL1, thiol-acrylamide gel AM1, pure acrylate gel PAC1 and pure acrylamide gel PAM1 were prepared with additional LAP and UV light as given in detail in Table S2, Supporting Information. The result of the storage modulus

of each gel is shown in **Figure 2**a. As expected, the storage modulus increases when increasing the concentration and the ratio of PEG crosslinker as it increases the density of crosslink network, resulting in stiffer gel. However, when increasing PEG while decreasing dPG ratios in order to keep the same concentration as AC3, the storage modulus significantly decreases since lowering dPG component can lower the crosslink density.

The fracture point test of each hydrogel sample type at a gel concentration of 20% (AC2, AL1, AM1, PAC1, and PAM1) was determined by an oscillating amplitude sweep test in the range of
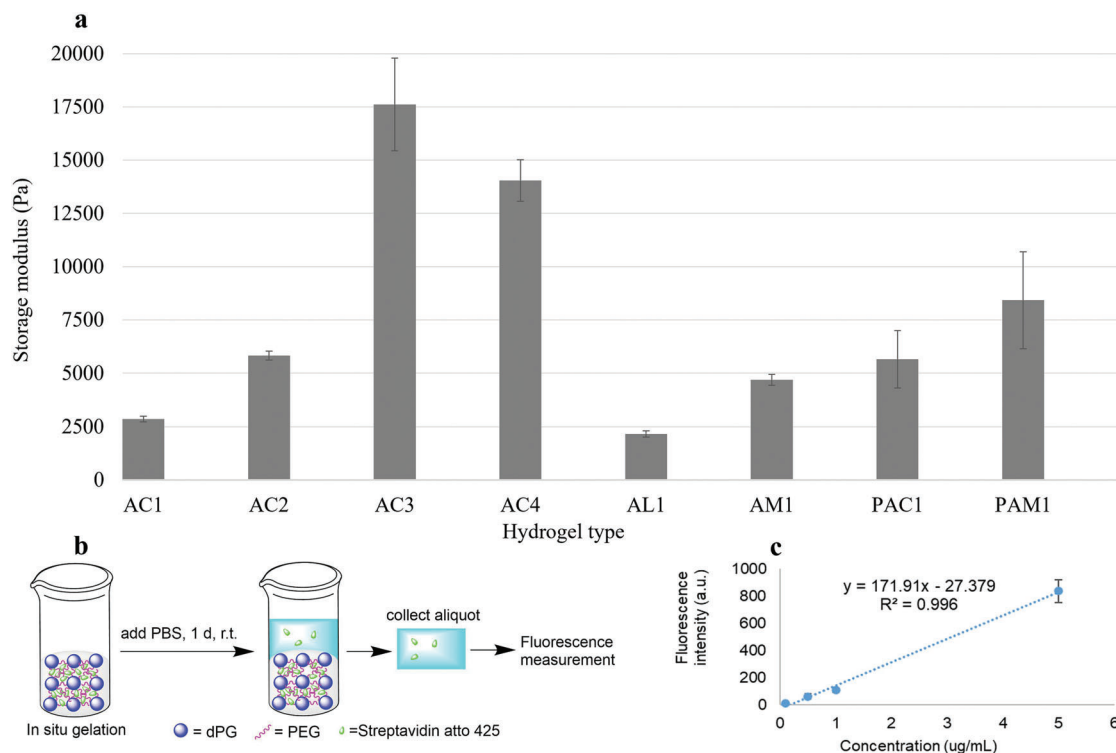
Figure 2. Characterization of hydrogels. a) Rheological measurements of the storage moduli of each hydrogel sample. b) Schematic procedure of the encapsulation efficiency test of a hydrogel after gelation in the presence of fluorescence-labeled streptavidin. c) Standard calibration curve of fluorescence-labeled streptavidin characterized by fluorescence measurements.

1–200% strain. This test can be used to preliminarily determine whether a hydrogel is elastic or brittle. The test measured the transition (crossover) point between storage modulus and loss modulus, where the storage modulus begins to decrease, and the loss modulus starts to increase. At this point, fracture or deformation cracking occurs at the macromolecular level. The results of the test are shown in Table S3, Supporting Information. PAC1 and PAM1 have low fracture value which indicates a brittle-type material while the remaining types (AC2, AL1, and AM1) are relatively elastic with high fracture point. These results explain that a solid hydrogel formed from a PEG crosslinker can impart elastic properties to a network structure due to its flexible linear chain. However, a hydrogel formed from only a dendritic and thus globular dPG component, despite its high storage modulus, can easily become brittle due to its hyperbranched structure.

2.3. Hydrogel Characterization and Determination of Encapsulation Efficiency

The model protein streptavidin was used for a proof-of-concept study to investigate the ability of the different hydrogel types which are usable for biosensing applications. Here, the hydrogel formation was tested and characterized by the usage of labeled streptavidin. The fluorescence-labeled streptavidin by Atto 425, a moderately hydrophilic coumarin-based structure with 90% quantum yield and excitation and emission maxima of 436 and 484 nm, respectively, was used for this study. The encapsulation efficiency of a hydrogel could be measured by quantify-

ing the fluorescence intensity of the fluorescent probe. To determine the encapsulation efficiency, a hydrogel with encapsulated fluorescence-labeled streptavidin was incubated overnight with phosphate buffer saline (PBS). The next day, the PBS aliquot on the gel was collected and measured with a fluorescence spectrometer to determine the corresponding intensity (Figure 2b). The detected intensity was calculated using the equation from the standard calibration curve of fluorescence-labeled streptavidin (Figure 2c) to determine the streptavidin concentration, which was later converted to its weight (µg). Once the weight in an aliquot was known, the weight of fluorescence-labeled streptavidin remaining in the hydrogel could be calculated, to obtain the encapsulation efficiency. Factors such as the molar ratio of PEG:dPG, the pH of a mixture, the storage conditions of the PEG-dithiol stock solution, and the gel concentration were screened by using thiol-acrylate gel type to find an optimum for the loading capacity of fluorescence-labeled streptavidin.

First, the encapsulation efficiency was investigated as a function of the different molar ratios of PEG:dPG. The molar ratio of dPG was kept constant while the molar ratio of PEG was increased by 2:1 (AC5), 3:1 (AC6), 5:1 (AC7), 7:1 (AC8), and 9:1 (AC9) of PEG:dPG and 3 µg of streptavidin was added in situ to each replicate sample (see **Table 1**). The encapsulation efficiency results are shown in **Figure 3**a. The AC5 sample exhibits the highest encapsulation efficiency of ≈70%, and the efficiency decreases with increasing PEG ratio. We assumed that the higher the hydrophilic PEG content, the stronger the swelling of the hydrogel occurs, resulting in network loosening and a higher leaching of streptavidin into the PBS aliquot. This assumption

ADVANCED
SCIENCE NEWS
www.advancedsciencenews.com

Macro-
molecular
Chemistry and Physics
www.mcp-journal.de

Table 1. Preparation of different gel types with in situ encapsulation of fluorescence-labeled streptavidin for the determination of encapsulation efficiency from different stock solution of precursors (45% w/v PEG-dithiol 3, 37.6% w/v dPG-acrylate 5, 42.3% w/v dPG-allyl 6, 26.4% w/v dPG-acrylamide 8, 5 mg mL^{-1} LAP). The volume of fluorescence-labeled streptavidin (1 mg mL^{-1}) were added 3 μL in all gel samples which were prepared at the total volume of 38 μL. Thiol-acrylate (AC), thiol-allyl (AL), thiol-acrylamide (AM), pure acrylate (PAC), and pure acrylamide (PAM).

Gel code	PEG		dPG		LAP	PBS	Mole ratio	Mole ratio	Conc.
	Volume [μL]	Mole [μmol]	Volume [μL]	Mole [μmol]	Volume [μL]	Volume [μL]	SH:ene	PEG:dPG	[%w/v]
AC5	6.5	0.49	6.4	0.24	-	22.1	4:6	2:1	14
AC6	9.7	0.73	6.4	0.24	-	18.9	6:6	3:1	18
AC7	16.1	1.21	6.4	0.24	-	12.5	10:6	5:1	25
AC8	22.5	1.69	6.4	0.24	-	6.1	14:6	7:1	33
AC9	28.6	2.14	6.4	0.24	-	0	18:6	9:1	40
AC10	4.7	0.35	4.6	0.17	-	25.7	4:6	2:1	10
AC11	9.3	0.7	9.2	0.34	-	16.5	4:6	2:1	20
AC12	14	1.05	13.6	0.51	-	7.4	4:6	2:1	30
AC13	16.3	1.22	15.9	0.6	-	2.8	4:6	2:1	35
AL2*	9.3	0.7	8.1	0.34	4.2	13.4	4:6	2:1	20
AM2*	9.3	0.7	13	0.34	4.2	8.5	4:5	2:1	20
PAC2*	-	-	20.3	0.76	4.5	10.2	-	-	20
PAM2*	-	-	28.9	0.76	4.5	1.6	-	-	20

*These samples contain 10 mol% LAP (based on PEG 3) and are exposed to 10 min UV.
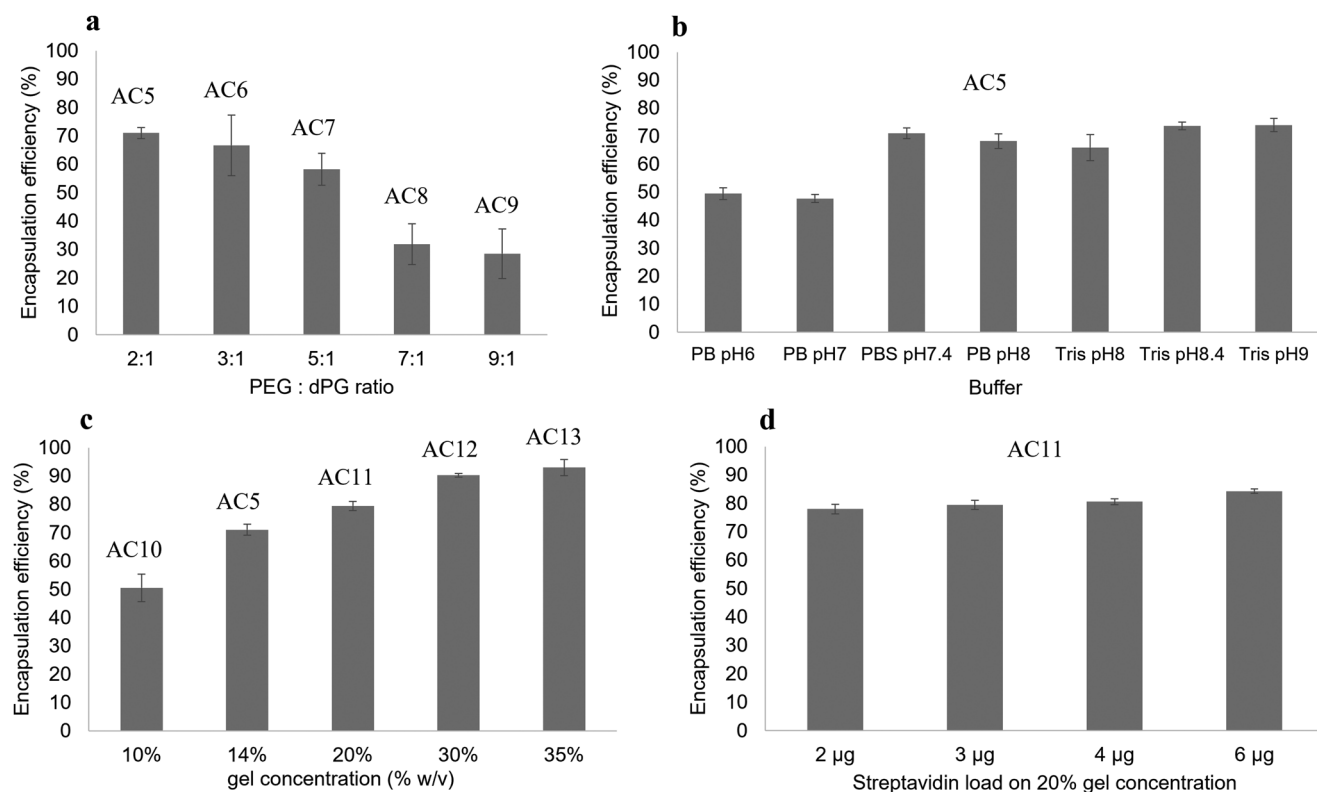
Figure 3. Screening of the encapsulation efficiency based on the variation of different parameters. a) Various molar ratios of PEG:dPG (2:1 [AC5], 3:1 [AC6], 5:1 [AC7], 7:1 [AC8], and 9:1 [AC9] ratio). b) Various biological buffers of gel type AC5. c) Gel concentrations (10% [AC10], 14% [AC5], 20% [AC11], 30% [AC12], and 35% w/v [AC13]). d) Loading of fluorescence-labeled streptavidin of 20% w/v gel concentration (AC11).

**ADVANCED
SCIENCE NEWS**

www.advancedsciencenews.com

Macro-molecular
Chemistry and Physics

www.mcp-journal.de

has been confirmed by the mass swelling ratio (Figure S1, Supporting Information) as the mass swelling ratio increases when increasing the molar ratio of PEG, resulting in enhancing hydrophilicity of the gel system to hold more water content inside a gel matrix. The lowest swelling value was identified from gel AC5 which has a low tendency to wrinkle, suitable for a confined space experiment (in this case, a 2 mL glass vial). This is because a well swelling hydrogel in a confined container expands dramatically in all directions after immersion in aqueous media, resulting in gel stresses, and eventually in wrinkling and cracking.[37,38]

Second, the encapsulation efficiency was studied based on the pH of a gel mixture and the state of the PEG-dithiol stock solution. The pH of hydrogel AC5 was varied from pH 6 to pH 9 using phosphate buffer (PB), PBS, and tris(hydroxymethyl)aminomethane (Tris) buffer solutions. Here, a higher pH of the mixture leads to higher encapsulation efficiency, as a more basic pH promotes thiolate formation,[39,40] that can react more efficiently with the double bond of an acrylate group,[41] leading to denser network formation and ultimately higher encapsulation efficiency (Figure 3b). The efficiency of the PBS pH 7.4 sample appears to be relatively high at 70% efficiency and comparable to those with higher pH values. Therefore, PBS pH 7.4 (physiological pH) solution was used to prepare hydrogels in all follow-up experiments. Furthermore, the storage conditions of PEG-dithiol 3 were studied by gel AC5. In case of PEG stock solution, the efficiency of a two-month-old PEG-dithiol solution stored in the refrigerator (≈4 °C) was comparable to the one with a freshly prepared stock-solution (Figure S2, Supporting Information). The encapsulation efficiency results from both stock solutions showed comparable result, suggesting that a PEG stock solution can be stored for at least two months.

Third, the encapsulation efficiency depended on the hydrogel concentration was conducted. Hydrogels ranging from 10% (AC10), 14% (AC5), 20% (AC11), 30% (AC12) to 35% w/v (AC13) were prepared. The result of the encapsulation efficiency is shown in Figure 3c. As expected, a hydrogel with the highest molar ratio (AC13) shows the highest efficiency as the higher concentration leads to higher crosslink density, thereby entrapping streptavidin in a better way. Gel AC12 and AC13 show comparable results of encapsulation efficiency, but AC10 and AC11 show a gap difference in encapsulation efficiency of almost 30%. Therefore, it is of interest to screen samples at 10% (AC10), 20% (AC11), and 30% w/v (AC12) gel concentrations and calculating their loading capacity factor.

Finally, the encapsulation efficiency was investigated as a function of loading with fluorescence-labeled streptavidin. The labeled Streptavidin was loaded in situ in varying amounts into a hydrogel with concentration of 10% (AC10), 20% (AC11), and 30% w/v (AC12) gel. The results of all gel concentrations show that the efficiency typically increases with an increasing streptavidin loading. However, Gel AC11 and AC12 showed no significant differences in the efficiency (Figures S3 and S4, Supporting Information). From an economic point of view, AC11 with 3 µg streptavidin loading would be a good candidate for further application studies, as it shows comparably high encapsulation efficiency at comparatively low material cost. Furthermore, no gel stress (wrinkle) was spotted for AC11.

In the cases of thiol-allyl and thiol-acrylamide gel types, The LAP photoinitiator, and UV light at a wavelength of 365 nm are required.[42–44] Both AL2 and AM2 hydrogels were tested by two main parameters: the amount of LAP and a UV exposure time. At first, the determination of the stability limit of Atto 425 dye must be performed since a typical fluorescence dye can get exhausted by a long UV exposure time. The resulting intensity of even after 20 min exposure shows no significant difference compared to the non-treated control (Figure S5, Supporting Information).
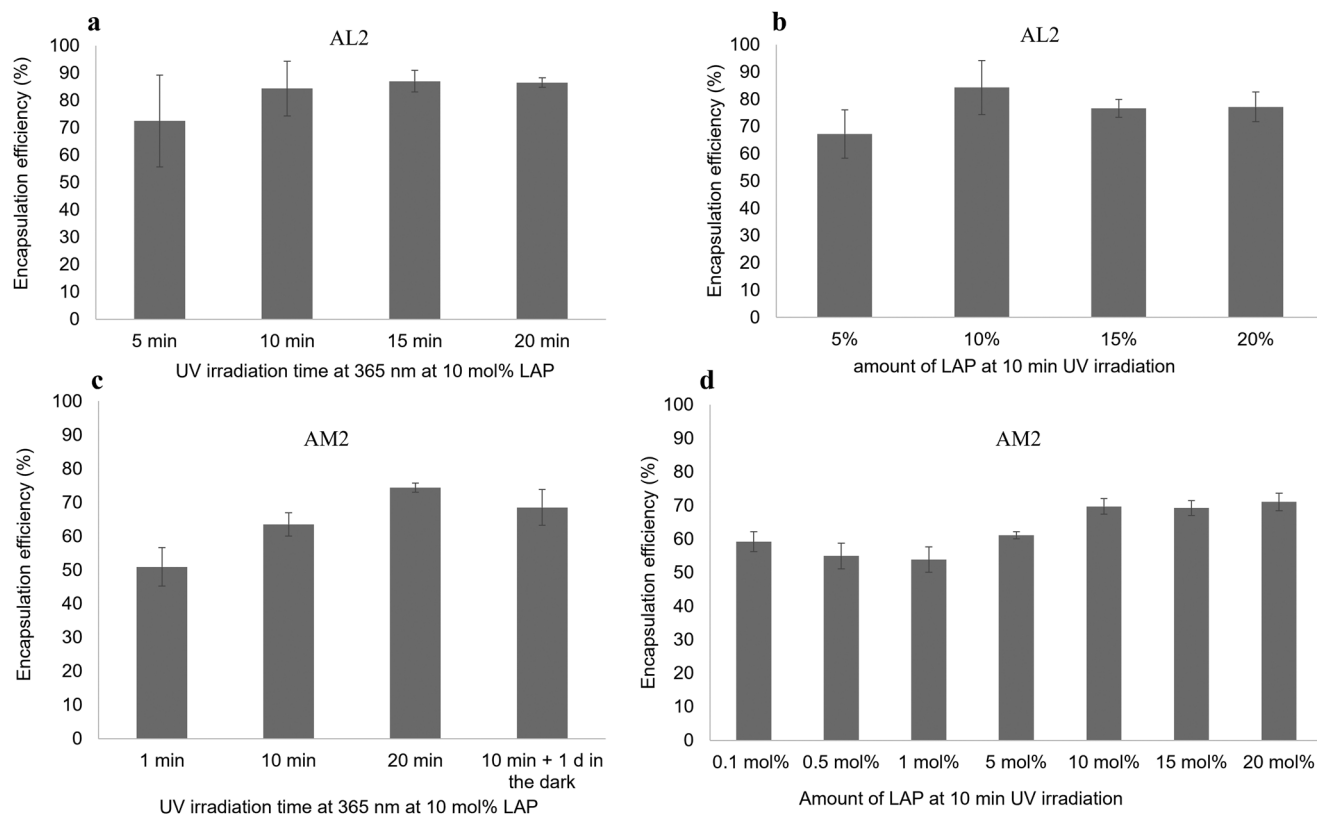
The encapsulation efficiency based on thiol-allyl gel (AL2) was investigated by studying the effect of a UV irradiation time while LAP amount was kept constant. Gel AL2 was exposed to UV light at different time periods from 5 to 20 min. The resulting encapsulation efficiency of a sample at a 10 min exposure seems to be sufficient to achieve high efficiency comparable to the ones with higher exposure times (**Figure 4**a). Besides that, the encapsulation efficiency based on various amount of LAP photo initiator was investigated. Gel AL2 was prepared by different amounts of LAP from 1 to 20 mol% at 10 min UV irradiation. Here, the sample with 10 mol% LAP has a relatively high encapsulation efficiency (≈80%) compared to the samples with 15 mol% and 20 mol% LAP (≈70%) (Figure 4b). However, the sample with 1 mol% LAP did not form a solid hydrogel in the experimental time frame.

Furthermore, encapsulation efficiency studies based on a thiol-acrylamide type hydrogel (AM2) were investigated. Beginning with the various exposure times which were applied to gel AM2 with slightly modified procedure, the 3 samples were incubated with PBS immediately after UV exposure at minute 1, 10, and 20 respectively, while another sample with 10 min exposure was kept at room temperature in the dark overnight before incubation. Interestingly, the encapsulation efficiency of the latter one improved, compared to the one at the same exposure but without a pause, while the others (without a pause) show increased efficiencies with elevated exposure times (Figure 4c). This is because a thiol-acrylamide reaction undergoes not only radical reaction but also addition reaction catalyzed by weak basic condition (pH7.4) as the Michael acceptor is electrophilic enough to be attacked by thiolate group of PEG-dithiol, resulting in the higher crosslink network and the higher efficiency.[41,45,46] Next, the encapsulation efficiency based on different amounts of LAP from 0.1 mol% to 20 mol% was studied at constant exposure time. Unlike thiol-allyl gel type which suffers from chain transfer side reactions,[32–34] thiol-acrylamide gel could form a rigid gel starting from 0.1 mol% LAP (Figure 4d). As expected, increasing amounts of LAP helps to improve the encapsulation efficiency and at 10 mol% LAP, a maximum is reached at 70%. In summary, 10 mol% LAP and a 10 min UV irradiation time are the best conditions to generate the hydrogels of pure acrylate (PAC2) and acrylamide (PAM2) among the screened parameters.

Despite their hard and brittle property, pure acrylate- (PAC2) and acrylamide- (PAM2) type hydrogels were investigated with respect to their encapsulation efficiency. The result shows that the two types of gels have comparable encapsulation efficiencies of 65–70% (Figure S6, Supporting Information).

2.4. Quantification of Accessible Binding Site of Streptavidin

The most important function of the streptavidin surfaces is the specific binding of biotin or biotinylated compounds. This has

Figure 4. Screening of the encapsulation efficiency of AL2 and AM2 gels at different conditions: a) the encapsulation efficiency result of AL2 based on different UV exposure times at 365 nm; b) the encapsulation efficiency of 20% w/v thiol-allyl hydrogel at 10 min UV exposure time based on different amounts of LAP photo initiator; c) the encapsulation efficiency of AM2 gel on different UV exposure times at 365 nm; and d) the encapsulation efficiency of AM2 at 10 min UV exposure time based on different amounts of LAP photo initiator.

been done not only in biosensing to detect the biotinylated compounds, but has also been used to enrich or separate these compounds. Streptavidin has 4 binding sites for biotin, and the sensitivity to biotin could be reduced by blocked or inaccessible binding pocket. Therefore, it is crucial to demonstrate not only the encapsulation efficiency but also the structural integrity as well as accessibility of the binding sites to realize biosensing applications with biotin. For all hydrogel types described above (thiol-acrylate, thiol-allyl, thiol-acrylamide, pure acrylate, and pure acrylamide), the accessible binding sites of streptavidin encapsulated in situ in a hydrogel matrix were determined. To quantify the accessible binding sites, the colorimetric HABA-streptavidin complex was used. HABA (4'-hydroxyazobenzene-2-carboxylic acid) is a dye molecule that has a much lower binding constant to streptavidin than biotin and thus can bind only moderately to the binding site of a streptavidin. The HABA-streptavidin complex shows an absorption maximum at 500 nm, while HABA alone shows an absorption maximum at 350 nm. When biotin is added to a solution of a HABA-streptavidin complex, biotin completely replaces HABA due to the strong binding affinity of streptavidin-biotin, which is superior to that of a HABA-streptavidin complex, resulting in a decrease in the absorption signal at 500 nm. In this experiment, the assay was divided into two parts. The first part was to quantify the binding sites with HABA (HABA assay), and the second part was to quantify the binding sites of the HABA-streptavidin complex with biotin (biotin assay).

In this method, a pure, non-fluorescently labeled streptavidin was encapsulated in situ in a hydrogel matrix (Table S2, Supporting Information). The hydrogel was treated with an excess of HABA solution, incubated overnight, and light absorption was then measured at 500 nm. The positive control was prepared by mixing a streptavidin and HABA solution with the same amount applied to the hydrogel samples. The resulting absorption of all types of hydrogel samples was compared to the value of the positive control, which was set as 4 intact binding sites to obtain the number of accessible binding sites. The result shows that the encapsulated streptavidin has an average of above 3 accessible binding sites as well as high binding capacity in all types of hydrogels (**Table 2**). This means that most of the binding sites of the encapsulated streptavidin are retained and thus accessible for binding with biotin.

Furthermore, quantification of the accessible binding site of encapsulated streptavidin by biotin was performed. In this way, instead of loading streptavidin into a hydrogel, the streptavidin-HABA complex was loaded. Then, an excess of biotin was added and incubated. The control was prepared by mixing HABA and biotin (same amount applied to the hydrogel samples) in the PBS solution. The absorbance was determined at 350 nm as a positive control, fixed at 4 binding sites, since theoretically all HABA molecules can be substituted by biotin and released into the solution. The negative control was performed at a wavelength of 500 nm assuming that no streptavidin-HABA complex

**ADVANCED
SCIENCE NEWS**

www.advancedsciencenews.com

[M] acro-
olecular
Chemistry and Physics

www.mcp-journal.de

Table 2. Number of accessible binding sites of in situ encapsulated streptavidin in all types of hydrogels, tested by HABA/biotin assay.

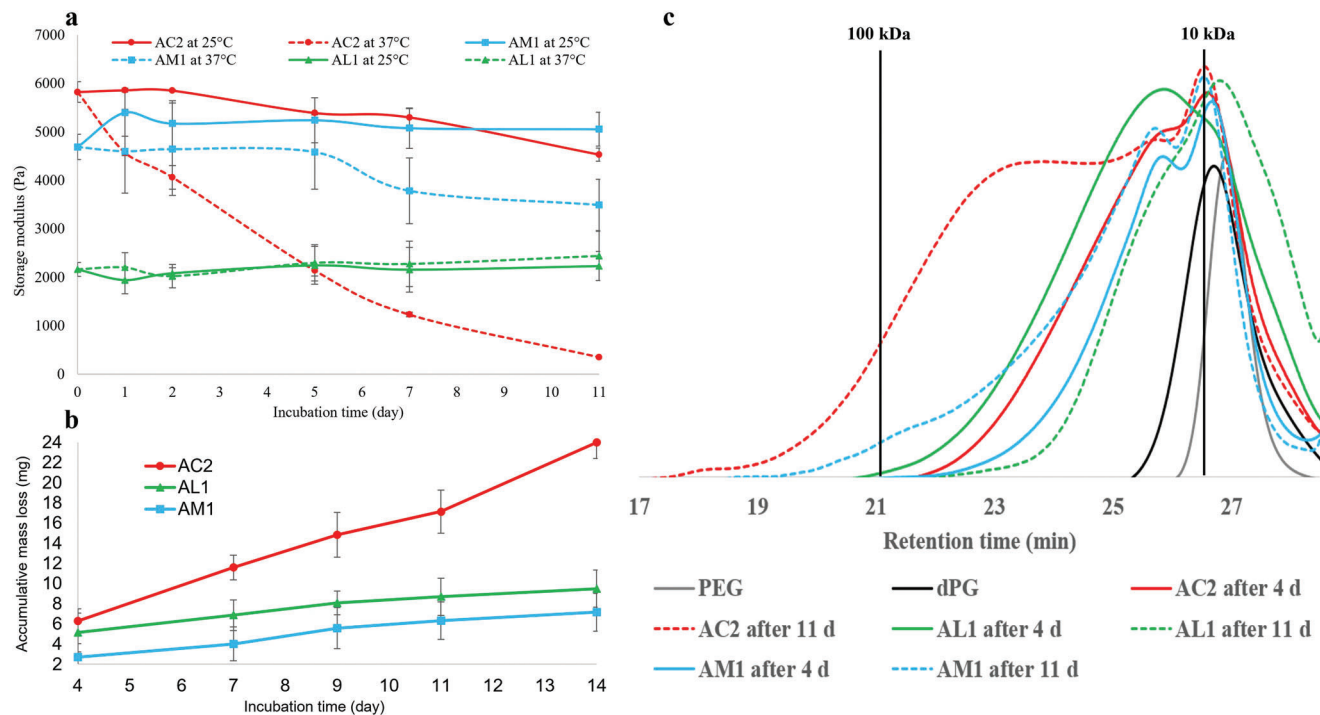| Hydrogel type	Accessible binding sites of encapsulated streptavidin					
	By HABA test			By biotin test		
	No. of Binding sites	SD	Binding capacity (microgram biotin/milliliter gel)	No. of Binding sites	SD	Binding capacity (microgram biotin/milliliter gel)
Thiol-acrylate	3.5	0.1	20.5	4.0	0.1	23.4
Thiol-allyl	3.4	0.1	19.9	3.1	0.1	18.2
Thiol-acrylamide	3.7	0.5	21.6	3.4	0.1	19.9
Pure acrylate	3.2	0.3	18.7	3.0	0.1	17.6
Pure acrylamide	3.1	0.1	18.2	3.1	0.1	18.2
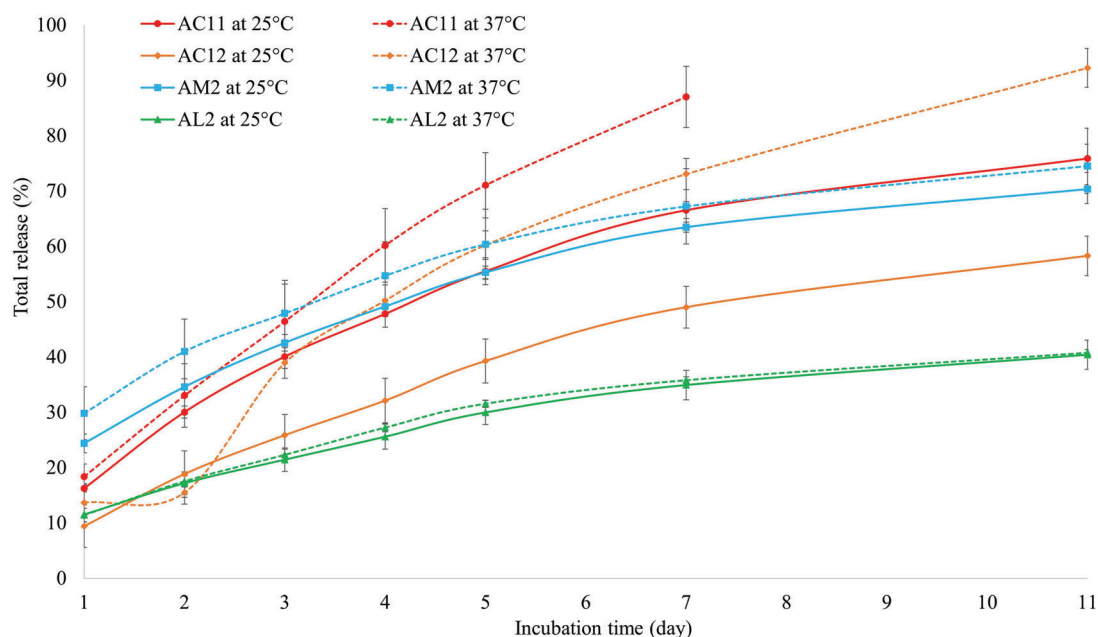
Figure 5. Release study of the in situ encapsulated fluorescence-labeled streptavidin in thiol-acrylate (AC11 and AC12), thiol-allyl (AL2), and thiol-acrylamide (AM2) hydrogels.

remained. The resulting binding sites and binding capacity are relatively similar to the previous experiment (Table 1). It can be concluded that in situ encapsulated-streptavidin hydrogel with different crosslinking chemistry types can retain most of the accessible binding sites (above 3 on average) of streptavidin as well as the binding capacity and can serve as an effective sensing platform for biotin and biotinylated species.

2.5. Kinetic Release Study and Degradation-Stability Test

To broaden the application horizon of this "thiol-click" hydrogel platform, release and stability studies are of interest for many application areas,[47–51] where the controlled release of a biomolecule or a drug has been studied at different temperatures and with different types of hydrogel platforms. In this particular case, the focus was on the stability of the hydrogels. In our study, a fluorophore-labeled streptavidin (Atto 425), was encapsulated in situ in the different hydrogel types, and the release of streptavidin was followed with by fluorescence intensity measurements, similar to the encapsulation efficiency measurement with slight modification. The experiment was performed at 25 and 37 °C, and the incubation time was extended from day 1, 2, 3, 4, 5, 7 to 11. The release of non-covalently immobilized streptavidin was controlled by the macromolecular network (structure and density) of a hydrogel and by non-covalent interactions. Thiol-acrylate (AC11 and AC12), -allyl (AL2), and -acrylamide (AM2) gels were tested. The results show that all samples generally have a tendency to release streptavidin over a longer period of time, especially at a higher temperature in combination with the acrylate-based crosslinking (**Figure 5**). Interestingly, gel AC11 at 37 °C became apparently softened by time and turned to solution in the last day. The reason lies to an ester bond from acrylate group, which was cleaved by hydrolysis, accelerated by high temperature.[52,53] Unlike AC11, gel AC12 with higher crosslink density was rigid enough to resist degradation through the end of the test. Gel AL2, on the

**ADVANCED
SCIENCE NEWS**

www.advancedsciencenews.com

**Macro-
molecular
Chemistry and Physics**

www.mcp-journal.de

Figure 6. Degradation study of thiol-acrylate (AC2), -allyl (AL1), and -acrylamide (AM1) hydrogels. a) Rheological characterization by oscillatory frequency sweep test at 1% strain and storage modulus at 1 Hz. b) Accumulative mass loss at 37 °C. c) Normalized gel permeations chromatogram of the incubated hydrogel samples at day 4 and day 11 at 37 °C in comparison to the precursor PEG and dPG.

other hand, shows slowest release with less than 40% even after 11 days, despite the fact that it has the lowest storage modulus (Figure 2) (or biggest mesh size [Figure S7, Supporting Information]) among them. The reason could come from the London dispersion interaction[54] between the large hydrophobic surface of a streptavidin[55,56] and thiol-allyl crosslinking region which is also hydrophobic, resulting in stable immobilization of streptavidin and slower release. It should be noted that besides the physical network density, the chemistry of the functional groups also has a great influence on the release, as it can be basically degradable or non-degradable.

To analyze the impact of the crosslinking chemistry, a degradation study of acrylate (AC2), allyl (AL1) and acrylamide (AM1) functional groups was performed by 4 main characterization methods: mechanical test by rheology, ^{1}H NMR spectroscopy, mass loss compilation, and molecular weight analysis by gel permeations chromatography (GPC). Starting with mechanical characterization by rheology, the resulting data was picked at 1 Hz in oscillatory frequency sweep test. The decrease of the storage modulus of AC type is obvious and get drastically accelerated at higher temperature as it is shown the clear sign of degradation, while the other types remain steady (**Figure 6**a).

In addition, the accumulative mass loss of AC2, AL1 and AM1 gels was calculated, and an aliquot of the sample was characterized by ^{1}H NMR and GPC. In case of ^{1}H NMR analysis, the water in PBS buffer was replaced by deuterium oxide and this was used for this experiment at only 37 °C to distinguish the unequivocal degradation study. The NMR spectrum of Gel AC2 clearly shows a sign of the higher peak intensity of not only an unreacted acrylate double bond (which was left since less PEG dithiol ratio,

2:1, was used) in the 5.5–7 ppm range, but also the main polymer backbone peaks at 3–4 ppm as well as at the reaction point (the peak of 2.8–2.9 ppm) compared to the others in the longer period (Figure S8, Supporting Information). This probably indicates that a large amount of the gel substances dissolve in the aliquot part, suggesting a degradation product, unlike AL1 and AM1 gels which did not show a signal of degradation as can be seen from the lower peak intensities developed by time. Furthermore, the accumulative mass loss and the GPC results can support the assumption. Accumulative mass loss was measured by accumulatively measuring the dry weight of substance in aliquot part. From the result, the mass loss of AC2 increases noticeably while the ones from gels AL1 and AM1 increase insignificantly slowly (Figure 6b). The degradation product of gel AC2 is further evidenced by the normalized GPC data as seen from the large shoulder peak which appears at almost close to 100 kDa after 11 days (Figure 6c).

3. Conclusions

A scalable thiol-click based hydrogel was constructed by reacting 6 kDa PEG dithiol with 10 kDa dendritic polyglycerol, which was functionalized with 3 different functional groups: acrylate, allyl, or acrylamide. Besides hydrogel characterization studies in terms of gel stability, flexibility and degradability, in situ encapsulated-streptavidin hydrogels were analyzed regarding to their encapsulation efficiency under various physicochemical conditions. Here high efficiencies and high accessible binding sites and binding capacities of streptavidin were found for all gel types. Furthermore, the release study of in situ encapsulated-streptavidin gel

**ADVANCED
SCIENCE NEWS**

www.advancedsciencenews.com

**Macro-
molecular
Chemistry and Physics**

www.mcp-journal.de

over several days was investigated. The encapsulated streptavidin from thiol-acrylate gel type leached out much faster than those from thiol-allyl and -acrylamide gels, due to ester-group degradation, which was experimentally proven by rheology measurements, ^{1}H NMR, GPC and accumulative mass loss experiments.

In conclusion, all hydrogel types performed well as biosensing platforms. Differences in the hydrogel structure and thus in their properties could be used for different applications. Thiol-acrylate based gels have the highest encapsulation efficiency of streptavidin. However, due to their degradability, they are only feasible for biosensing applications with incubations and experimental times of less than 1 day. Acrylate containing hydrogels could further be used for applications requiring their ability to degrade such as wound healing[57] or cell encapsulation,[58] whereas a less or non-degradable alternative, radical-mediated thiol-allyl and thiol-acrylamide based hydrogels could be applied in tissue engineering[30] or bio-ink application[59] where a gel remains stable over a long period of time.

4. Experimental Section

Materials: All chemicals were purchased were purchased from Merck KGaA, Darmstadt, Germany and/or its affiliates and used without any further purification, unless otherwise stated. Diethyl ether (100%) was purchased from VWR chemicals. *N*,*N*-Dimethylformamide (DMF, 99.8%) was purchased from Acros Organics. Triphenylphosphine (99%) was purchased from Alfa Aesar. Sodium hydroxide (pellets), Sodium hydroxide (99.5%), dichloromethane (DCM, 99%) and ethyl acetate were purchased from Fischer Scientific. Micro fluorescence cuvette (ES-Quartz glass) with the optical path length of Optical path length 10×4 mm was purchased from Portmann Instruments. UV bypass filter with 365 nm monochrome light and 49 mm diameter was purchased from Vision Light Tech B.V. The average weight molecular weight of 10 kDa of dPG was prepared as previously reported[60–62] with the improved method.[63]

Instrumentals: All NMR spectra (^{1}H and ^{13}C) were recorded at 300 K by on a Jeol Eclipse 500 MHz (Tokyo, Japan) or a Bruker AVANCE III 700 MHz spectrometer (Billerica, MA, USA). Chemical shifts δ were reported in ppm and the deuterated solvent peak was used as a standard. The elemental assessment was performed by Vario EL CHNS element analyzer by Elementar Analysensysteme GmbH (Langenselbold, Germany). All GPC chromatograms were recorded in water with an Agilent 1100 equipped with an automatic injector, isopump, and Agilent 1100 differential refractometer (Agilent Technologies, Santa Clara, CA, USA). The PSS Suprema (precolumn), 1× with pore size of 30 Å, 2× with pore size of 1000 Å column, was calibrated against Pullulan standards prior to measurements. All fluorescence data were resulted from JASCO FP-6500 spectrometer. The absorbance of the quantification of streptavidin binding site was obtained from a microplate reader (TECAN infinite M200Pro).

Rheology: All the rheology data of hydrogel samples were characterized by Malvern Instruments Kinexus equipped with the parallel plate of 8 mm diameter and the average normal force of estimate 0.1 N at 25 °C. The data were analyzed by an oscillatory frequency sweep strain controlled test with 1% strain (which was obtained from a linear viscoelastic range of an amplitude sweep test) and the reported storage modulus (G′) of a rigid hydrogel were picked at 1 Hz. The rupture point of a hydrogel was determined by oscillatory amplitude sweep test ranging from 1–200% strain at a constant 1 Hz.

Functionalization of PEG(OMs)$_2$ 2: PEG 1 (6 kDa, 20 g, 3.3 mmol, 1 equiv.) was first dried at 70 °C under vacuum overnight. The dried PEG was then purged with Argon gas and cooled down to room temperature and was dissolved in anhydrous DCM (100 mL). Triethylamine (TEA, 2.77 mL, 20 mmol, 6 equiv.) was added to the solution and the reaction flask was then cooled on ice bath. Methanesulfonyl chloride (1.03 mL, 13.3 mmol, 4 equiv.) was added dropwise to the solution and the reac-

tion then was stirred overnight. Afterward the ice bath was removed and the crude product was washed thrice with brine. The DCM layer was then dried with Na$_2$SO$_4$ and concentrated on the rotary evaporator. The concentrated crude was then precipitated in cooled diethyl ether. After being dried overnight under vacuum, the precipitate product results in a white powder with 95% isolated yield. ^{1}H NMR (500 MHz, CDCl$_3$, δ [ppm]): 3.07 (3H, s), 3.48 – 3.78 (m), 4.37 (2H, t) (Figure S9, Supporting Information).

Functionalization of PEG Dithiol 3: Dimesylated PEG 2 (PEG(OMs)$_2$, 19 g, 3.2 mmol, 1 equiv.) was dissolved in 1-propanol (100 mL) and thiourea (1.02 g, 13.3 mmol, 4 equiv.) was then added to the solution. The solution was refluxed overnight to obtain diisothiouronium PEG intermediate. After 1-propanol was removed from the mixture, NaOH (0.53 g, 13.3 mmol, 4 equiv.) and water (100 mL) were added and the solution was then refluxed overnight. Afterward, tris(2-carboxyethyl)phosphine (TCEP, 1.67 g, 6.7 mmol, 2 equiv.) was added and the reaction was run for 2 h. The product was purified by first adding NaCl to the reaction mixture until saturated point, then extracting the product with DCM thrice and drying it with Na$_2$SO$_4$, concentrating the DCM layer and finally precipitating it in cooled diethyl ether. The precipitate was allowed to dry under vacuum overnight to later obtain PEG dithiol product 3 as a pale yellowish powder with an 88% isolated yield. ^{1}H NMR (500 MHz, CDCl$_3$, δ [ppm]): 1.59 (1H, t), 2.69 (2H, quat), 3.48–3.78 (m). Elemental analysis; N 0.13; C 54.24; S 2.02; H 8.47 (Figure S10, Supporting Information).

Functionalization of dPG Acrylate 5: Dried dPG 4 10 kDa (4.94 g, 0.49 mmol, 1 equiv.) was dissolved in DMF (50 mL). The reaction flask was then cooled with ice bath and TEA (0.88 mL, 6.42 mmol, 13 equiv.) was added to the solution. Acryloyl chloride (0.4 mL, 4.94 mmol, 10 equiv., aimed to have ≈5% acrylate functional groups on dPG) was added dropwise to the mixture and the reaction flask was allowed to stir overnight. Afterward, the mixture was concentrated and purified by dialysis by using 2 kDa cutoff benzoylated cellulose dialysis tube in water for 2 d. After the purification, the mixture was concentrated and stocked as an aqueous solution (80% isolated yield). The ^{1}H NMR shows the peaks of double bond and the main backbone peak. The estimate calculation of a number of the functional groups relies on the comparison between the integral of the repeating unit peak which refers to five protons and the integral of the double bond peaks. As for the dPG acrylate 5, the authors assumed that one repeating unit glycidol contains one free hydroxy group. If 100% functionalization happens, it means one repeating unit (five protons) contains one proton peak of the double bond. Thus, the integral of 0.05 of a proton peak refers to 5% acrylate functional group. As aforementioned, one repeating unit glycidol (M_w 74 g mol^{-1}) contains one free OH group. So, in one polymer molecule (M_w 10 000 g mol^{-1}), there were 135 free OH groups by average estimation and dPG acrylate with a 5% functional group corresponding to roughly 6 groups of acrylates. ^{1}H NMR (500 MHz, D$_2$O, δ (ppm)): 0.88 (3H, broad s, initiator backbone), 1.38 (2H, broad s, initiator backbone), 3.44–4.32 (m, backbone repeating units), 6.05 (1H, broad s), 6.26 (1H, broad s) and 6.50 (1H, broad s) (Figure S11, Supporting Information).

Functionalization of dPG Allyl 6: To a DMF (10 mL) solution of dried dPG 4 (0.87 g, 0.087 mmol, 1 equiv.) was added NaH (0.021 g, 0.87 mmol, 10 equiv. aimed for circa 5% allyl functional groups on dPG) and the reaction mixture was run for 1 h at room temperature. The mixture was then cooled down in an ice bath and allyl bromide (0.11 mL, 1.3 mmol, 15 equiv.) was added gradually to the mixture. The reaction was stirred overnight and subjected then to dialysis against water by using 2 kDa cutoff dialysis tube for 2 d. The purified product was concentrated and stocked as an aqueous solution (82% isolated yield). ^{1}H NMR (500 MHz, D$_2$O, δ [ppm]): 0.91 (3H, broad s, initiator backbone), 1.40 (2H, broad s, initiator backbone), 3.34–4.20 (m, backbone repeating units), 5.27 (1H, broad s), 5.35 (1H, broad s) and 5.99 (1H, broad s) (Figure S12, Supporting Information).

Functionalization of dPG Amine 7: Dried dPG 4 (5 g, 0.5 mmol, 1 equiv.) was dissolved in DMF (50 mL) and to a solution of dPG was added TEA (0.9 mL, 6.5 mmol, 13 equiv.). The reaction flask was then cooled down with ice bath and methanesulfonyl chloride (0.39 mL, 5 mmol, 10 equiv. aimed for roughly 5% mesyl groups on dPG) was later added dropwise. The solution was allowed to run overnight. Afterward, NaN$_3$ (0.65 g,

**ADVANCED
SCIENCE NEWS**

www.advancedsciencenews.com

**Macro-
molecular
Chemistry and Physics**

www.mcp-journal.de

10 mmol, 20 equiv.) was added to the mixture and it was then stirred and heated up at 60 °C for 2 d. Later the crude mixture was subjected to dialysis with 2 kDa cutoff tube against water for 2 d. Then the crude product was lyophilized and collected as a viscous sticky liquid. Afterward, to the DMF (40 mL) solution of crude dPG azide was added the tetrahydrofuran (THF, 30 mL) solution of triphenylphosphine (3.28 g, 12.5 mmol, 25 equiv.) and the mixture was maintained in clear solution and stirred overnight. Later water (5 mL) was added to the solution and the mixture was allowed to stir overnight. The purification was then taken place by first washing the mixture with DCM followed by ethyl acetate, and then dialyzing the aqueous crude with 2 kDa cutoff tube against water for 2 d. The purified aqueous product was subsequently concentrated and lyophilized overnight, resulted in pale yellowish honey-like liquid (70% isolated yield). ^{1}H NMR (700 MHz, D$_2$O, δ [ppm]): 0.90 (3H, broad s, initiator backbone), 1.39 (2H, broad s, initiator backbone), and 2.73–4.02 (m, backbone repeating units), (Figure S13, Supporting Information). ^{13}C NMR (700 MHz, D$_2$O, δ [ppm]): 43.1 (s, 2nd CH$_2$-NH$_2$), 60.9–79.8 (m, polymer backbone) (Figure S14, Supporting Information).

Quantification of an Amino Group on dPG Amine (dPG NH(Boc)): The amino functionalized dPG can be quantified by ^{1}H NMR end-group analysis. dPG amine 7 was reacted with excess of di-*tert*-butyl dicarbonate ((Boc)$_2$O) and then purified by dialysis against water, resulting in dPG NH(Boc), after ^{1}H NMR characterization, the integral of tert-butyloxycarbonyl (Boc) group was related to the integral of the dPG backbone, resulting in 4% amine functional groups. ^{1}H NMR (500 MHz, D$_2$O, δ [ppm]): 0.86 (3H, broad s, initiator backbone), 1.42 (9H, s), 3.12–4.06 (m, backbone repeating units), (Figure S15, Supporting Information).

Functionalization of dPG Acrylamide 8: To a DMF (10 mL) solution of dPG amine 7 (1 g, 0.1 mmol, 1 equiv.) was added TEA (0.21 mL, 1.5 mmol, 15 equiv.) and the reaction mixture was cooled down in an ice bath. Then acryloyl chloride (0.1 mL, 1.2 mmol, 12 equiv.) was added dropwise to the reaction mixture and it was allowed to run overnight. Afterward, water 10 mL was added to the mixture and the pH was adjusted to pH 9 and it was stirred at 50 °C for 2 h. then the mixture was purified by dialysis with 2 kDa cutoff tube against water for 2 d. the dialyzed product was concentrated and collected as a pale yellowish aqueous solution (79% isolated yield). ^{1}H NMR (500 MHz, D$_2$O, δ (ppm)): 0.7 (3H, broad s, initiator backbone), 1.19 (2H, broad s, initiator backbone), 3.17–3.89 (m, backbone repeating units), 5.61 (1H, broad s), 6.04 (1H, broad s) and 6.11 (1H, broad s) (Figure S16, Supporting Information).

General Procedure of Encapsulation Efficiency Test: To prepare the test with sample AC11, PEG dithiol 3 (in PBS solution, 0.7 μmol, 9.3 μL), dPG acrylate 5 (0.34 μmol, 9.2 μL), fluorescence-labeled streptavidin (in PBS solution, 3 μg, 3 μL) and PBS (16.5 μL) were mixed according to the Table 1. The mixture was left at room temperature in the dark overnight. Then 700 μL PBS was added on top of the gel and it was incubated at room temperature overnight in the dark with shaking. Afterward, the volume of an aliquot on top of the gel was measured and determined by fluorescence spectroscopy. The fluorescence intensity was then calculated to quantify the amount of streptavidin staying in the solution and the one left inside the gel. This protocol was applied to all hydrogel samples except the study of UV exposure time of gel AM2.

Quantification of Accessible Binding Site of Encapsulated Streptavidin by HABA: The determination of the binding site of the streptavidin encapsulated in thiol-acrylate, thiol-allyl or thiol-acrylamide hydrogels were in the same manner. To quantify the binding site of streptavidin encapsulated thiol-acrylate hydrogel (20% w/v, 38 μL, 2:1 mole ratio of PEG:dPG), PEG dithiol 3 (in PBS solution, 0.7 μmol, 9.3 μL), dPG acrylate 5 (0.34 μmol, 9.2 μL), non-labeled streptavidin (in PBS solution, 50 μg, 12.5 μL), and PBS (7 μL) were mixed. In case of thiol-allyl and thiol-acrylamide hydrogels, a mixture (with additional 10 mol% of LAP added) was subjected to 365 nm UV light for 10 min. Then all samples were placed in the dark at room temperature overnight. To each sample was subsequently added PBS (150 μL) and HABA (1 μg, 1 μL) and all samples were subsequently incubated with shaking at room temperature overnight. Afterward, the UV absorbance of HABA-streptavidin complex of each sample was measured at 500 nm.

Quantification of Accessible Binding Site of Encapsulated Streptavidin by Biotin: The binding site of encapsulated streptavidin of each gel type can be determined in the similar way. To quantify the binding site of streptavidin encapsulated thiol-acrylate hydrogel (20% w/v, 38 μL, 2:1 mole ratio of PEG:dPG), PEG dithiol 3 (in PBS solution, 0.7 μmol, 9.3 μL), dPG acrylate 5 (0.34 μmol, 9.2 μL), HABA-Streptavidin complex (in PBS solution, 50 μg, 12.5 μL), and PBS (7 μL) were mixed. The sample was placed in the dark overnight. PBS (150 μL) and biotin (5 μg, 5 μL) were then added to the sample and it was shaken and incubated at room temperature overnight. In the next day, the UV absorbance of biotin was measured at 350 nm.

Calculation of the Mesh Size of a Hydrogel: The mesh size of the thiol-acrylate (AC2), -allyl (AL1), and -acrylamide (AM1) hydrogels at 20%w/v and 2:1 mole ratio was directly calculated from the storage modulus value received from oscillatory frequency sweep test at 1 Hz shown on Figure 2. A mesh size can be calculated from the classical theory of rubber elasticity as shown below:[47,64,65]

$$r = \left(\frac{6RT}{\pi N_{AV} G} \right)^{\frac{1}{3}} \tag{1}$$

where r is mesh size (nm), R is gas constant (8.314 m^3·Pa·K^{-1}·mol^{-1}), T is temperature (K), π is Pi constant (3.142), N_{AV} is Avogadro's number (6.022 × 10^{23} mol^{-1}), and G is storage shear modulus (Pa). The resulting mesh size is shown in Figure S7, Supporting Information.

Preparation of an In Situ Encapsulated-Streptavidin Hydrogel for the Release Study: The preparation of a release study is similar to the experiment of encapsulation efficiency but has differences in the period of time of incubation and the washing. All samples were prepared according to the Table 1. Thiol-allyl (AL2) and -acrylamide (AM2) gels were exposed to UV light at 365 nm for 10 min. All samples were then incubated with 600 μL PBS solution from day 1 till day 11. The aliquot was collected at day 1, 2, 3, 4, 5, 7 and 11 and each time after the fluorescence intensity of an aliquot was measured, the taken aliquot was replenished with 600 μL fresh PBS solution to the respective hydrogel sample to be incubated until the next collection time. After the calculation, the percentage of release was reported as total release as it was summed from the beginning to the end of the measurement.

Preparation of a Hydrogel for the Degradation Study: Thiol-acrylate (AC2), -allyl (AL1), and -acrylamide (AM1) hydrogels were prepared according to Table S2, Supporting Information. After the gel was settled overnight, the gel was removed from the mold and put to the bigger container. A 600 μL phosphate-buffered saline (PBS) solution was then put to the container and it was incubated for 11 days. The gel strength was measured at day 1, 2, 5, 7, and 11 by the rheometer with the condition mentioned earlier at 25 and 37 °C. In the case of a degradation study by NMR, gel permeation chromatography (GPC) and mass loss experiments, all the samples were prepared in the similar manner but had a difference in using deuteron PBS which was prepared by lyophilizing the normal PBS solution and then redissolving back in the same volume with D$_2$O. The incubation was run at 37 °C for 14 days and the aliquot was collected and determined by ^{1}H NMR at day 4, 7, 9, 11, and 14. Each collected aliquot was later lyophilized and weighted to be calculated as a dry mass of a gel fragment which was found in the aliquot for mass loss experiment. The lyophilized aliquot at day 4 and day 11 of each sample was later determined by GPC.

Supporting Information

Supporting Information is available from the Wiley Online Library or from the author.

Conflict of Interest

The authors declare no conflict of interest.

Data Availability Statement

The data that support the findings of this study are available in the supplementary material of this article.

Keywords

3D hydrogels, encapsulation efficiency, release and degradation study, streptavidin, thiol-click chemistry

[1] A. Herrmann, R. Haag, U. Schedler, *Adv. Healthcare Mater.* **2021**, *10*, 2100062.

[2] A. Herrmann, L. Kaufmann, P. Dey, R. Haag, U. Schedler, *ACS Appl. Mater. Interfaces* **2018**, *10*, 11382.

[3] P. C. Weber, D. H. Ohlendorf, J. J. Wendoloski, F. R. Salemme, *Science* **1989**, *243*, 85.

[4] S. K. Avrantinis, R. L. Stafford, X. Tian, G. A. Weiss, *ChemBioChem* **2002**, *3*, 1229.

[5] F. Liu, J. Z. H. Zhang, Y. Mei, *Sci. Rep.* **2016**, *6*, 27190.

[6] P. H. E. Hamming, J. Huskens, *ACS Appl. Mater. Interfaces* **2021**, *13*, 58114.

[7] L. Välimaa, K. Pettersson, M. Vehniäinen, M. Karp, T. Lövgren, *Bioconjugate Chem.* **2003**, *14*, 103.

[8] J. M. Alonso, A. Reichel, J. Piehler, A. del Campo, A. del Campo, *Langmuir* **2008**, *24*, 448.

[9] R. D'Agata, P. Palladino, G. Spoto, *Beilstein J. Nanotechnol.* **2017**, *8*, 1.

[10] S. Li, H. Liu, N. He, *J. Nanosci. Nanotechnol.* **2010**, *10*, 4875.

[11] Y. Maeda, T. Yoshino, M. Takahashi, H. Ginya, J. Asahina, H. Tajima, T. Matsunaga, *Appl. Environ. Microbiol.* **2008**, *74*, 5139.

[12] J. Pivetal, F. M. Pereira, A. I. Barbosa, A. P. Castanheira, N. M. Reis, A. D. Edwards, *Analyst* **2017**, *142*, 959.

[13] A. Jo, R. Zhang, I. C. Allen, J. S. Riffle, R. M. Davis, *Langmuir* **2018**, *34*, 15783.

[14] A. Hennig, P. M. Dietrich, F. Hemmann, T. Thiele, H. Borcherding, A. Hoffmann, U. Schedler, C. Jäger, U. Resch-Genger, W. E. S. Unger, *Analyst* **2015**, *140*, 1804.

[15] M.-Y. Hong, Y.-J. Kim, J. W. Lee, K. Kim, J.-H. Lee, J.-S. Yoo, S.-H. Bae, B.-S. Choi, H.-S. Kim, *J. Colloid Interface Sci.* **2004**, *274*, 41.

[16] P. Dey, M. Adamovski, S. Friebe, A. Badalyan, R.-C. Mutihac, F. Paulus, S. Leimkühler, U. Wollenberger, R. Haag, *ACS Appl. Mater. Interfaces* **2014**, *6*, 8937.

[17] K. Awsiuk, P. Petrou, A. Thanassoulas, J. Raczkowska, *Langmuir* **2019**, *35*, 3058.

[18] X. Duan, Y. Li, N. K. Rajan, D. A. Routenberg, Y. Modis, M. A. Reed, *Nat. Nanotechnol.* **2012**, *7*, 401.

[19] F. Reisbeck, S. Wedepohl, M. Dimde, A.-C. Schmitt, J. Dernedde, M. Álvaro-Benito, C. Freund, R. Haag, *J. Mater. Chem. B* **2021**, *10*, 96.

[20] R. Randriantsilefisoa, J. L. Cuellar-Camacho, M. S. Chowdhury, P. Dey, U. Schedler, R. Haag, *J. Mater. Chem. B* **2019**, *7*, 3220.

[21] W. Liang, S. Bhatia, F. Reisbeck, Y. Zhong, A. K. Singh, W. Li, R. Haag, *Adv. Funct. Mater.* **2021**, *31*, 2010630.

[22] C. E. Ziegler, M. Graf, M. Nagaoka, H. Lehr, A. M. Goepferich, *Biomacromolecules* **2021**, *22*, 3223.

[23] A. Oehrl, S. Schötz, R. Haag, *Macromol. Rapid Commun.* **2020**, *41*, 1900510.

[24] J. J. Roberts, S. J. Bryant, *Biomaterials* **2013**, *34*, 9969.

[25] A. A. Aimetti, A. J. Machen, K. S. Anseth, *Biomaterials* **2009**, *30*, 6048.

[26] C. E. Hoyle, A. B. Lowe, C. N. Bowman, *Chem. Soc. Rev.* **2010**, *39*, 1355.

[27] C. E. Hoyle, C. N. Bowman, *Angew. Chem., Int. Ed.* **2010**, *49*, 1540.

[28] S. H. Mahadevegowda, M. C. Stuparu, *Eur. J. Org. Chem.* **2017**, *2017*, 570.

[29] S. Roller, H. Zhou, R. Haag, *Mol. Diversity* **2005**, *9*, 305.

[30] D. L. Elbert, J. A. Hubbell, *Biomacromolecules* **2001**, *2*, 430.

[31] N. Hammer, F. P. Brandl, S. Kirchhof, V. Messmann, A. M. Goepferich, *Macromol. Biosci.* **2015**, *15*, 405.

[32] R. C. Laible, *Chem. Rev.* **1958**, *58*, 807.

[33] S. J. Oh, D. R. Kinney, W. Wang, P. L. Rinaldi, *Macromolecules* **2002**, *35*, 2602.

[34] M. B. Larsen, S.-J. Wang, M. A. Hillmyer, *J. Am. Chem. Soc.* **2018**, *140*, 11911.

[35] F. Dénès, M. Pichowicz, G. Povie, P. Renaud, *Chem. Rev.* **2014**, *114*, 2587.

[36] I. Degirmenci, M. L. Coote, *J. Phys. Chem. A* **2016**, *120*, 1750.

[37] M. A. Blot, *Appl. Sci. Res., Sect. A* **1963**, *12*, 168.

[38] V. Trujillo, J. Kim, R. C. Hayward, *Soft Matter* **2008**, *4*, 564.

[39] D. Bermejo-Velasco, A. Azémar, O. P. Oommen, J. Hilborn, O. P. Varghese, *Biomacromolecules* **2019**, *20*, 1412.

[40] I. M. Kolthoff, W. Stricks, R. C. Kapoor, *J. Am. Chem. Soc.* **1955**, *77*, 4733.

[41] D. P. Nair, M. Podgórski, S. Chatani, T. Gong, W. Xi, C. R. Fenoli, C. N. Bowman, *Chem. Mater.* **2014**, *26*, 724.

[42] A. K. Nguyen, P. L. Goering, V. Reipa, R. J. Narayan, *Biointerphases* **2019**, *14*, 021007.

[43] J. S. Ribeiro, A. Daghrery, N. Dubey, C. Li, L. Mei, J. C. Fenno, A. Schwendeman, Z. Aytac, M. C. Bottino, *Biomacromolecules* **2020**, *21*, 3945.

[44] J. D. Mccall, K. S. Anseth, *Biomacromolecules* **2012**, *13*, 2410.

[45] M. Porel, J. S. Brown, C. A. Alabi, *Synlett* **2015**, *26*, 565.

[46] J. S. Brown, A. W. Ruttinger, A. J. Vaidya, C. A. Alabi, P. Clancy, *Org. Biomol. Chem.* **2020**, *18*, 6364.

[47] J. Li, D. J. Mooney, *Nat. Rev. Mater.* **2016**, *1*, 16071.

[48] T. Shirakura, T. J. Kelson, A. Ray, A. E. Malyarenko, R. Kopelman, *ACS Macro Lett.* **2014**, *3*, 602.

[49] G. W. Ashley, J. Henise, R. Reid, D. V. Santi, *Proc. Natl. Acad. Sci. USA* **2013**, *110*, 2318.

[50] A. Puiggalí-Jou, E. Cazorla, G. Ruano, I. Babeli, M.-P. Ginebra, J. García-Torres, C. Alemán, *ACS Biomater. Sci. Eng.* **2020**, *6*, 6228.

[51] S. Sheth, E. Barnard, B. Hyatt, M. Rathinam, S. P. Zustiak, *Front. Bioeng. Biotechnol.* **2019**, *7*, 410.

[52] X. Tong, J. Lai, B.-H. Guo, Y. Huang, *J. Polym. Sci., Part A: Polym. Chem.* **2011**, *49*, 1513.

[53] A. Metters, J. Hubbell, *Biomacromolecules* **2005**, *6*, 290.

[54] J. P. Wagner, P. R. Schreiner, *Angew. Chem., Int. Ed.* **2015**, *54*, 12274.

[55] D. Shao, K. Tapio, S. Auer, J. J. Toppari, V. P. Hytönen, M. Ahlskog, *Langmuir* **2018**, *34*, 15335.

**ADVANCED
SCIENCE NEWS**

www.advancedsciencenews.com

Macro-molecular
Chemistry and Physics

www.mcp-journal.de

[56] I. Le Trong, N. Humbert, T. R. Ward, R. E. Stenkamp, *J. Mol. Biol.* **2006**, *356*, 738.

[57] Q. Xu, L. Guo, S. A, Y. Gao, D. Zhou, U. Greiser, J. Creagh-Flynn, H. Zhang, Y. Dong, L. Cutlar, F. Wang, W. Liu, W. Wang, W. Wang, *Chem. Sci.* **2018**, *9*, 2179.

[58] X. Li, S. A, Q. Xu, F. Alshehri, M. Zeng, D. Zhou, J. Li, G. Zhou, W. Wang, *ACS Appl. Bio Mater.* **2020**, *3*, 4756.

[59] S. Stichler, T. Jungst, M. Schamel, I. Zilkowski, M. Kuhlmann, T. Böck, T. Blunk, J. Teßmar, J. Groll, *Ann. Biomed. Eng.* **2017**, *45*, 273.

[60] R. Haag, A. Sunder, J.-F. Stumbé, *Angew. Chem., Int. Ed* **1996**, *38*, 17.

[61] A. Sunder, R. Hanselmann, H. Frey, R. Mülhaupt, *Macromolecules* **1999**, *32*, 4240.

[62] H. Frey, R. Haag, *Rev. Mol. Biotechnol.* **2002**, *90*, 257.

[63] M. Wallert, J. Plaschke, M. Dimde, V. Ahmadi, S. Block, R. Haag, *Macromol. Mater. Eng.* **2021**, *306*, 2000688.

[64] A. J. Kuijpers, G. H. M. Engbers, J. Feijen, S. C. De Smedt, T. K. L. Meyvis, J. Demeester, J. Krijgsveld, S. A. J. Zaat, J. Dankert, *Macromolecules* **1999**, *32*, 3325.

[65] K. S. Anseth, C. N. Bowman, L. Brannon-Peppas, *Biomaterials* **1996**, *17*, 1647.

Thiol-Click Based Polyglycerol Hydrogels as Biosensing Platform with In Situ Encapsulated Streptavidin Probes

Boonya Thongrom, Mathias Dimde, Uwe Schedler* and Rainer Haag*

Thiol-Click Based Polyglycerol Hydrogels as Biosensing Platform with *in situ* Encapsulated Streptavidin Probe

Boonya Thongrom, Mathias Dimde, Uwe Schedler, and Rainer Haag**

Table S1. Gelation screening of thiol-acrylate hydrogel which is based on the mole ratio of PEG:dPG.

PEG dithiol (µmol)	dPG acrylate (µmol)	Ratio of PEG:dPG	Concentration (%w/v)	Solid gel formation
0.45	1.37	1:3	14	not solid
0.59	1.78	1:3	19	not solid
0.69	2.11	1:3	22	not solid
0.67	1.37	1:2	16	not solid
0.87	1.78	1:2	20	not solid
1.03	2.11	1:2	24	not solid
0.30	0.30	1:1	4	yes
0,60	0.30	2:1	6	yes
0.90	0.30	3:1	7	yes
1.58	0.30	5:1	11	yes
2.23	0.30	7:1	14	yes
2.87	0.30	9:1	18	yes

Table S2. Preparation of different gel types for the flexibility and fraction point test and determination of accessible binding site of encapsulated streptavidin from different stock solution of precursors (45% w/v PEG dithiol, 42.3% w/v dPG allyl, 5 mg/mL LAP, 4 mg/mLStreptavidin/Streptavidin HABA complex).

Gel type	Gel code	PEG		dPG		LAP	PBS	Strep /Strep-HABA	Mole ratio	Conc.
		Volume (µL)	Mole (µmol)	Volume (µL)	Mole (µmol)	Volume (µL)	Volume (µL)	(µL)	PEG:dPG	(% w/v)
Thiol-acrylate	AC1[#]	19.5	1.46	19.2	0.72	-	75.3	-	2:1	14
Thiol-acrylate	AC2[#]	27.9	2.09	24.3	1.03	-	58.8	-	2:1	20
Thiol-acrylate	AC3[#]	38.1	2.86	15	0.56	-	60.9	-	5:1	20
Thiol-acrylate	AC4[#]	41.1	3.08	11.7	0.44	-	61.2	-	7:1	20
Thiol-allyl	AL1	27.9	2.09	24.3	1.03	12.4	49.4	-	2:1	20
Thiol-acrylamide	AM1[#]	27.9	2.09	39	1.03	12.4	34.7	-	2:1	20
Pure acrylate	PAC1[#]	-	-	60.9	2.29	13.5	39.6	-	-	20
Pure acrylamide	PAM1[#]	-	-	86.7	2.29	13.5	13.8	-	-	20
Thiol-acrylate	AC14*	9.4	0.7	8.1	0.34	-	8	12.5	2:1	20
Thiol-allyl	AL3	8.2	0.7	9.3	0.34	4.2	3.8	12.5	2:1	20
Thiol-acrylamide	AM3*	9	0.7	9.3	0.34	4.2	3	12.5	2:1	20
Pure acrylate	PAC3*	-	-	18.1	0.76	4.5	2.9	12.5	-	20
Pure acrylamide	PAM3*	-	-	19.9	0.76	4.5	1.1	12.5	-	20

[#]prepared from 37.6% w/v dPG acrylate, 26.4% w/v dPG acrylamide

*prepared from 42% w/v dPG acrylate, 38.4% w/v dPG acrylamide

Table S3. Fracture point test of each hydrogel types performed by oscillatory amplitude sweep test at 1 – 200% stain, 1 Hz and 25 °C.

| Sample	Fracture point	SD	Results

| AC2 | 118% strain | 21.6 | Elastic |
AL1	>200% strain	n.a.	Elastic
AM1	>200% strain	n.a.	Elastic
PAC1	32% strain	7.5	hard but brittle
PAM1	9% strain	9.3	hard but brittle
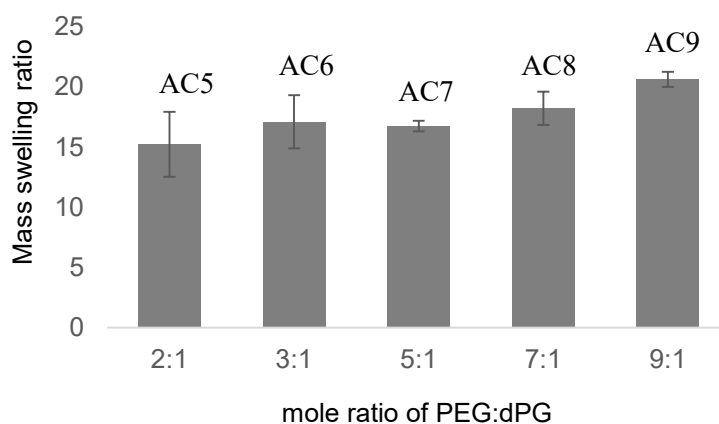
Figure S1. Mass swelling ratio of thiol-acrylate hydrogel based on the different ratios of PEG:dPG sample (**AC5** – **AC9** respectively).
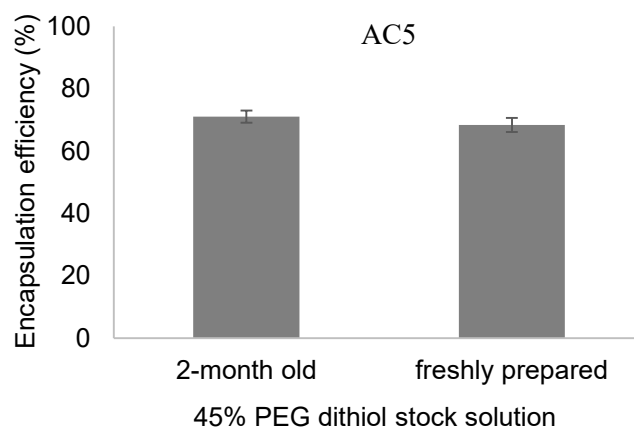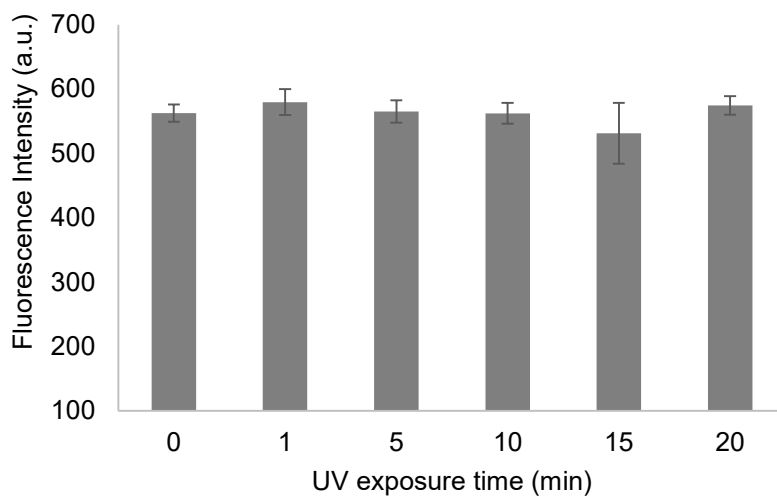

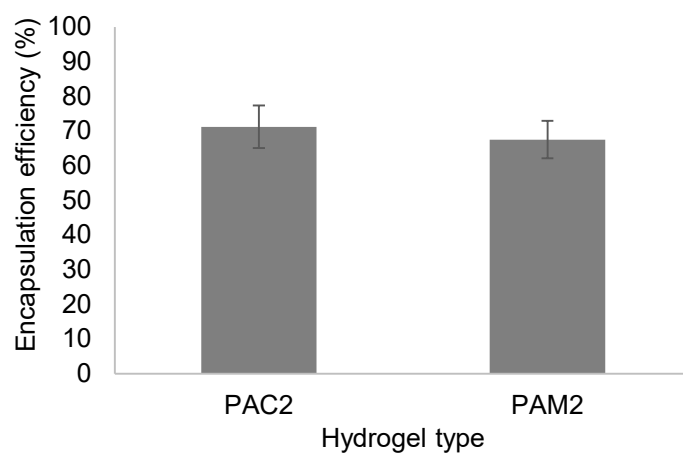**Figure S2.** Encapsulation efficiency of 14% w/v thiol-acrylate hydrogel (**AC5**) based on the storage condition of PEG dithiol stock solution.
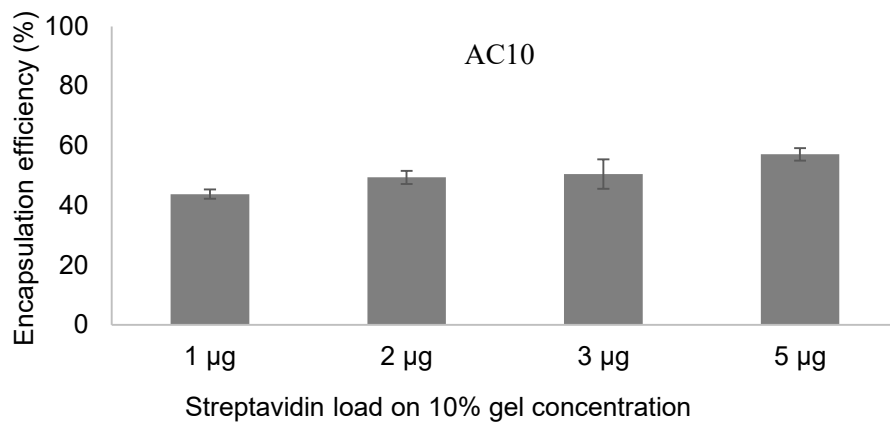
Figure S3. Encapsulation efficiency based on the loading of streptavidin Atto 425 at 10% w/v gel concentration.
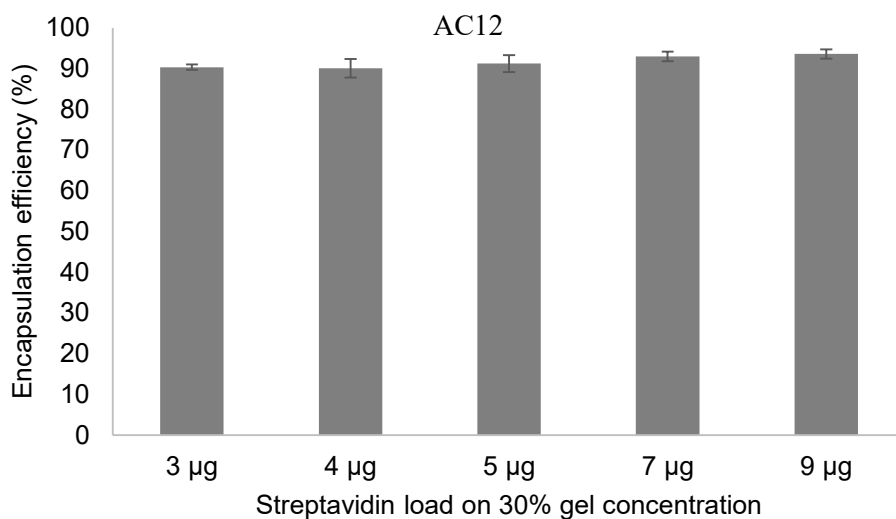
Figure S4. Encapsulation efficiency based on the loading of streptavidin Atto 425 at 30% w/v gel concentration.
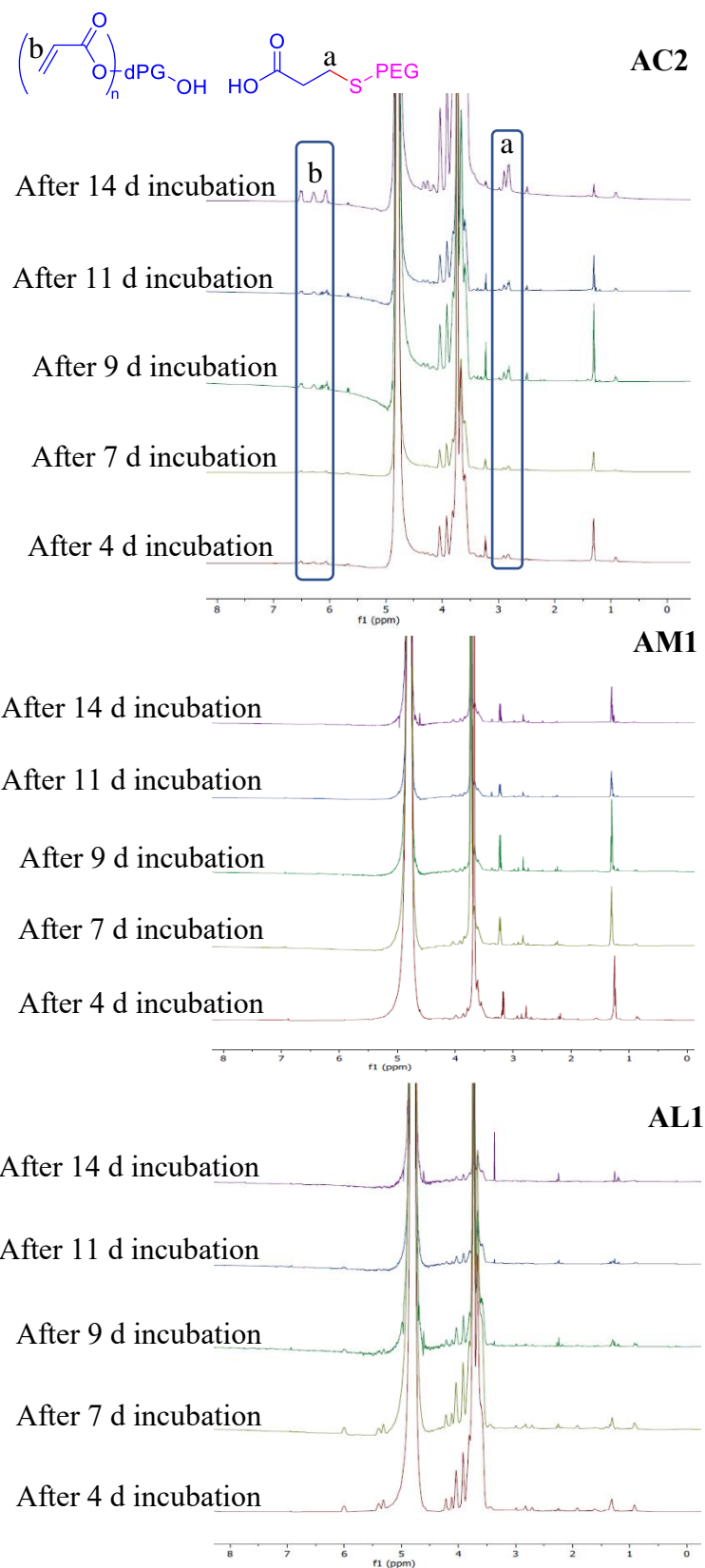
Figure S6. Encapsulation efficiency of pure acrylate (PAC2) and acrylamide (PAM2) type hydrogels at 10 min UV exposure at 365 nm.
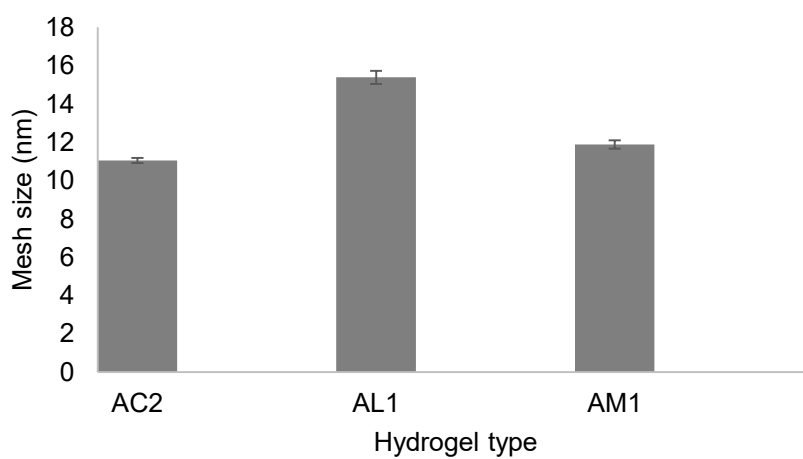
Figure S7. Mesh size, which is calculated by the storage modulus at 1 Hz from frequency sweep test at 25 °C, of three different types of hydrogels, thiol-acrylate (AC2), -allyl (AL1) and -acrylamide (AM1).
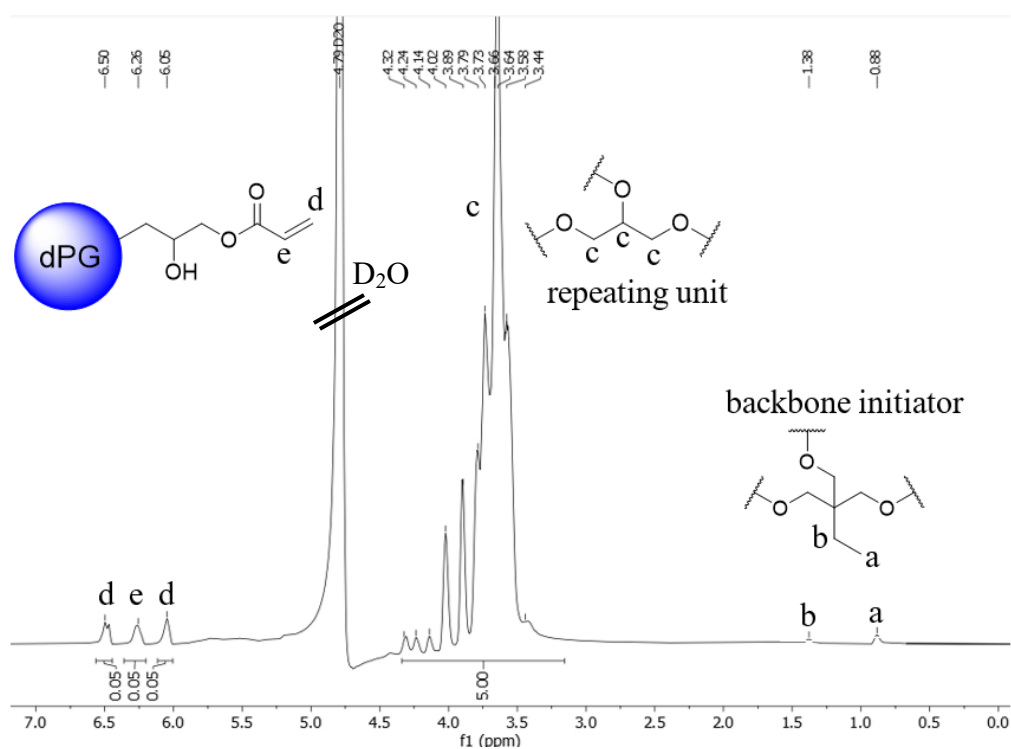
Figure S8. ^{1}H NMR spectra of the aliquot of 20% w/v thiol-acrylate (**AC2**), -acrylamide (**AM1**) and -allyl (**AL1**) hydrogel samples after 4,7,9,11 and 14 days of incubation at 37 °C.
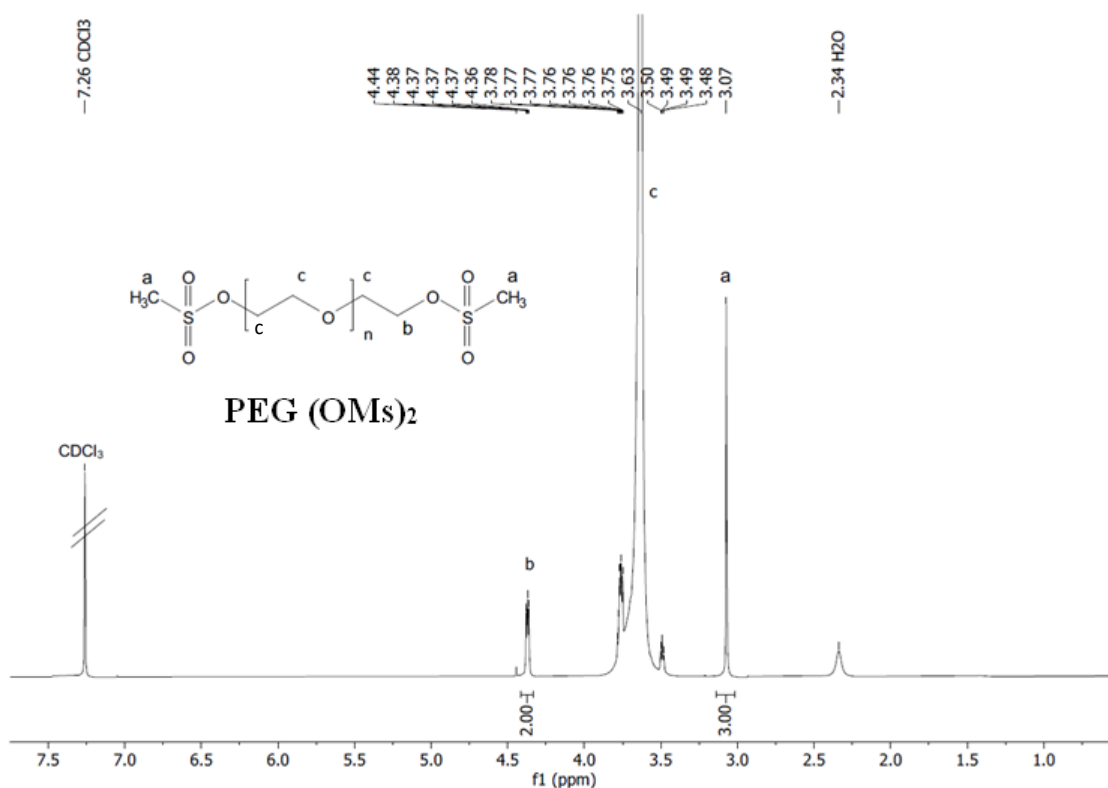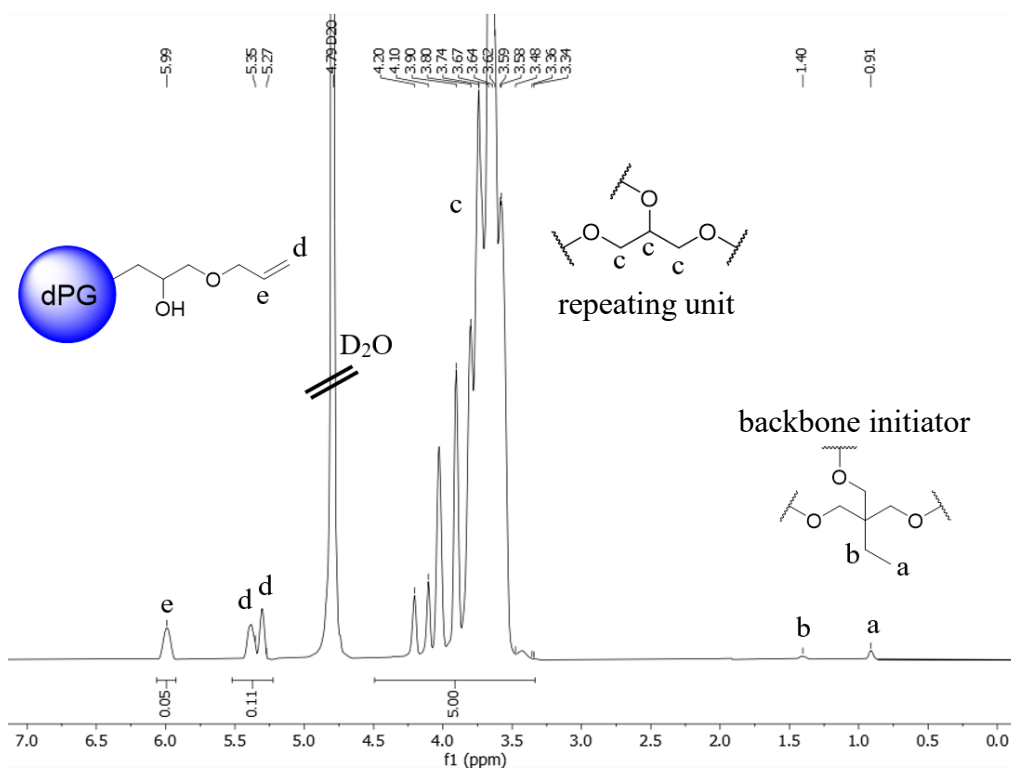

Figure S9. ^{1}H NMR (500 MHz, CDCl$_3$, δ (ppm)) of PEG(OMs)$_2$ **2.**
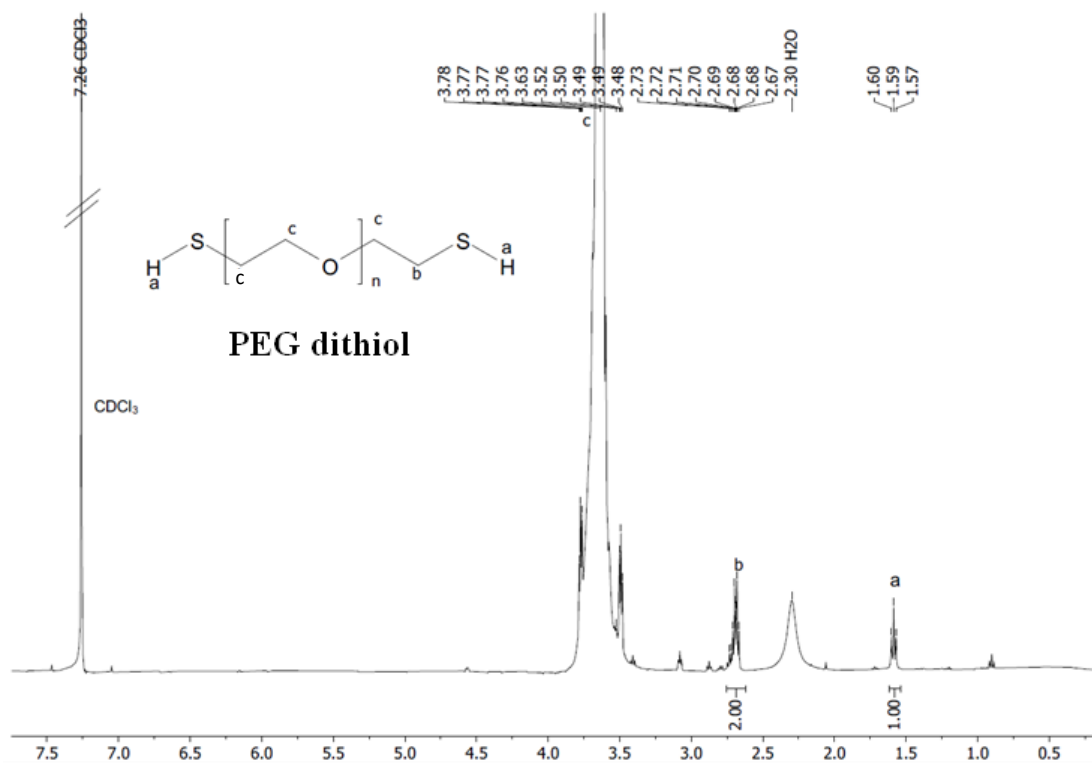
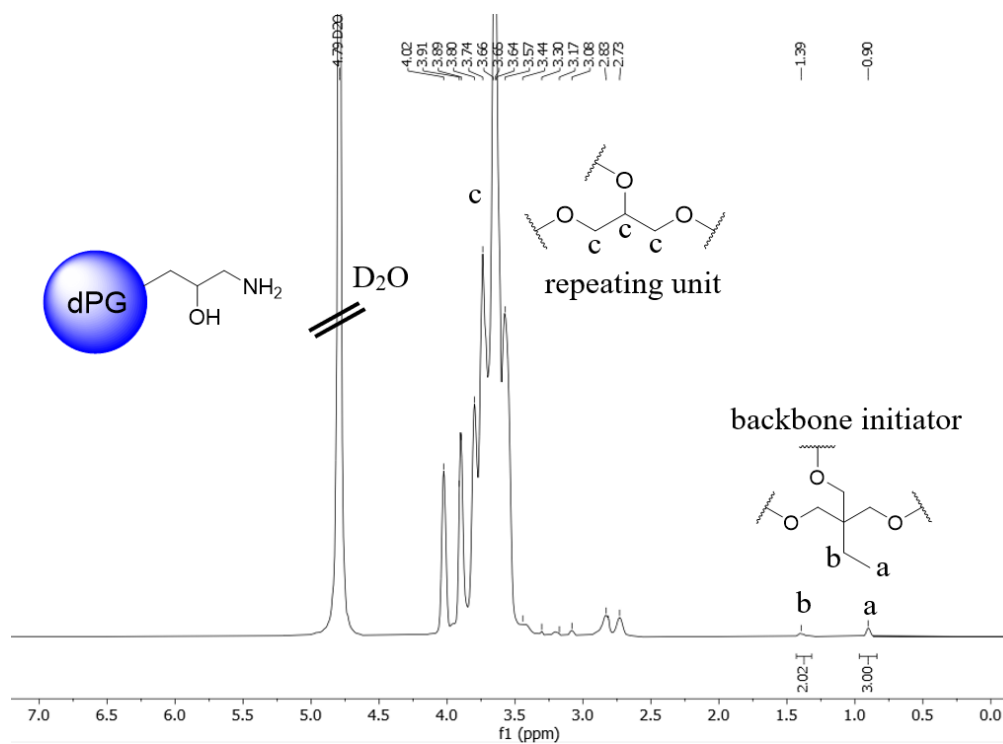**Figure S10**. ^{1}H NMR (500 MHz, CDCl$_3$, δ (ppm)) of PEG-dithiol **3.**

Figure S11. ^{1}H NMR (500 MHz, D$_2$O, δ (ppm)) of dPG-acrylate **5** (5%).

Figure S12. ^{1}H NMR (500 MHz, D$_2$O, δ (ppm)) of dPG-allyl **6** (5%).

Figure S13. ^{1}H NMR (700 MHz, D$_2$O, δ (ppm)) of dPG-amine **7.**
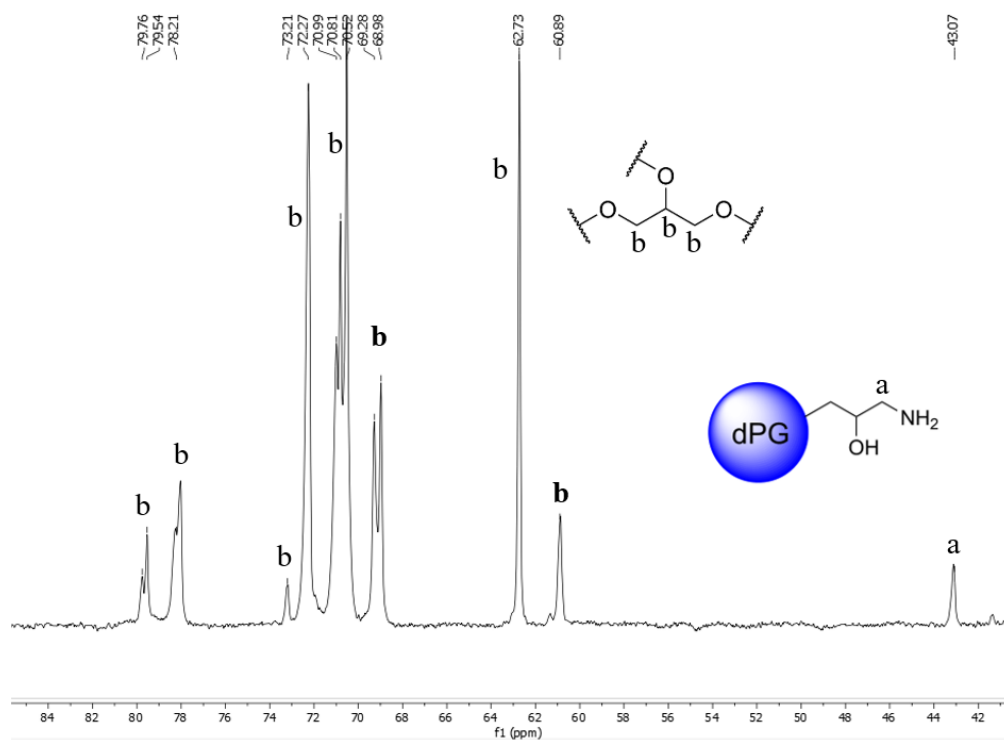
Figure S14. ^{13}C NMR (700 MHz, D$_2$O, δ (ppm)) of dPG-amine **7**.
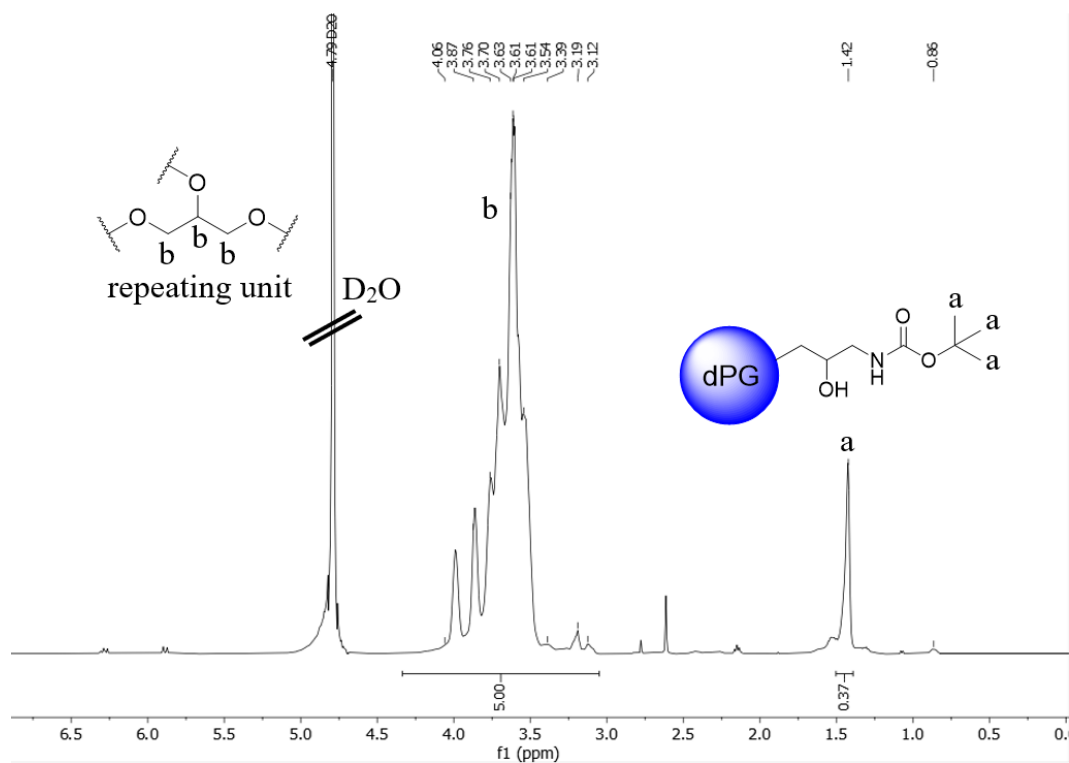
Figure S15. ^{1}H NMR (500 MHz, D$_2$O, δ (ppm)) of dPG-NH(Boc) (4%).
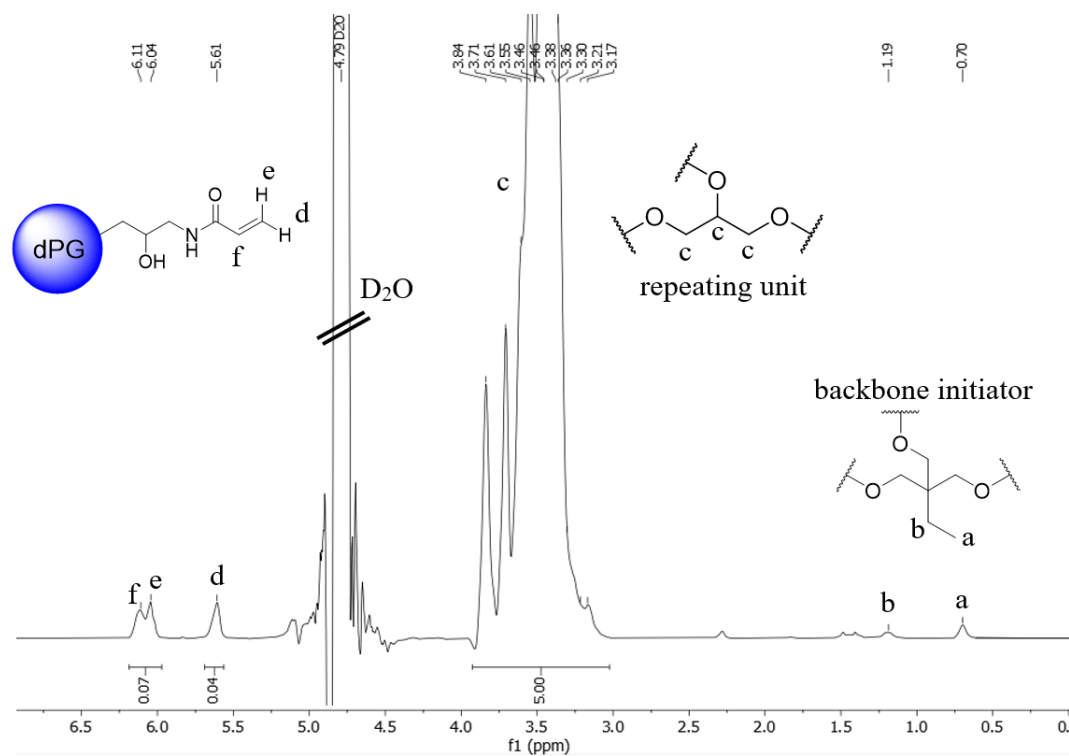
Figure S16. ^{1}H NMR (700 MHz, D$_2$O, δ (ppm)) of dPG-acrylamide **8** (4%).

4.2 Scaffold Flexibility Controls Binding of Herpes Simplex Virus Type 1 with Sulfated Dendritic Polyglycerol Hydrogels Fabricated by Thiol-Maleimide Click Reaction

Boonya Thongrom,+ Antara Sharma,+ Chuanxiong Nie, Elisa Quaas, Marwin Raue, Sumati Bhatia* and Rainer Haag*
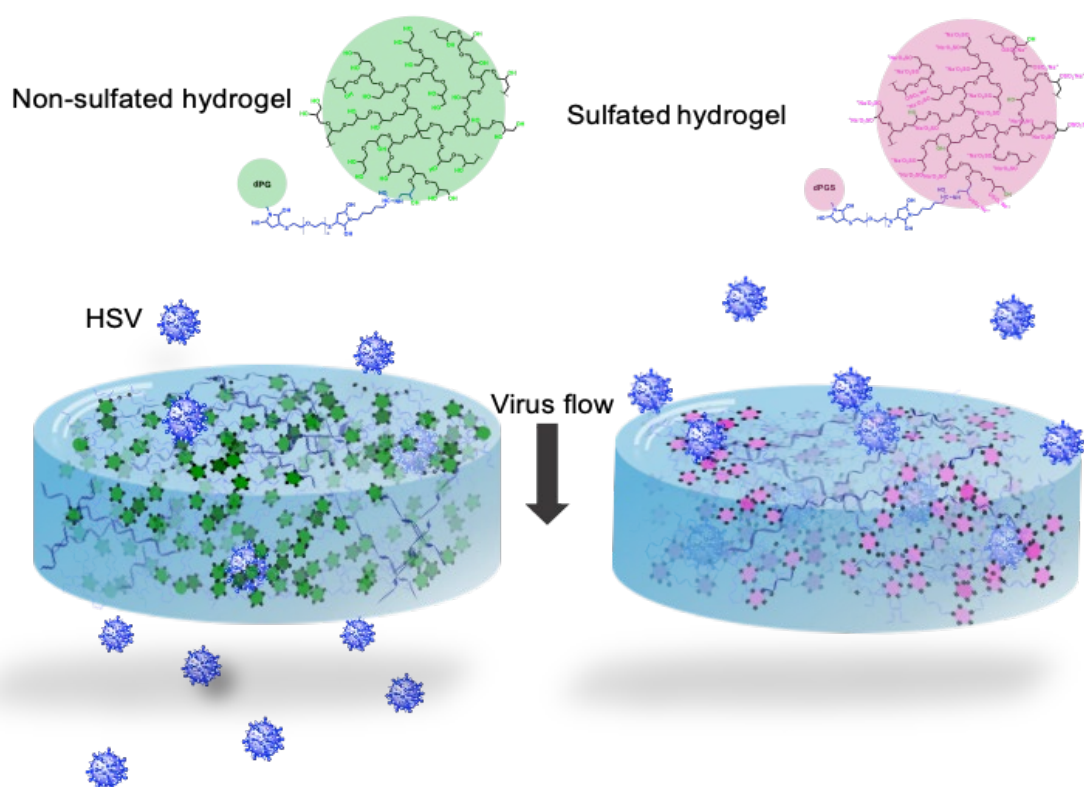
Figure 13. *Graphical Abstract. Reprinted with permission from Ref.*[138] *Copyright © 2022 John Wiley & Sons.*

Contributions of authors

Boonya Thongrom performed all syntheses of gel components, and the rheological characterizations and wrote the experimental parts. Antara Sharma analyzed all the data from gelation and rheological studies and wrote the introduction and result, and discussion parts. Chuanxiong Nie conducted the virus-binding assay. Elisa Quaas did the cytotoxicity tests of all gel components. Marwin Raue assisted in PEG dithiol synthesis and helped prepare the hydrogel samples. Sumati Bhatia and Rainer Haag supervised the project, gave the project idea and scientific advice as well as proofread and corrected the manuscript.

RESEARCH ARTICLE

# Scaffold Flexibility Controls Binding of Herpes Simplex Virus Type 1 with Sulfated Dendritic Polyglycerol Hydrogels Fabricated by Thiol-Maleimide Click Reaction

Boonya Thongrom, Antara Sharma, Chuanxiong Nie, Elisa Quaas, Marwin Raue, Sumati Bhatia,* and Rainer Haag*

Herpes Simplex Virus-1 (HSV-1) with a diameter of 155–240 nm uses electrostatic interactions to bind with the heparan sulfate present on the cell surface to initiate infection. In this work, the initial contact using polysulfate-functionalized hydrogels is aimed to deter. The hydrogels provide a large contact surface area for viral interaction and sulfated hydrogels are good mimics for the native heparan sulfate. In this work, hydrogels of different flexibilities are synthesized, determined by rheology. Gels are prepared within an elastic modulus range of 10–1119 Pa with a mesh size of 80–15 nm, respectively. The virus binding studies carried out with the plaque assay show that the most flexible sulfated hydrogel performs the best in binding HSV viruses. These studies prove that polysulfated hydrogels are a viable option as HSV-1 antiviral compounds. Furthermore, such hydrogel networks are also physically similar to naturally occurring mucus gels and therefore may be used as mucus substitutes.

1. Introduction

Herpes Simplex Virus-1 (HSV-1) is a part of the Herpesviridae family, which is known to target oral, pharyngeal, and genitals.[1] The virus is supported by a wide range of hosts, including humans. HSV-1 has a high seroprevalence of ≈80% in adults. It is an enveloped virus around 155–240 nm in diameter.[1,2] HSV-1 can be a cause of morbidity and mortality in newborns and immunocompromised patients, and antivirals such as acyclovir (ACV) and ganciclovir are often prescribed to reduce the frequency, duration, and severity of infection.[3,4]

B. Thongrom, A. Sharma, C. Nie, E. Quaas, M. Raue, S. Bhatia, R. Haag
Institut für Chemie und Biochemie
Freie Universität Berlin
Takustraße 3, Berlin 14195, Germany
E-mail: sumati@zedat.fu-berlin.de; haag@chemie.fu-berlin.de

DOI: 10.1002/mabi.202100507

HSV-1 uses its surface glycoprotein to bind to heparan sulfate proteoglycans (HSPG) to start the infection in host cells. Because the virus entry is primarily driven by electrostatic interactions, many drug designs have been inspired by the sulfate-dominant interactions.[5] This deals with the problem on the long-term scale, disabling the formation of a virus-reservoir. Previously, Dey et al. fabricated sulfated dendritic polyglycerol (dPGS) nanogels as synthetic heparan sulfate mimics of a range of flexibilities as well as sizes.[6] While all the nanogels were successful in inhibiting virus, the more flexible nanogels showed higher efficacy. Recently, our group has also published a new series of dendronized linear polysulfates as multivalent inhibitors to prevent HSV entry. However, in this case, highly flexible sulfated linear polyglycerol (lPGS) was compared with more rigid sulfated architectures. Here also, the flexible lPGS was highly successful in intervening with the infection process, showing 295 times greater efficacy than heparin.[7]

Recently, hydrogels are emerging as important platforms for multiple applications in the biomedical arena.[8,9] Hydrogels are formed when macromolecules crosslink by physical or chemical means to form water-swollen networks. They have a number of characteristics which make them particularly attractive for biomedical applications. For example, due to their structural similarity to living tissues, they are highly biocompatible; moreover they are able to provide low interfacial tension with the nearby tissues in the body.[10] They can also be non-invasively injected and fill in any required shape at the injection point.[11] In addition to other biomedical applications, they have been used in virus-trapping and containment. Zhang et al. used glycosylated hydrogels to trap the Norovirus.[12] Importantly, mucus hydrogels within the body, function in a similar way providing the first line of defense against pathogenic attack.[13]

The role of scaffold flexibility for virus binding is very important, yet, macroscopic materials with different stiffness have not been studied for this application. In this paper, we extend the understanding of scaffold flexibility with polyglycerol-based hydrogels. We have designed sulfated hydrogels by a click conjugation approach. Here we have employed polyethylene gly-

ADVANCED
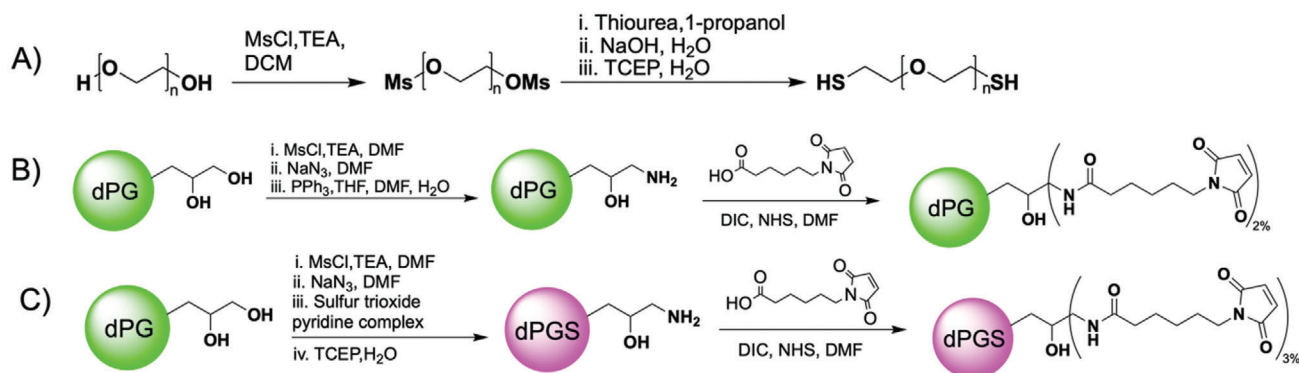**SCIENCE NEWS**
www.advancedsciencenews.com

M acro-molecular
Bioscience
www.mbs-journal.de

Scheme 1. Synthesis of A) PEG dithiol, B) dPG maleimide, C) dPGS maleimide.

col (PEG) dithiol and (dendritic polyglycerol sulfate) dPGS-maleimide as the macromolecular components to linear and crosslinking units, respectively. This ball-and-chain type system forms a hydrogel as a Michael-click reaction occurs between the linear PEG-dithiol and the maleimides decorating dPGS. These new sulfated hydrogels were studied by rheology and could prevent viral infection depending on the scaffold flexibility. The large surface area and highly negatively charged system allow virus binding by multivalent polyelectrolyte interactions.

2. Discussion

2.1. Design of Gel Components

We hypothesized that a ball-and-chain type polymers would further interconnect and crosslink to form a hydrogel matrix. Thus, two gel components need to be synthesized with the perspective of a facile and quick hydrogel reaction recipe. Hence, while the linear PEG "chain" component was functionalized with thiol groups, the crosslinking dPG and dPGS units were both decorated with maleimide functional groups such that the Michael addition click reaction would occur between the thiol and the maleimide units, respectively. Furthermore, in order to quantify the effect of the sulfate groups as well as to observe the individual efficacy of the matrix itself, hydrogels without sulfate, i.e., with PEG and dPG were also synthesized. These gels were then compared in separate rheology and virus binding assays.

2.1.1. Synthesis of PEG Dithiol

Commercially available PEG with a molecular weight of 6 kDa was first mesylated and subsequently purified by precipitation resulting in $PEG(OMs)_2$ in the form of a white powder. In order to synthesize PEG dithiol, $PEG(OMs)_2$ was first allowed to react with dithiourea, wherein the intermediate diisothiouronium PEG was formed. This was immediately followed by basic hydrolysis to finally obtain PEG dithiol, $PEG(SH)_2$. Tris(2-carboxyethyl) phosphine (TCEP) was added as reducing agent at this point, and purification thereafter by extraction and precipitation resulted in pure $PEG(SH)_2$, as confirmed by ^1H NMR spectroscopy. The synthesis is depicted in **Scheme 1**A.

2.1.2. Synthesis of dPG Maleimide

dPG was synthesized following the procedure in literature. dPG maleimide was synthesized in four steps. First of all, dPG was mesylated. To the mesylated product, sodium azide was added to form $dPGN_3$ following a substitution reaction. The resulting mixture containing the product was purified by dialysis. dPG amine was synthesized by the reduction of $dPGN_3$ with triphenylphosphine (TPP). Dichloromethane (DCM) wash and dialysis of the crude product resulted in pure $dPGNH_2$. This was corroborated by ^1H NMR and ^{13}C NMR spectroscopy results. Finally, the amine group was reacted with the active (N-hydroxy Succinimid)NHS ester formed by the reaction of NHS and N,N-Diisopropylcarbodiimide (DIC) resulting in the formation of dPG maleimide. Pure dPG maleimide was obtained by dialysis of the crude product against water, confirmed thereafter by ^1H NMR studies. The synthetic steps are shown in Scheme 1B.

2.1.3. Synthesis of dPGS Maleimide

dPGS maleimide was prepared in a similar fashion to dPG maleimide, as depicted in Scheme 1C. dPGN3 was synthesized in the same manner as mentioned above. To the same reaction mixture, sulfur trioxide pyridine complex was added and subsequently the crude mixture was first neutralized and then purified by dialyizing it against first brine, followed by water. The obtained product was then reduced and purified by dialysis. The consequent dried dPGS amine was obtained in the form of a yellow powder, the purity of which was determined by ^1H NMR spectroscopy. Afterward, dPG maleimide was synthesized by the reaction of dPGS amine with NHS and DIC. After purification by dialysis against water, the final product was obtained as a pale yellow powder. The synthetic purity and 84% degree of sulfation were confirmed by ^1H NMR spectroscopy and elemental analysis, respectively.

2.2. Synthesis of Gels

Two types of gel series were constructed. dPG maleimide gels, i.e., gels represented by "HG" were created from PEG dithiol and dPG maleimide. Further, to identify the importance of the decorating functional groups, dPGS maleimide gels (represented by

Table 1. Composition of different non-sulfated (HG) and sulfated (HGS) gel types depicting the amounts and ratios of the gel components (10% w/v PEG, 16% w/v dPG, and 10% w/v dPGS) used per 100 µL volume.

Gel code	Gel type	PEG:dPG/dPGSMol ratio	Gel components volume[µL]		Total gel volume [µL]	Gel concentration [% w/v]
			PEG	dPG/dPGS		
HG 8%	dPG maleimide	2.5:1	48	20	100	8.0
HG 7%	dPG maleimide	2.5:1	42	17.5	100	7.0
HG 6%	dPG maleimide	2.5:1	36	15	100	6.0
HG 5%	dPG maleimide	2.5:1	30	12.5	100	5.0
HG 4%	dPG maleimide	2.5:1	24	10	100	4.0
HGS 8%	dPGS maleimide	2.5:1	34.3	45.7	100	8.0
HGS 6%	dPGS maleimide	2.5:1	25.8	34.2	100	6.0
HGS 5%	dPGS maleimide	2.5:1	21.5	28.5	100	5.0
HGS 4%	dPGS maleimide	2.5:1	17.2	22.8	100	4.0
HGS 3%	dPGS maleimide	2.5:1	12.9	17.1	100	3.0

"HGS") were synthesized from the reaction between PEG dithiol and dPGS maleimide. The synthetic procedure was rapid and simple: the Phosphate buffer saline (PBS) solution of two gel components as well as an additional PBS were vortexed together so as to amount to a total of 100 µL gel volume in the ratios indicated in **Table 1**. Further, the gels at 37 °C were allowed to swell for 1 h, and oscillatory rheology experiments were carried out to determine their mechanical properties and pore sizes. The ratio of the two reacting components in this case, PEG-dithiol and dPG maleimide was maintained to be the same as 2.5:1, respectively, in every gel decreasing the overall gel components concentration.

Increasing dilution of gel components allowed a decrease in the number of crosslinks, and thus gel elasticity decreased and conversely its viscosity increased, as can also be clearly visualized in **Figure 1**B–E. Initially, with an overall gel concentration of 8%, the rigidity of the HGS 8% gels (Figure 1B) is very high. For this reason, it maintains a quite rigid structure which does not flow within the measured time period.[14] Spinnability or the ability of thread-formation is a unique property arising from non-Newtonian flow, where the existence of both elastic and viscous properties is an important prerequisite. As such, spinnability increases in viscoelastic compounds with an increase in viscosity.[14] As the gel concentration decreases from 5% to 3% (Figure 1C–E), their viscosity increases. Gel HGS 5% (Figure 1C) is also quite elastic as it hardly flows when pressure is applied and quickly recoils to its previous position as pressure is removed. It does not display spinnability suggesting a very low viscous characteristic as well. Conversely gels HGS 4% and HGS 3% (Figure 1D,E, respectively), are both soft flowable gels. They are not able to maintain their conformation with the increasing pressure. In fact HGS 3% appears to be a viscous liquid; however, as evidenced by its very high spinnability, it maintains some elasticity and thus its network structure as well.
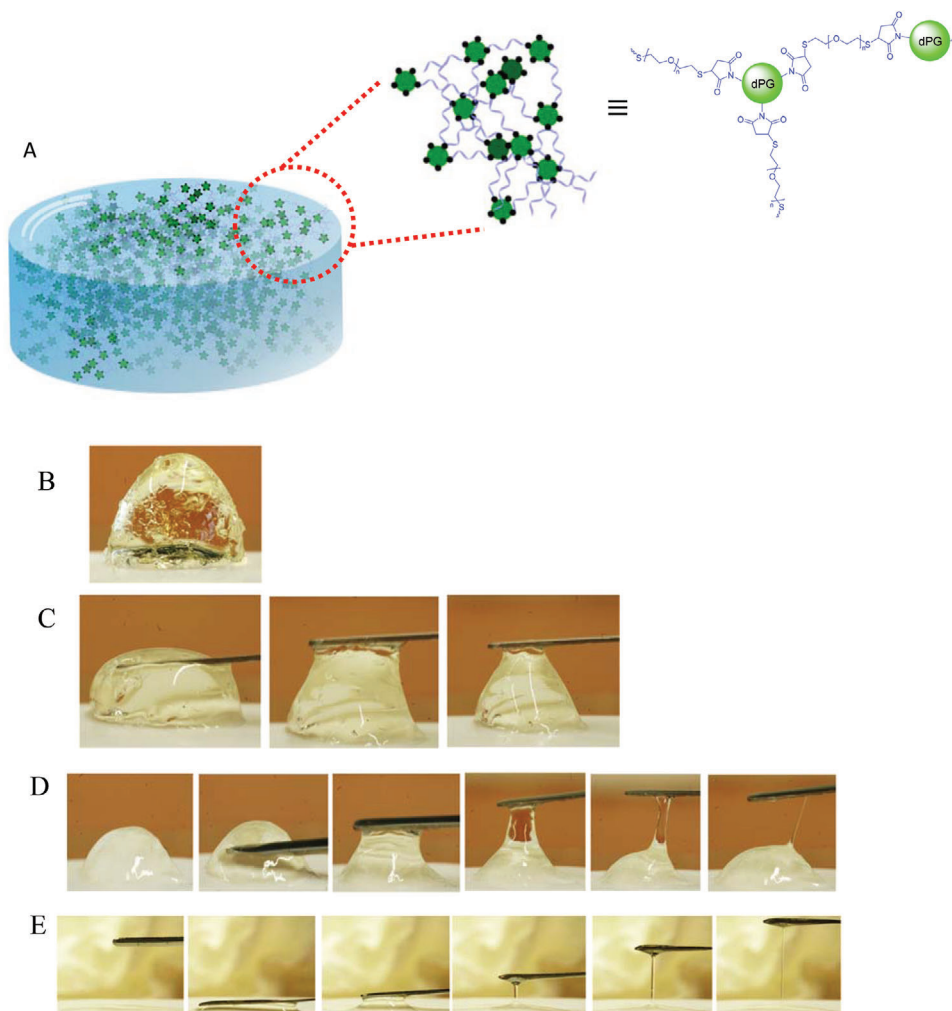
2.3. Oscillatory Rheology

A substance's viscoelastic properties are essentially indicative of its mechanical properties and can be determined by oscillatory rheology experiments. A strain-sweep test was carried out over

the entire series to establish the linear viscoelastic region (LVE) so that consecutive oscillatory rheology experiments would be conducted in this region. These viscoelastic experiments allowed the deduction of the storage modulus, G' and the loss modulus, G'' as a function of the radial frequency, ω. Moreover, the experiments were conducted at 25 °C and at the physiological temperature 37 °C, where the viscoelastic properties of the swollen gels were measured as well. The results of the experiments at 37 °C are shown in **Figure 2**, while the results of the swollen gels are shown in **Figure 3**.

The rheological behavior of the non-sulfated gels "HG" is shown in Figures 2A and 3A at 37 °C in the initial and swollen states after 1-h incubation with excess water, respectively. All the gels displayed notable elastic-dominated behavior, thus providing ample proof of the stability of the crosslinks. In Figure S8 (Supporting Information), the behavior of these gels at 25 °C can be seen. The difference caused by the increase in temperature to the physiological temperature is negligible. Interestingly, the swollen state causes a notable difference in the viscoelastic behavior in all these gels. As can be seen in **Table 2**, there is a general trend of decrease in the elastic character of this gel as the gels become more swollen.

The viscoelastic behavior of the sulfated "HGS" gels at 37 °C is shown in Figures 2B and 3B while their behavior at 25 °C can be seen in Figure S9 (Supporting Information). All gels in this series can be seen to behave in a similar fashion. An increase in both moduli is seen for all cases with increasing frequency, as expected. Further, as with the HG series, all HGS gels are elastic-dominated, indicating the existence of permanent crosslinking in a solid gel matrix. In comparison to the non-sulfated HGs, the general trend of elasticity was more toward the lower end. This can be explained by the electrostatic repulsion present within these gels contributed by the sulfate groups. An increase in temperature from 25 to 37 °C did not affect the rheological properties in this case. However, a significant decrease was observed in the elastic modulus of all the sulfated gels when they were in the swollen state, as can be seen in Table 2. This occurs due to the increase in the general pore size with swelling and this affect is particularly pronounced due to the high-water attraction of charged sulfate groups, exemplified by gel HGS 4% wherein more than 2

**ADVANCED
SCIENCE NEWS**

www.advancedsciencenews.com

**{M} acro-
olecular
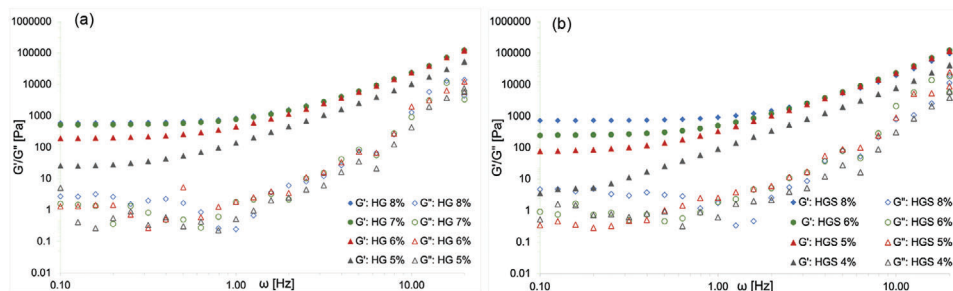Bioscience**

www.mbs-journal.de

Figure 1. A) Pictorial representation of the hydrogel and its internal matrix structure (inset). The dPG units (green) are decorated with maleimide groups (black) which then react with PEG dithiol (blue) in a Michael-click reaction to result in the formation of the hydrogel. Sulfated gels B) HGS 8%, C) HGS 5%, D) HGS 4%, E) HGS 3%. Each gel displays a clear difference in its physical properties, which are dependent upon its rheological properties. Gel HGS 8% maintains a firm structure, while the viscous trait dominates in gel HGS 3%.
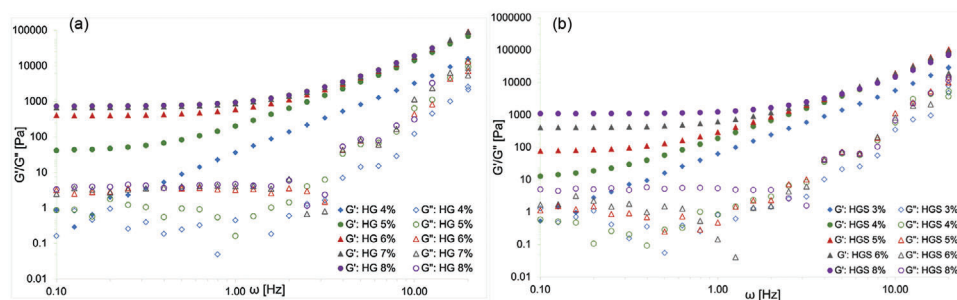
Figure 2. Storage (G') and loss (G'') moduli as a function of radial frequency (ω) of A) HG gels and B) HGS gels at 37 °C, for samples in which the gel component ratios were varied systemically.

times decrease of the elastic modulus was observed in the swollen state comparison to the initial state at 37 °C. Moreover, the change in the viscoelastic properties is more distinct in this case in comparison to the non-sulfated gels. Out of all the sulfated hydrogels, the HGS 3% was the most viscous, with its shear modulus in the non-swollen state being only 10 Pa. The rheological behavior of the non-swollen HGS 3% network was consistent with the rest of the hydrogels in the series. For most part the elastic modulus remained higher than the viscous modulus, except for in the lower frequency range in the very beginning, as shown in Figure 2B.

**ADVANCED
SCIENCE NEWS**

www.advancedsciencenews.com

{M}acro-
molecular
Bioscience

www.mbs-journal.de

Figure 3. Storage (G´) and loss (G″) moduli as a function of radial frequency (ω) of A) swollen HG gels and B) swollen HGS gels at 37 °C, for samples in which the gel component ratios were varied systemically. Gels HG 4% and HGS 3% could not be measured in a swollen state as they were too viscous and miscible when more water was introduced.

Table 2. Shear modulus G_0 and estimated mesh size of hydrogel series HG and HGS in the initial and swollen states at 37 °C.

Hydrogel[a]	37 °C (Initial state)		37 °C (Swollen state)	
	Shear modulus [G_0 Pa^{-1}]	Mesh size [ξ nm^{-1}]	Shear modulus [G_0 Pa^{-1}]	Mesh size [ξ nm^{-1}]
HG 4%	5	91	–	–
HG 5%	67	39	43	46
HG 6%	433	21	234	26
HG 7%	716	18	556	19
HG 8%	766	18	630	19
HGS 3%	10	76	–	–
HGS 4%	40	47	17	62
HGS 5%	111	33	118	33
HGS 6%	442	21	283	24
HGS 8%	1119	15	748	18

[a] Initial state refers to the hydrogel as soon as it forms after mixing, and swollen state refers to the hydrogel after 1 h of incubation with excess water.

The existence of a stable network was also seen by spinnability. As with all other gels in this series, it is expected that its shear modulus would decrease further with swelling. For this reason, its behavior in the swollen state could not be determined, as the viscosity of the gel was quite high and therefore became miscible on the addition of PBS. However, the nature of the crosslinks remained stable as the swollen gels showed spinnability as well. In fact, the HGS 3% also show some similarities to naturally occurring gel mucus. As their shear modulus in the swollen state would be lower than 10 Pa, they would be in the approximate shear modulus range of healthy lung mucus, which is about 1–2 Pa.[15] Moreover, lung mucus also exhibits a similar rheological pattern, maintaining a plateau at lower frequencies, and then an increase above 10 Hz.

The plateau modulus is the frequency range wherein an overall linear behavior of the storage and loss moduli is seen. Materials like hydrogels possess a complex rheological profile owing to the presence of a defined internal structure. While the macrorheology, or its bulk rheological properties such as viscoelasticity govern its functions such as lubrication and interaction with surfaces, its microrheological properties determine the diffusion behavior of small components like pathogens or drugs, within the

hydrogel matrix. While a larger mesh size allows free diffusion of a smaller component, when the two are comparable, steric hindrance on movement becomes significant. Thus precise control over the mesh size is pertinent to its application.[16] In order to calculate the mesh size, the G´ value at 0.3 Hz frequency was chosen and then substituted in the simplified equation G′ = kT/ξ^3, where k is the Boltzmann constant, T is the temperature, and ξ is the mesh size.[17–19] As a rule, mesh sizes increase as the crosslinking density is decreased.[20] The lowest mesh sizes would therefore be predicted as corresponding to the least elastic hydrogel. Indeed, among the initially formed sulfated and non-sulfated hydrogel HG 4% and HGS 3% had the largest mesh size at ≈91 and 76 nm, respectively owing to the low crosslinking density. It was found that HSV measuring 180 nm in size were slowed down in mucus with mesh size of ≈100 nm, with up to a 1000-fold decrease in compared to water.[21] The mesh size of the sulfated HGS 3% and 4% gels approaches this and can therefore can be considered as suitable candidates for hindering HSV.
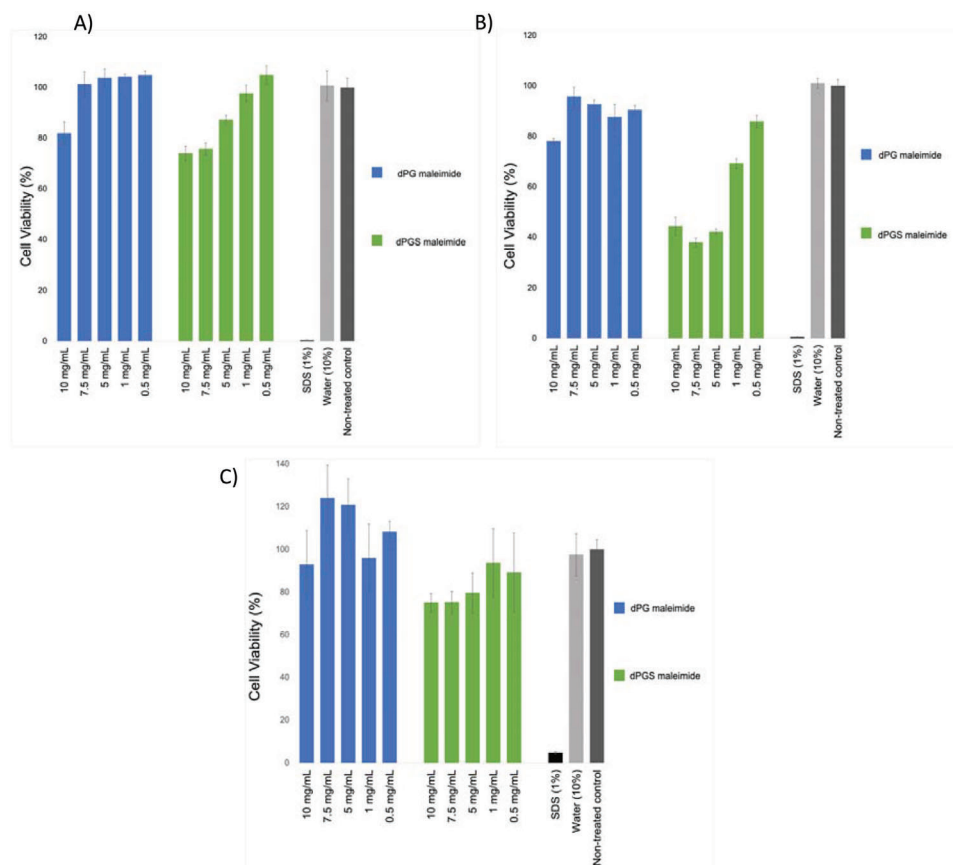
2.4. Cytotoxicity Studies

The cytotoxicity tests of gel components were performed against different cell types with CCK-8 kit. The Vero E6 (**Figure** 4A) was used, generally applied for infection assays and virus propagation studies. Moreover, the human lung cell lines A549 and HBE were also employed to diversify the study (Figure 4B,C, respectively). A slight decrease in the cell viability was observed with the addition of sulfated compounds, as expected. A high tolerance of the gel components for all the cell lines was observed, and the tolerance of dPGS decreased only at the concentration >1 mg mL^{-1}. dPG maleimide showed high cell viability throughout the tested range for all cell lines. A549, Vero E6, as well as the HeLa cell lines were treated with PEG dithiol and a high tolerance was noted in every case. These results are shown in Figure S10 (Supporting Information). Overall, all the experiments proved a high tolerance for all the gel components involved rendering them safe to be applied for future treatments.

2.5. Binding of HSV

The HSV-1 binding of the hydrogels was established by plaque reduction assays. For this purpose, the hydrogel was initially incubated with the virus solution with moderate shaking for 1 h.

ADVANCED
SCIENCE NEWS
www.advancedsciencenews.com

Macro-
molecular
Bioscience
www.mbs-journal.de

Figure 4. Cytotoxicity tests were conducted for the components of both hydrogel series, dPG-maleimide and dPGS-maleimide, as shown in A) Vero-E6 cell line, B) A549 cell line, and C) HBE cell line. For each case, the presence of sulfate groups on the gel negatively affected the cell viability results.

Afterward, the number of viral particles in the supernatant is titrated by plaque assays on Vero E6 cells. The binding with virus was revealed by reduced virus titer in the supernatant as shown in **Figure 5**.

We did not observe any significant reduction in the HSV titer with the non-sulfated control gels or gel component dPG-maleimide. The sulfated gel types (HGS 8%, HGS 6%, HGS 5%, HGS 4%, HGS 3%) showed much higher binding abilities of up to 30 times higher than their non-sulfated counterparts. HSV viruses electrostatically bind with heparan sulfate on the host cells through their surface glycoprotein. Due to the presence of sulfate groups in the HGS gels, virus binding became significantly more efficacious in comparison to HG gels. This was observed not only for every hydrogel but also for the individual sulfated and non-sulfated gel components (dPG-maleimide and dPGS-maleimide). However, as the gels HGS 8%–5% are quite stiff, their sulfate groups are less exposed even after swelling, and thus do not interact with as many HSV particles as the softer gels would. This has a negative effect on their binding performance, as can be seen in Figure 5. The effects of network structure on virus binding were revealed by the comparison among sulfated hydrogels with different stiffness. The more viscous gel HGS 3% being slightly better than the HGS 4%, showed a higher HSV interaction than the more elastic gels HGS 5%–8% in the series. The remaining virus titer in the supernatant treated with HGS
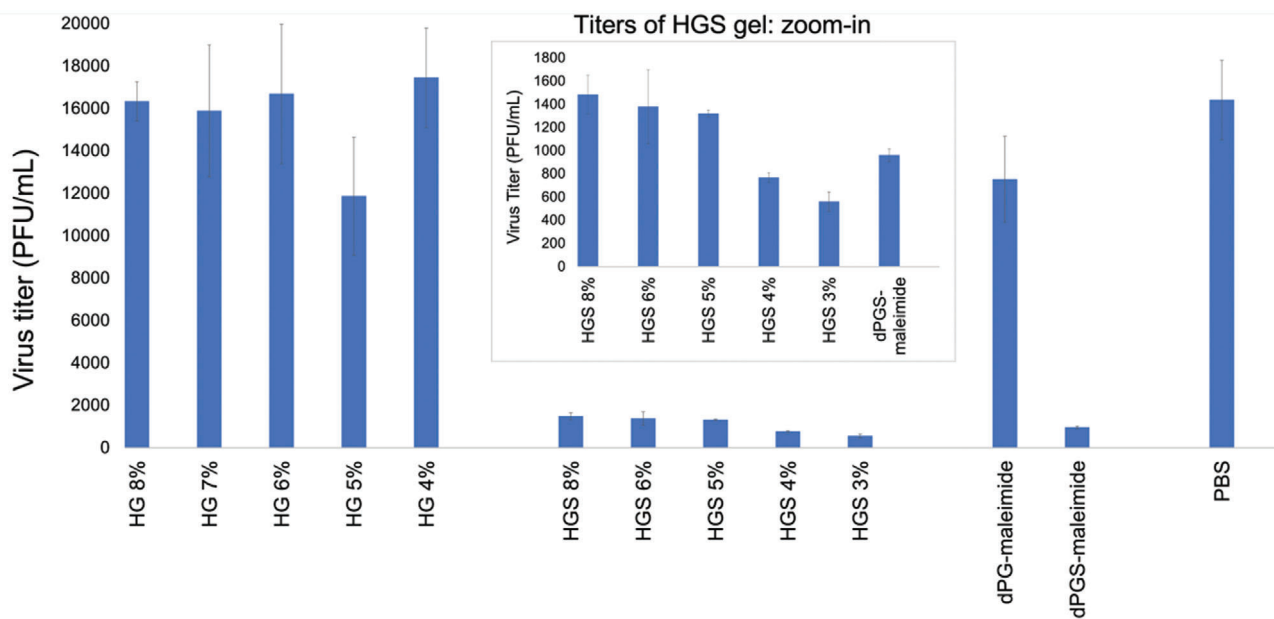
3% gel was 560 PFU mL^{-1} whereas for HGS 8%, the remaining virus titer was still 1483 PFU mL^{-1}. The loosely bound network in the more flexible sulfated hydrogels might allow the exposition of more sulfate groups while binding with the virus and thus is definitely a plus for HSV binding and inhibition.

Sulfated hydrogels HGS were compared with the 2.3×10^{-3} M sulfated gel component dPGS-maleimide ($\approx$4.6% w/v). As can be seen in Table S1 (Supporting Information), the concentration of sulfated gel component in the HGS 4% ($\approx$1.1 $\times$ 10^{-3} M dPGS) and HGS 3% ($\approx$0.9 $\times$ 10^{-3} M dPGS) are 2–2.5 times lower and all sulfate groups are not fully exposed because of 3D network formation, still the performance of these gel types were slightly higher than the dPGS-maleimide itself because of large contact surface area with the virus and high flexibility.

Thus, sulfated gels proved to be the most compelling candidates for HSV-1 binding. Moreover, the network structure also played a significant role in this study, where higher flexibility allowed higher binding capacity.

3. Conclusion

This study demonstrates the flexibility of a sulfated hydrogels network as an important parameter for its ability to bind HSV-1 virus. In order to deduce the best candidate, polyether-based hydrogels were prepared using thiol-maleimide click chemistry

**ADVANCED
SCIENCE NEWS**

www.advancedsciencenews.com

**[M]acro-
molecular
Bioscience**

www.mbs-journal.de

Figure 5. Efficacy of HSV-1 binding by hydrogels. The figure characterizes the virus titers after treatment with various samples. Inset: virus titers of gel series HGS, as well as dPGS-maleimide. Values are expressed as mean ± SD, $n = 3$. dPGS-maleimide (5% w/v) and dPG-maleimide (8% w/v) were applied in the HSV binding assay.

based on dPG-maleimide as a crosslinker and PEG-dithiol as the linear component. Two sets of hydrogels were compared, distinguished by the presence of hydroxyl groups in one series and sulfate groups in the other series. Furthermore, hydrogels were prepared within each series such that their flexibility was tuned reduction of the linear component. A range of flexibilities with shear moduli between 1 and 1200 Pa were achieved. The presence of sulfate groups on hydrogels is crucial for HSV binding, rheology dependent parameters also played an important role. The sulfated hydrogels show 10–30 times stronger HSV binding than the non-sulfated controls. Furthermore, gels followed a general trend of having higher virus titer reduction as their flexibilities increased. Notably, HGS 3% proved to be the most suitable virus-binding candidate, showing an even higher binding capacity than the highly sulfated dendritic crosslinker dPGS-maleimide. These polysulfated hydrogel networks can mimic the antiviral function of mucus and may find future applications in this area.

4. Experimental Section

Materials: All chemicals were purchased from Merck KGaA, Darmstadt, Germany and/or its affiliates and used without any further purification, unless otherwise stated. The solvents used herein, i.e., diethyl ether (100%) and *N,N*-dimethylformamide (99.8%) were bought from VWR chemicals and Acros Organics, respectively, while DCM (99%) and ethyl acetate were both obtained from Fischer Scientific. Sodium hydroxide in the form of pellets, as well as in a 99.5% solution, was also procured from Fischer Scientific. Triphenylphosphine (99%) was purchased from Alfa Aesar. dPG of ≈6 kDa average molecular weight was prepared as previously reported[22–24] with the improved method.[25] For purification carried out with dialysis, Spectra Por dialysis tubing (MWCO = 2000 g mol⁻¹) (Carl Roth GmbH, Karlsruhe, Germany).

Cell viability assays were performed with a CCK-8 Kit from Sigma Aldrich according to the manufacturing instructions. A549, HBE, HeLa, and Vero

E6 cells were obtained from Leibniz-Institut DSMZ—Deutsche Sammlung von Mikroorganismen und Zellkulturen GmbH and cultured in DMEM supplemented with 10% (v/v) FBS, 100 U mL⁻¹ penicillin and 100 μg mL⁻¹ streptomycin.

Instrumentals: The Jeol Eclipse 500 MHz (Tokyo, Japan) or a Bruker AVANCE III 700 MHz spectrometer (Billerica, MA, USA) instruments were used to measure all the NMR spectra of all the compounds (¹H and ¹³C) reported here were recorded at 300 K. Chemical shifts δ were reported in ppm and the deuterated solvent peak was used as a standard. Vario EL CHNS element analyzer (Elementar Analysensysteme GmbH (Langenselbold, Germany)) was used to carry out the elemental analysis of all relevant compounds reported in this work. All the rheology data reported here was measured and characterized by the Kinexus rheometer (NETZSCH GmbH, Selb, Germany). A parallel plate, 8 mm in diameter was used for all the measurements, with the average normal force maintained at ≈0.1 N at 25 and 37 °C. The data were analyzed by an oscillatory frequency sweep strain-controlled test with 1% strain (which is obtained from a linear viscoelastic range of an amplitude sweep test) and the reported storage modulus (G´) of a rigid hydrogel were picked at 0.3 Hz.

Synthesis of Gel Components: PEG(OMs)₂: Dried PEG (20 g, 3.3 mmol, 1 eq., 6 kDa) was dissolved in a dichloromethane (DCM) solution (100 mL), and subsequently cooled down in an ice bath. Then triethylamine (TEA, 2.77 mL, 20 mmol, 6 eq.) was added to the solution, followed by the dropwise addition of methanesulfonyl chloride (1.03 mL, 13.3 mmol, 4 eq.). The reaction was allowed to run overnight. Afterward, the crude product was purified; the DCM layer was washed thrice with brine before drying it with Na₂SO₄. It was then precipitated in cooled diethyl ether. The purified precipitate was then allowed to dry overnight under vacuum, finally resulting in a white powder with 95% isolated yield. ¹H NMR: (500 MHz, CDCl₃, δ (ppm)): 3.07 (3H, s), 3.48–3.78 (m), 4.37 (2H, t) (Figure S1, Supporting Information).

Synthesis of PEG Dithiol (PEG(SH)2):   PEG(OMs)₂ (19 g, 3.2 mmol, 1 eq.) and thiourea (1.02 g, 13.3 mmol, 4 eq.) were added to a solution of 1-propanol. The solution was refluxed overnight to obtain diisothiouronium PEG as the intermediate product. Without any further purification, 1-propanol was immediately removed from the intermediate, followed by the addition of NaOH (0.53 g, 13.3 mmol, 4 eq.) and water (100 mL). The reaction mixture was allowed to reflux overnight. Afterward, tris(2-

**ADVANCED
SCIENCE NEWS**

www.advancedsciencenews.com

**Macro-
molecular
Bioscience**

www.mbs-journal.de

carboxyethyl)phosphine (TCEP, 1.67 g, 6.7 mmol, 2 eq.) was added to the mixture and stirred for 2 h prior to the purification. To purify, NaCl was added to the mixture until the point of saturation, followed by the precipitation of the product was extracted three times into DCM. The DCM layer was then dried by Na_2SO_4, after which it was precipitated in cooled diethyl ether. The precipitate was dried in vacuo overnight. PEG dithiol was obtained as a pale yellowish powder in 88% isolated yield. ^{1}H NMR (500 MHz, $CDCl_3$, δ (ppm)): 1.59 (1H, t), 2.69 (2H, quat), 3.48–3.78 (m). Elemental analysis; N = 0.13; C = 54.24; S = 2.02; H = 8.47 (Figure S2, Supporting Information).

Synthesis of dPGNH$_2$: Dried dPG (5 g, 0.5 mmol, 1 eq.) and TEA (0.7 mL, 5 mmol, 10 eq.) were added to a solution of *N,N*-dimethyl formamide (DMF, 50 mL) and the reaction mixture was subsequently cooled using an ice bath. Methanesulfonyl chloride (0.31 mL, 4 mmol, 8 eq. to target roughly 5% mesyl groups on dPG) was added dropwise to the stirring mixture. The reaction mixture was then stirred overnight. NaN_3 (0.65 g, 10 mmol, 20 eq.) was then added to the reaction flask and thereafter heated at 60 °C for 2 days. Afterward, the crude mixture was purified in water by dialysis (MWCO = 2 kDa) for 2 days. After purification, water was first removed from the flask and DMF (40 mL) was then added to it. Separately a tetrahydrofuran (THF, 30 mL) solution of triphenylphosphine (TPP, 3.28 g, 12.5 mmol, 25 eq.) was prepared in another flask. The contents of the latter were then added gradually to the former DMF solution flask. The reaction flask was allowed to stir overnight, with additional care that phase separation did not take place. Afterward, water (5 mL) was added to the reaction mixture and stirred again overnight at room temperature overnight. Finally, the product was purified by a DCM wash, repeated three times and later dialyzed against water (MWCO = 2 kDa) for 2 days. The product obtained was then dried and collected as a pale yellowish liquid with a honey-like consistency in 70% isolated yield. ^{1}H NMR (700 MHz, D_2O, δ (ppm)): 0.90 (3H, broad s, initiator backbone), 1.39 (2H, broad s, initiator backbone), 2.73–4.02 (m, backbone repeating units), (Figure S3, Supporting Information). ^{13}C NMR (700 MHz, D_2O, δ (ppm)): 43.07 (s, 2nd carbon next to amino group), 60.89–79.76 (m, polymer backbone) (Figure S4, Supporting Information).

Synthesis of dPG Maleimide: dPGNH$_2$ (1.4 g, 0.14 mmol, 1 eq.), 6-maleimidohexanoic acid (0.15 g, 0.7 mmol, 5 eq.), and *N*-hydroxysuccinimide (0.13 g, 1.12 mmol, 8 eq.) were added to DMF (20 mL). *N,N'*-diisopropylcarbodiimide (DIC, 0.17 mL, 1.12 mmol, 8 eq.) was then added to the mixture and it was allowed to stir overnight at room temperature. The crude mixture was afterward subjected to dialysis against water (MWCO = 2 kDa) for 2 days. The purified product was later collected and kept in an aqueous solution with 85% isolated yield. ^{1}H NMR (700 MHz, D_2O, δ (ppm)): 0.92 (3H, broad s, initiator backbone), 1.32 (2H, broad s), 1.61 (4H, broad s), 2.28 (2H, broad s), 3.26–4.04 (m, backbone repeating units), 6.89 (2H, broad s) (Figure S5, Supporting Information).

Synthesis of dPGSNH$_2$: An initial mixture was made by the addition of dPG (6 g, 0.6 mmol, 1 eq.) and TEA (0.83 mL, 6 mmol, 10 eq.) were added to DMF (60 mL). The mixture was then cooled down with the help of an ice bath. Subsequently methanesulfonyl chloride (0.37 mL, 4.8 mmol, 8 eq.) was added dropwise to the stirring solution, which was then allowed to stir overnight. Following the addition of NaN_3 (0.62 g, 9.6 mmol, 16 eq.), the reaction mixture was allowed to stir as it was heated to 60 °C. After 2 days, sulfur trioxide pyridine complex (23.87 g, 150 mmol, 250 eq.) was added to the mixture and then allowed to run for 2 days at room temperature. The crude mixture was purified by first neutralizing the solution with NaOH and then dialyzing it first against brine, followed by water for 2 more days. Dialysis tubes with a 2 kDa molecular weight cut-off were used for both these cases. After purification, TCEP (1.38 g, 4.8 mmol, 8 eq.) was added to the aqueous solution and it was allowed to stir for 3 days. The crude mixture was then purified by dialysis against water (MWCO = 2 kDa) carried out for 2 days. Finally, the aqueous solution of the product was lyophilized overnight and collected as a solid pale yellow powder with 65% isolated yield with 4% as degree of sulfation. ^{1}H NMR (600 MHz, D_2O, δ (ppm)): 0.93 (3H, broad s, initiator backbone), 3.45–4.74 (m, backbone repeating units), elemental analysis: N 0.84, C 20.52, S 14.94, H 3.71(Figure S6, Supporting Information).

Synthesis of dPGS Maleimide: 6-maleimidohexanoic acid (0.07 g, 0.35 mmol, 7 eq.), and *N*-hydroxysuccinimide (0.05 g, 0.45 mmol, 9 eq.) were added to a solution of DMF (5 mL). This was followed by the addition of DIC (0.07 mL, 0.45 mmol, 9 eq.) and the mixture was stirred. After 30 min, the aqueous solution (5 mL) of dPGSNH$_2$ (1 g, 0.05 mmol, 1 eq.) was added to the reaction mixture and then allowed to stir overnight at room temperature. The crude product was purified by dialyzing the mixture against water with for 2 days (MWCO = 2 kDa). Finally, the aqueous solution was lyophilized and the final product was obtained as a solid, pale yellow powder in 87% isolated yield. ^{1}H NMR (700 MHz, D_2O, δ (ppm)): 0.94 (3H, broad s, initiator backbone), 1.30 (2H, broad s), 1.62 (4H, broad s), 2.26–2.29 (2H, broad s), 2.48–2.52 (2H, broad s), 3.40–4.75 (m, backbone repeating units), 6.93 (2H, broad s). Elemental analysis: N 1.95, C 21.75, S 16.23, H 3.62 (Figure S7, Supporting Information).

Cytotoxicity Studies: All cell experiments were conducted according to German genetic engineering laws and German biosafety guidelines in the laboratory (safety level 1). A549, HBE, and Vero E6 cells were seeded in a 96-well plate at a density of 5×10^4 cells mL^{-1} in 90 µL DMEM medium per well over night at 37 °C and 5% CO_2. 10µL of sample (solved in deionized water) were added in serial dilutions including positive (1% SDS) and negative controls (medium, H_2O) and incubated for another 24 h at 37 °C and 5% CO_2. For background subtraction, also wells containing no cells but only sample were used. After 24 h incubation the CCK8 solution was added (10 µL well^{-1}) and absorbance (450 nm/650 nm) was measured after $\approx$3 h incubation of the dye using a Tecan plate reader (Infinite pro200, TECAN-reader Tecan Group Ltd.). Measurements were performed in triplicates and repeated three times. The cell viability was calculated by setting the non-treated control to 100% and the non-cell control to 0% after subtracting the background signal using the Excel software.

Virus Binding Assay: The samples were disinfected by UV-irradiation first for 30 min. Then they were incubated with HSV-1-GFP solution (300 µL, $\approx$20 000 PFU mL^{-1}) for 1 h with constant shaking. Afterward, the virus particles in the solution was titrated by a plaque assay on the VeroE6 line with DMEM (0.9% methylcellulose) as overlay medium. The plaques were counted after 2 days with a fluorescence microscope (Axio, Zeiss, Germany).

Supporting Information

Supporting Information is available from the Wiley Online Library or from the author.

Conflict of Interest

The authors declare no conflict of interest.

Author Contributions

B.T. and A.S. contributed equally to this work.

Data Availability Statement

The data that support the findings of this study are available in the supplementary material of this article.

Keywords

click chemistry, HSV-1, hydrogel, polysulfates, rheology, virus binding

[1] P. G. Arduino, S. R. Porter, *J. Oral Pathol. Med.* **2008**, *37*, 107.
[2] R. F. Laine, A. Albecka, S. Van De Linde, E. J. Rees, C. M. Crump, C. F. Kaminski, *Nat. Commun.* **2015**, *6*, 5980.
[3] C. Dogrammatzis, H. Waisner, M. Kalamvoki, *Viruses* **2021**, *13*, 17.
[4] S. Crimi, L. Fiorillo, A. Bianchi, C. D'Amico, G. Amoroso, F. Gorassini, R. Mastroieni, S. Marino, C. Scoglio, F. Catalano, P. Campagna, S. Bocchieri, R. De Stefano, M. T. Fiorillo, M. Cicciù, *Viruses* **2019**, *11*, 463.
[5] B. Ziem, W. Azab, M. F. Gholami, J. P. Rabe, N. Osterrieder, R. Haag, *Nanoscale* **2017**, *9*, 3774.
[6] P. Dey, T. Bergmann, J. L. Cuellar-Camacho, S. Ehrmann, M. S. Chowdhury, M. Zhang, I. Dahmani, R. Haag, W. Azab, *ACS Nano* **2018**, *12*, 6429.
[7] P. Pouyan, C. Nie, S. Bhatia, S. Wedepohl, K. Achazi, N. Osterrieder, R. Haag, *Biomacromolecules* **2021**, *22*, 1545.
[8] H. Kamata, X. Li, U.-I. Chung, T. Sakai, *Adv. Healthcare Mater.* **2015**, *4*, 2360.
[9] A. Herrmann, R. Haag, U. Schedler, *Adv. Healthcare Mater.* **2021**, *10*, 2100062.
[10] B. Gyarmati, B. Vajna, Á. Némethy, K. László, A. Szilágyi, *Macromol. Biosci.* **2013**, *13*, 633.
[11] T. J. Sanborn, P. B. Messersmith, A. E. Barron, *Biomaterials* **2002**, *23*, 2703.
[12] Y. Zhang, Q. Yao, C. Xia, X.i Jiang, P. G. Wang, *ChemMedChem* **2006**, *1*, 1361.
[13] R. Bansil, B. S. Turner, *Curr. Opin. Colloid Interface Sci.* **2006**, *11*, 164.
[14] N. Tsurutaro, *Bull. Chem. Soc. Jpn.* **1952**, *25*, 88.
[15] S. K. Lai, Y.-Y. Wang, D. Wirtz, J. Hanes, *Adv. Drug Delivery Rev.* **2009**, *61*, 86.
[16] J. Li, D. J. Mooney, *Nat. Rev. Mater.* **2016**, *1*, 16071.
[17] A. Sharma, B. Thongrom, S. Bhatia, B. von Lospichl, A. Addante, S. Y. Graeber, D. Lauster, M. A. Mall, M. Gradzielski, R. Haag, *Macromol. Rapid Commun.* **2021**, *42*, 2100303.
[18] B. Von Lospichl, S. Hemmati-Sadeghi, P. Dey, T. Dehne, R. Haag, M. Sittinger, J. Ringe, M. Gradzielski, *Colloids Surf., B* **2017**, *159*, 477.
[19] Y. Tsuji, X. Li, M. Shibayama, **2018**, *4*, 50.
[20] K. S. Anseth, C. N. Bowman, L. Brannon-Peppas, *Biomaterials* **1996**, *17*, 1647.
[21] S. S. Olmsted, J. L. Padgett, A. I. Yudin, K. J. Whaley, T. R. Moench, R. A. Cone, *Biophys. J.* **2001**, *81*, 1930.
[22] H. Frey, R. Haag, *J. Biotechnol.* **2002**, *90*, 257.
[23] A. Sunder, R. Hanselmann, H. Frey, R. Mülhaupt, *Macromolecules* **1999**, *32*, 4240.
[24] R. Haag, A. Sunder, J.-F. Stumbé, *J. Am. Chem. Soc.* **2000**, *122*, 2954.
[25] M. Wallert, J. Plaschke, M. Dimde, V. Ahmadi, S. Block, R. Haag, *Macromol. Mater. Eng.* **2021**, *306*, 2000688.

Scaffold Flexibility Controls Binding of Herpes Simplex Virus Type 1 with Sulfated Dendritic Polyglycerol Hydrogels Fabricated by Thiol-Maleimide Click Reaction

Boonya Thongrom,[+] Antara Sharma,[+] Chuanxiong Nie, Elisa Quaas, Marwin Raue, Sumati Bhatia* and Rainer Haag*

Institut für Chemie und Biochemie, Freie Universität Berlin, Takustraße 3, 14195 Berlin, Germany.
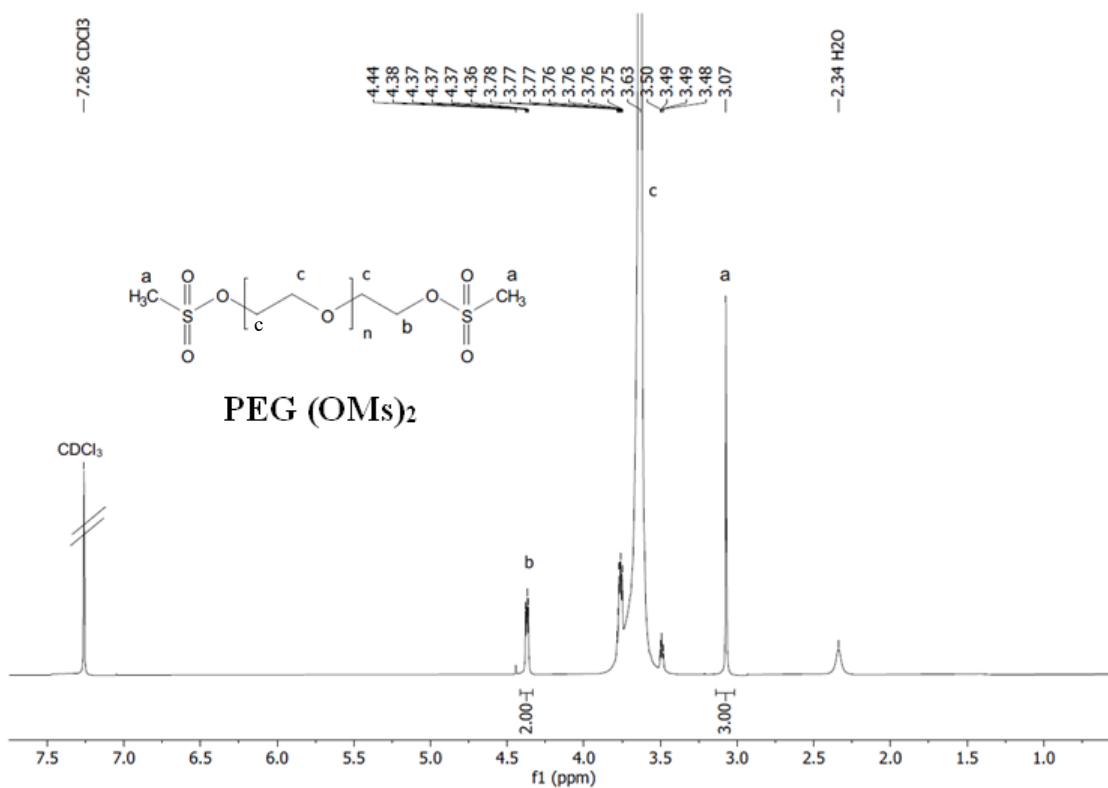
Figure S1. ^{1}H NMR (500 MHz, CDCl$_3$, δ (ppm)) of PEG (OMs)$_2$
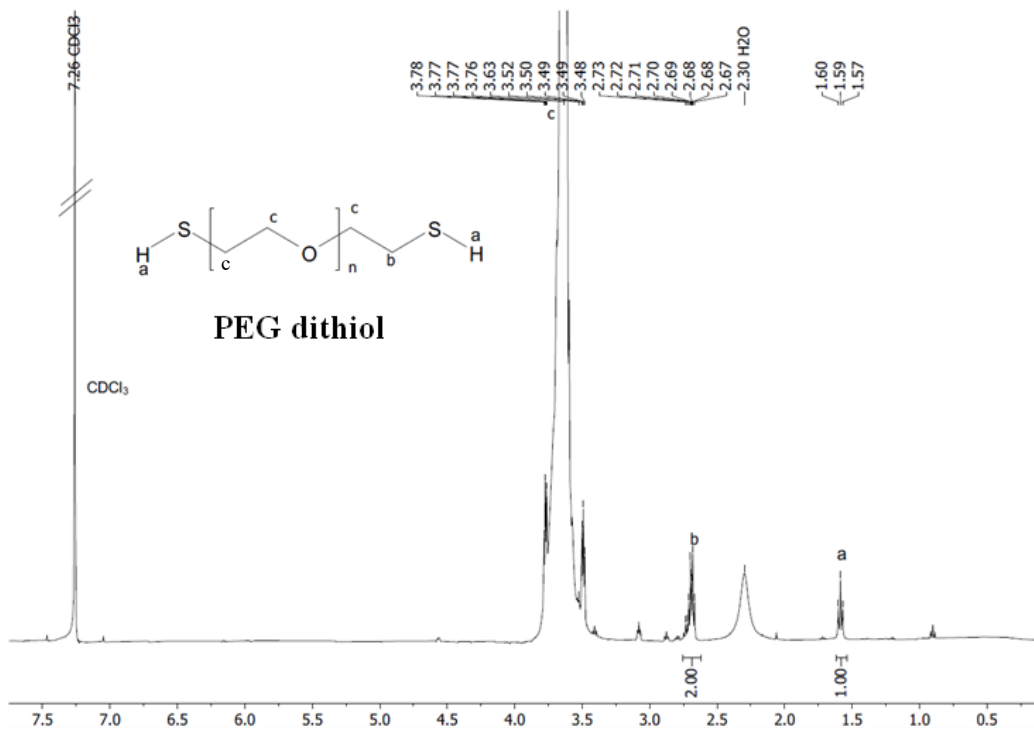
Figure S2. ^{1}H NMR (500 MHz, CDCl$_3$, δ (ppm)) of PEG dithiol
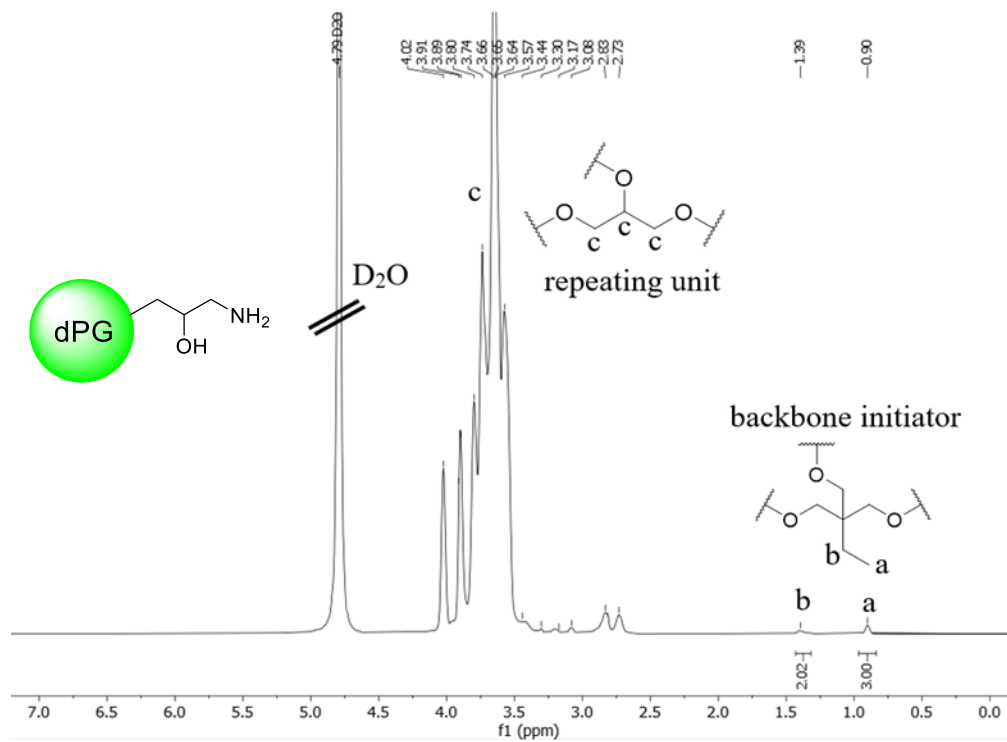
Figure S3. ^{1}H NMR (700 MHz, D$_2$O, δ (ppm)) of dPGNH$_2$
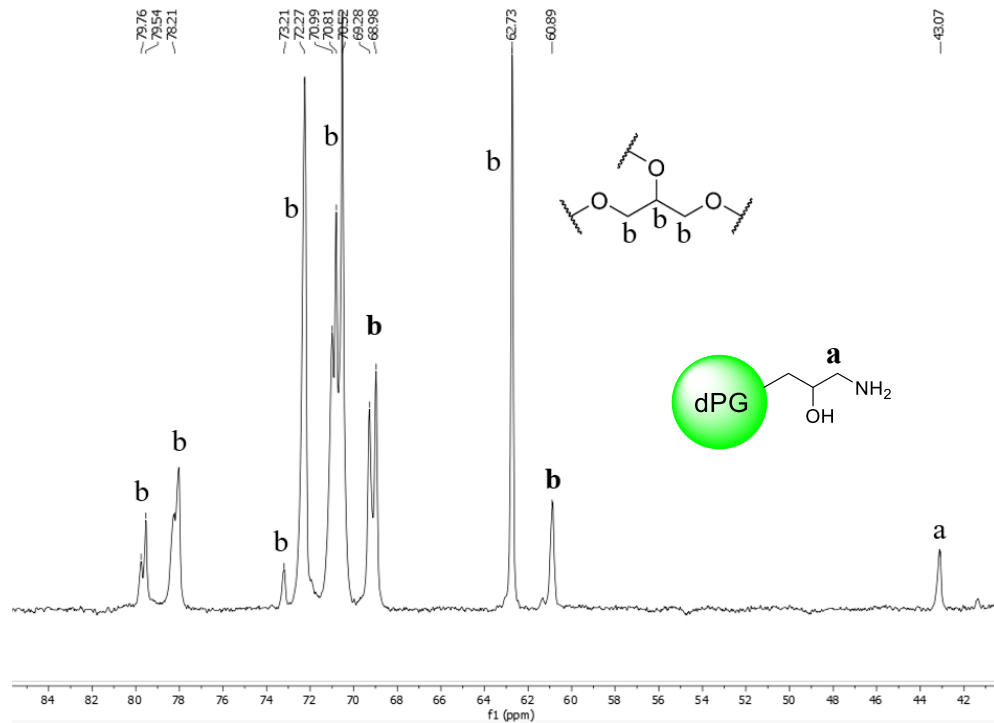
Figure S4. ^{13}C NMR (700 MHz, D$_2$O, δ (ppm)) of dPGNH$_2$
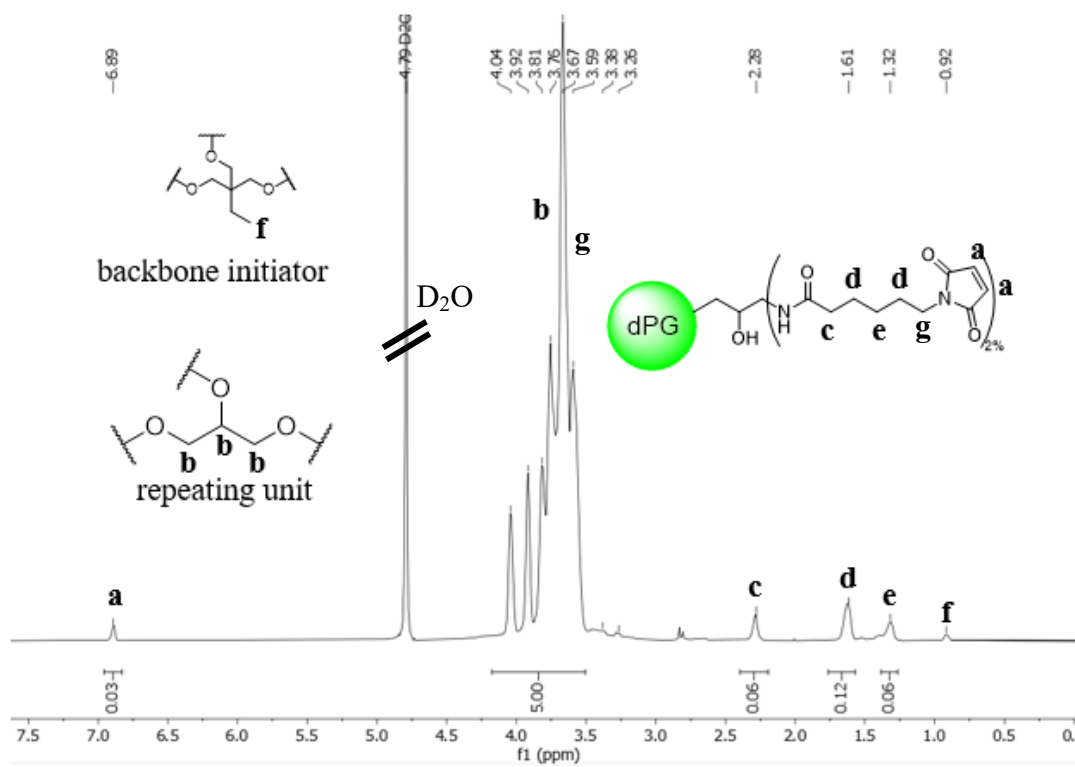
Figure S5. ^1H NMR (700 MHz, D$_2$O, δ (ppm)) of dPG maleimide
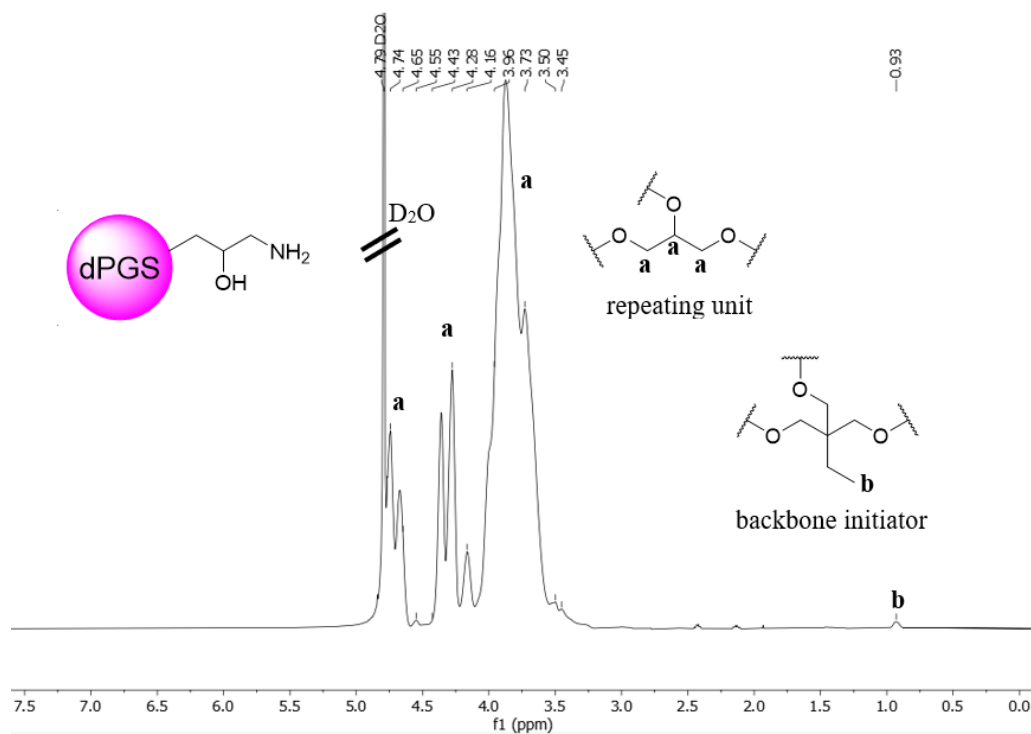
Figure S6. ^{1}H NMR (600 MHz, D₂O, δ (ppm)) of dPGSNH₂
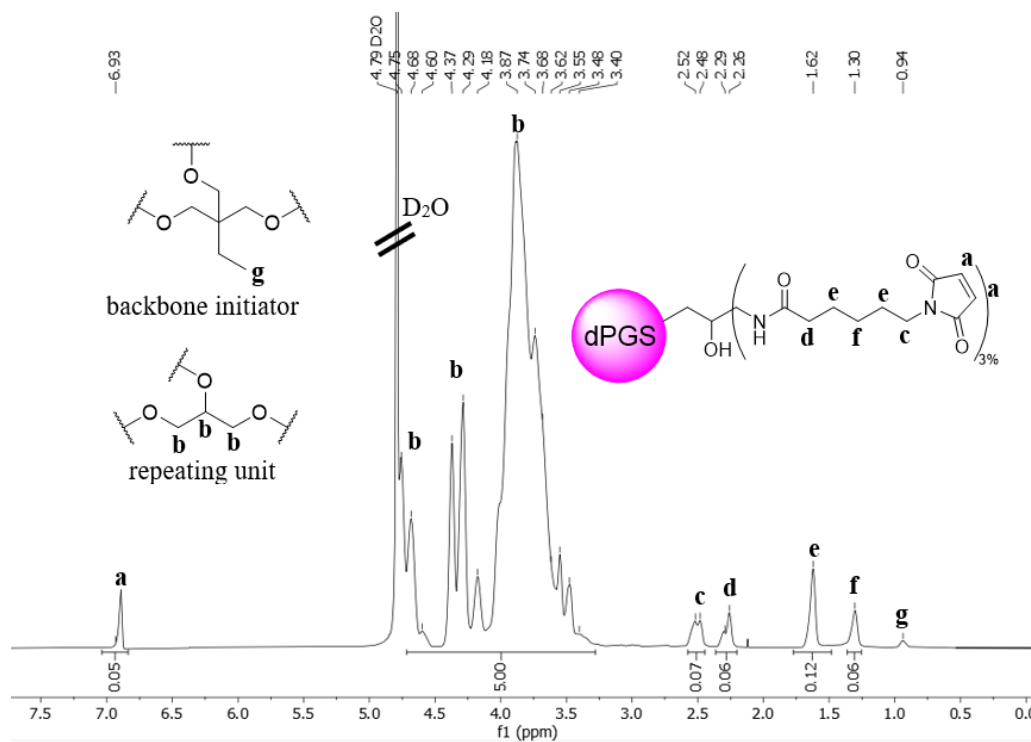
Figure S7. ^{1}H NMR (700 MHz, D₂O, δ (ppm)) of dPGS maleimide
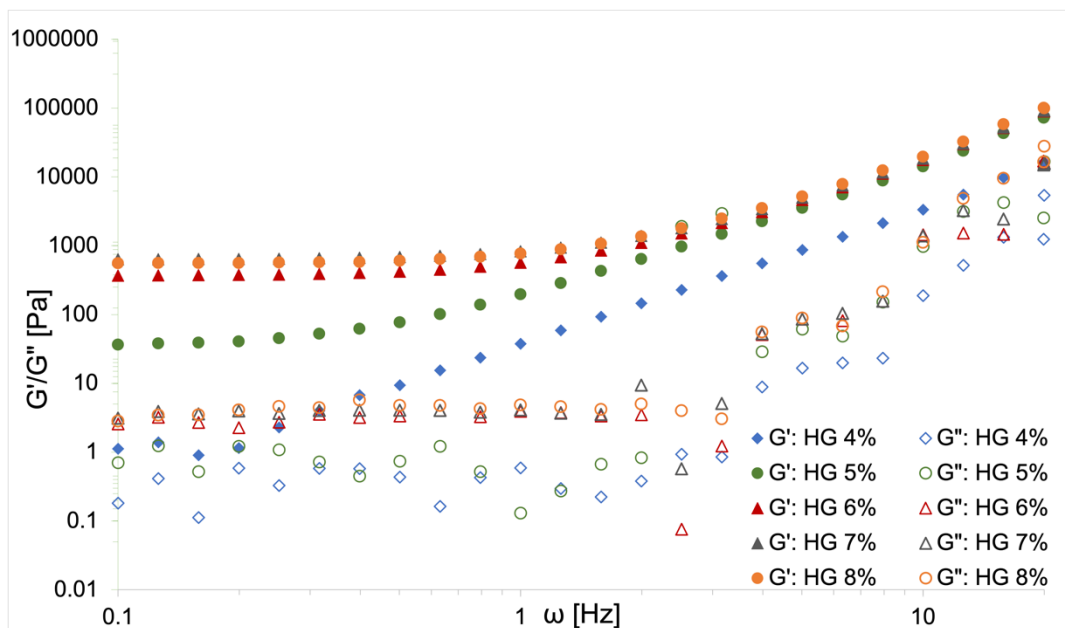
Figure S8. Storage (G') and loss (G") moduli as a function of radial frequency (ω) of MM gels at 25 ºC, for samples in which the gel component ratios were varied systemically.
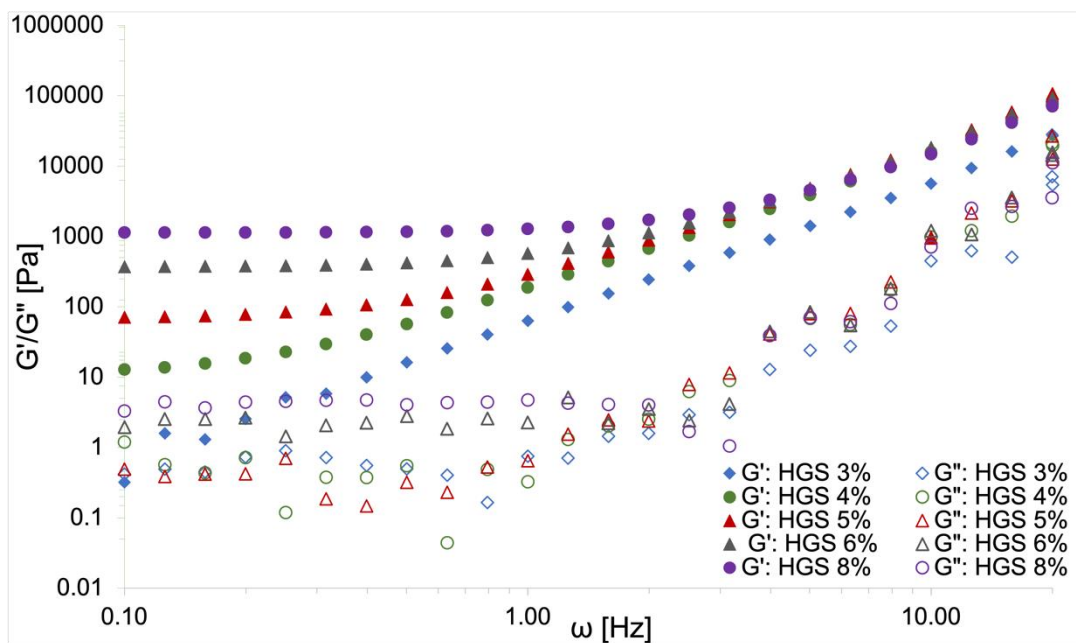
Figure S9. Storage (G') and loss (G") moduli as a function of radial frequency (ω) of and MS gels at 25 ºC, for samples in which the gel component ratios were varied systemically.

65

5
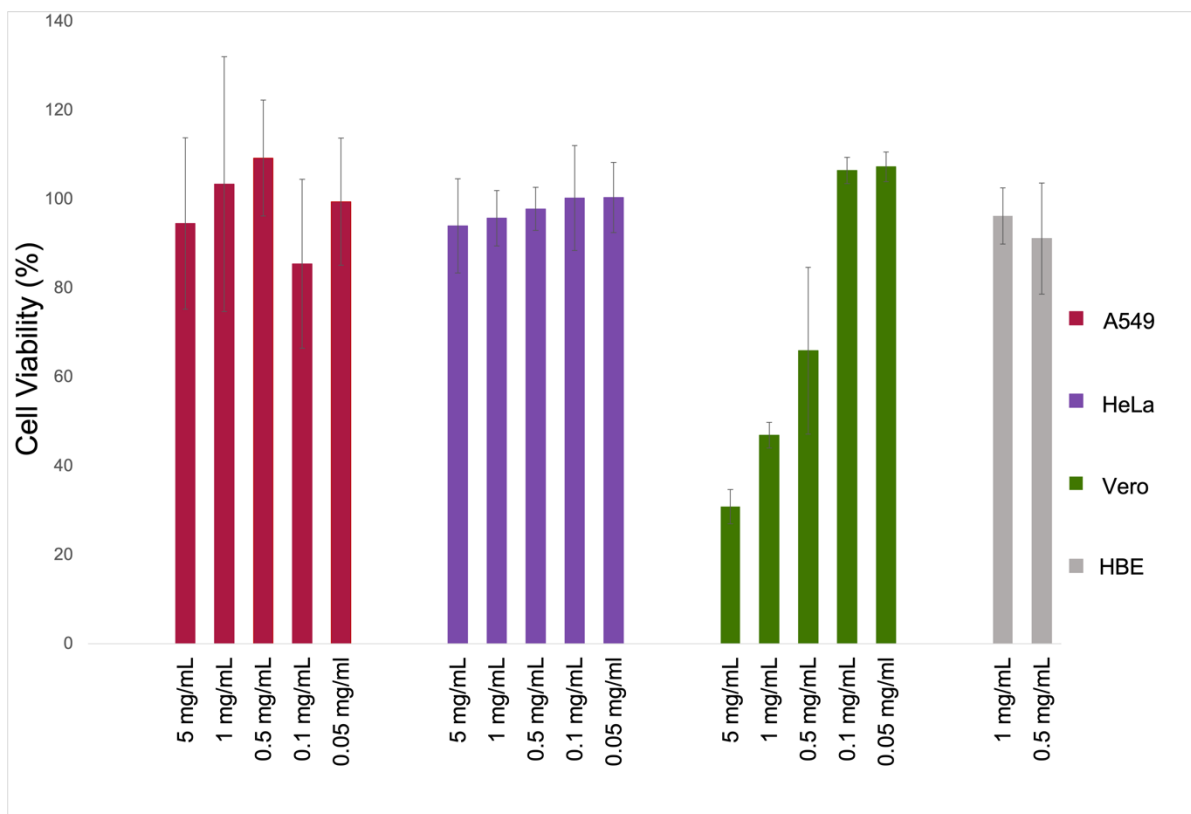
Figure S10. Cytotoxicity tests results of PEG-dithiol with A549, HeLa, Vero E6, and HBE cell lines.

Table S1. Composition of non-sulfated (HG) and sulfated (HGS) gels, depicting the amounts and ratios of the gel components used per 100 μL gels, such as the concentration of the gel components, overall gel concentration, as well as the concentration of the dPG or dPGS gel components within each gel.

Gel Code	Gel Type	PEG:dPG Mol Ratio	Gel Components (μmol)		Gel Concentration (% w/v)	dPG/dPGS Concentration (mM)
			PEG	dPG		
HG 8%	dPG maleimide	2.5:1	0.80	0.32	8.0	3.2
HG 7%	dPG maleimide	2.5:1	0.70	0.28	7.0	2.8
HG 6%	dPG maleimide	2.5:1	0.60	0.24	6.0	2.4
HG 5%	dPG maleimide	2.5:1	0.50	0.20	5.0	2.0
HG 4%	dPG maleimide	2.5:1	0.40	0.16	4.0	1.6
HGS 8%	dPGS maleimide	2.5:1	0.57	0.23	8.0	2.3
HGS 6%	dPGS maleimide	2.5:1	0.43	0.17	6.0	1.7
HGS 5%	dPGS maleimide	2.5:1	0.36	0.14	5.0	1.4
HGS 4%	dPGS maleimide	2.5:1	0.29	0.11	4.0	1.1
HGS 3%	dPGS maleimide	2.5:1	0.22	0.09	3.0	0.9
	dPG maleimide	-	-	0.32	3.2*	3.2
	dPGS maleimide	-	-	0.23	4.6*	2.3

*concentration of the gel component precursors

5. Summary and Conclusion

The research projects in this dissertation are aimed at the development of the 3D hydrogel network as a gel substrate for biosensing and antiviral applications. The hydrogel is fabricated by a multivalent dPG polymer and linear PEG crosslinker via thiol-ene click chemistry. The advantages of using the combination of dPG and PEG are the ease of modification and design for any applications by playing on the multivalency of the dPG molecule as well as the simple fine-tuning of viscoelasticity of the hydrogel. Besides, they are biocompatible and nontoxic to biosystems.

In the first project, the hydrogel is designed as a gel platform for the *in situ* encapsulation of streptavidin which is a biosensing probe to detect biotin, as a streptavidin-biotin binding is one of the strongest noncovalent interactions in nature. dPG which is functionalized by either acrylate, allyl, or acrylamide is crosslinked with linear dithiolated PEG to form a hydrogel. By employing fluorescence-labeled streptavidin, the encapsulation efficiency of each hydrogel sample type can be determined, based on many factors such as the mole ratio between PEG and dPG, gel concentrations, pH, loading capacity, and so on. The encapsulation efficiency of all gel types at the same condition shows 70% on average. The accessible binding site (or sensing performance) of encapsulated streptavidin toward free biotin is well preserved with 3 accessible binding sites on average. This implies that hydrogels are an excellent substrate for biosensing applications. Furthermore, the degradation study indicates that the hydrogel which contains an ester bond can be degradable and can be used for other applications such as wound healing or cell encapsulation.

In the second project, the hydrogel is intended for a virus-binding study. To bind a virus via electrostatic interaction, the hydrogel is decorated with negatively charged sulfate groups, which are already proven to be effective to inhibit a virus at its positively charged receptor binding domains. Therefore, the sulfated hydrogel is made from sulfated dPG which contains maleimide as a crosslinking point and a PEG dithiol linear crosslinker. The stiffness of this hydrogel is varied from stiff to viscous slimy consistency, in order to study the effect of the hydrogel scaffold flexibility. Interestingly, the slimy hydrogel with a highly flexible network shows the best result at binding HSV type 1, even slightly better than the pure solution of a higher amount of sulfated dPG. This shows that the flexibility of the network is also taken into account in trapping the virus. Above all, all sulfated hydrogel samples show much better performance at virus binding than their non-sulfated version under the same conditions.

6. Zusammenfassung

Die Forschungsprojekte in dieser Doktorarbeit zielen auf die Entwicklung eines 3D-Hydrogelnetzwerks als Gelsubstrat für Biosensoren und antivirale Anwendungen ab. Das Hydrogel wird durch ein multivalenten dPG-Polymer und einen linearen PEG Vernetzer über Thiol-en-Click-Chemie hergestellt. Die Vorteile der Kombination von dPG und PEG liegen in der leichten Modifizierbarkeit und dem Design für beliebige Anwendungen, indem nur die Multivalenz des dPG-Moleküls genutzt wird, sowie in der einfachen Feinabstimmung der Viskoelastizität des Hydrogels. Außerdem sind sie biokompatibel und ungiftig für Biosysteme.

Im ersten Projekt wird das Hydrogel als Gelplattform für die in-situ-Einkapselung von Streptavidin entwickelt, einer Biosensorsonde zum Nachweis von Biotin, da die Streptavidin-Biotin-Bindung eine der stärksten nicht-kovalenten Wechselwirkungen in der Natur ist. dPG, das entweder mit Acrylat, Allyl oder Acrylamid funktionalisiert ist, wird mit linearem dithioliertem PEG vernetzt, um ein Hydrogel zu bilden. Durch die Verwendung von fluoreszenzmarkiertem Streptavidin kann die Verkapselungseffizienz jedes Hydrogel-Probentyps bestimmt werden, basierend auf vielen Faktoren wie dem Molverhältnis zwischen PEG und dPG, den Gelkonzentrationen, dem pH-Wert, und der Beladungskapazität. Die Verkapselungseffizienz aller Geltypen beträgt bei gleichen Bedingungen im Durchschnitt 70 %. Die zugängliche Bindungsstelle (oder Sensorleistung) des eingekapselten Streptavidins gegenüber freiem Biotin bleibt mit ~3 bindungsstellen gut erhalten. Dies deutet darauf hin, dass Hydrogele ein hervorragendes Substrat für Biosensorik-Anwendungen sind. Darüber hinaus weist die Abbaustudie darauf hin, dass das Hydrogel, das eine Esterbindung enthält, abbaubar ist und für andere Anwendungen wie Wundheilung oder Zellverkapselung verwendet werden kann.

Im zweiten Projekt wurde das Hydrogel für eine Virusbindungsstudie verwendet. Um ein Virus über eine elektrostatische Wechselwirkung zu binden, wird das Hydrogel mit einem negativ geladenen Sulfat dekoriert, was sich bereits bei Heparansulfat als wirksam erwiesen hat, um ein Virus an seiner positiv geladenen Receptor-Bindungsstelle zu hemmen. Daher wird das sulfatierte Hydrogel aus sulfatiertem dPG hergestellt, das Maleimid als Vernetzungspunkt und PEG-Dithiol als linearen Vernetzer enthält. Die Steifigkeit dieses Hydrogels wird von fest bis hin zu zähflüssiger, schleimiger Konsistenz variiert, um die Flexibilität des Hydrogelgerüsts zu untersuchen. Interessanterweise zeigt das schleimige Hydrogel mit einem hochflexiblen Netzwerk die besten Ergebnisse bei der Bindung von HSV Typ 1, sogar etwas besser als die

reine Lösung mit einer höheren Menge an sulfatiertem dPG. Dies zeigt, dass auch die Flexibilität des Netzwerks beim Einfangen des Virus berücksichtigt wird. Vor allem zeigen alle sulfatierten Hydrogelproben unter den gleichen Bedingungen eine viel bessere Leistung bei der Virusbindung als ihre nicht sulfatierte Version.

7. References

[1]   E. Caló, V. v. Khutoryanskiy, *Eur Polym J* **2015**, *65*, 252–267.

[2]   J. Li, D. J. Mooney, J. A. Paulson, *Nat Rev Mater* **2016**, *1*, 16071.

[3]   X. M. Bustamante-Marin, L. E. Ostrowski, *Cold Spring Harb Perspect Biol* **2017**, *9*, 1–17.

[4]   B. Demouveaux, V. Gouyer, C. Robbe-Masselot, F. Gottrand, T. Narita, J. L. Desseyn, *Scientific Reports* **2019**, *9*, 1–11.

[5]   J. K. A. Langowski, S. Singla, A. Nyarko, H. Schipper, F. T. van den Berg, S. Kaur, H. C. Astley, S. W. S. Gussekloo, A. Dhinojwala, J. L. van Leeuwen, *Front Zool* **2019**, *16*, 1–17.

[6]   I. S. Haslam, E. W. Roubos, M. L. Mangoni, K. Yoshizato, H. Vaudry, J. E. Kloepper, D. M. Pattwell, P. F. A. Maderson, R. Paus, *Biological Reviews* **2014**, *89*, 618–655.

[7]   S. T. L. Jales, R. de M. Barbosa, A. C. de Albuquerque, L. H. v. Duarte, G. R. da Silva, L. M. A. Meirelles, T. M. S. da Silva, A. F. Alves, C. Viseras, F. N. Raffin, T. F. A. de L. Moura, *Journal of Composites Science* **2022**, *6*, 231–245.

[8]   J. H. Hamman, *Molecules* **2008**, *13*, 1599–1616.

[9]   S. Liu, T. Jiang, R. Guo, C. Li, C. Lu, G. Yang, J. Nie, F. Wang, X. Yang, Z. Chen, *ACS Appl Bio Mater* **2021**, *4*, 2769–2780.

[10]   C. Kilic Bektas, V. Hasirci, *Biomater Sci* **2019**, *8*, 438–449.

[11]   H. Cruz, M. Yap Gabon, S. Salehin, T. Seviour, B. Laycock, I. Pikaar, *Environmental Science and Ecotechnology* **2021**, *6*, 100097.

[12]   D. Chan, J.-C. Chien, E. Axpe, L. Blankemeier, S. W. Baker, S. Swaminathan, V. A. Piunova, D. Yu Zubarev, C. L. Maikawa, A. K. Grosskopf, J. L. Mann, H. Tom Soh, E. A. Appel, D. Chan, J. Chien, L. Blankemeier, H. T. Soh, E. Axpe, J. L. Mann, E. A. Appel, S. W. Baker, S. Swaminathan, V. A. Piunova, D. Yu Zubarev, C. L. Maikawa, A. K. Grosskopf, J. L. Mann, H. Tom Soh, E. A. Appel, *Advanced Materials* **2022**, *34*, 2109764.

[13]   S. Correa, A. K. Grosskopf, H. Lopez Hernandez, D. Chan, A. C. Yu, L. M. Stapleton, E. A. Appel, *Chem Rev* **2021**, *121*, 11385–11457.

[14]   A. Herrmann, R. Haag, U. Schedler, *Adv Healthc Mater* **2021**, *10*, 2100062.

[15]   M. Harun-Ur-Rashid, T. Foyez, I. Jahan, K. Pal, A. bin Imran, *RSC Adv* **2022**, *12*, 9445–9465.

[16]   C. Nie, P. Pouyan, D. Lauster, J. Trimpert, Y. Kerkhoff, G. P. Szekeres, M. Wallert, S. Block, A. K. Sahoo, J. Dernedde, K. Pagel, B. B. Kaufer, R. R. Netz, M. Ballauff, R. Haag, *Angewandte Chemie International Edition* **2021**, *60*, 15870–15878.

[17]   W. Hu, Z. Wang, Y. Xiao, S. Zhang, J. Wang, *Biomater Sci* **2019**, *7*, 843–855.

[18]   Y. Gao, K. Peng, S. Mitragotri, *Advanced Materials* **2021**, *33*, 2006362.

[19]   Hartmuth C. Kolb, M. G. Finn, K. Barry Sharpless, *Angewandte Chemie International Edition* **2001**, *40*, 2004–2021.

[20]   D. P. Nair, M. Podgórski, S. Chatani, T. Gong, W. Xi, C. R. Fenoli, C. N. Bowman, *Chemistry of Materials* **2014**, *26*, 724–744.

[21]   S. Bashir, M. Hina, J. Iqbal, A. H. Rajpar, M. A. Mujtaba, N. A. Alghamdi, S. Wageh, K. Ramesh, S. Ramesh, *Polymers (Basel)* **2020**, *12*, 1–60.

[22]   R. D. Kasai, D. Radhika, S. Archana, H. Shanavaz, R. Koutavarapu, D. Y. Lee, J. Shim, *International Journal of Polymeric Materials and Polymeric Biomaterials* **2022**, 1–11.

[23]   A. Singh, K. Sharma, V. K. Garg, G. Garg, *Int. J Pharm Sci Rev Res* **2010**, *4*, 97–105.

[24]   F. Sabbagh, I. I. Muhamad, *J Inorg Organomet Polym Mater* **2017**, *27*, 1439–1449.

[25]   S. Sheth, E. Barnard, B. Hyatt, M. Rathinam, S. P. Zustiak, *Front Bioeng Biotechnol* **2019**, *7*, 410.

[26]   H. Chamkouri, *Am J Biomed Sci Res* **2021**, *11*, 485–493.

[27]   J. George, C. C. Hsu, L. T. B. Nguyen, H. Ye, Z. Cui, *Biotechnol Adv* **2020**, *42*, 107370.

[28]   K. Chen, Y. Feng, Y. Zhang, L. Yu, X. Hao, F. Shao, Z. Dou, C. An, Z. Zhuang, Y. Luo, Y. Wang, J. Wu, P. Ji, T. Chen, H. Wang, *ACS Appl Mater Interfaces* **2019**, *11*, 36458–36468.

[29]   C. Norioka, Y. Inamoto, C. Hajime, A. Kawamura, T. Miyata, *NPG Asia Mater* **2021**, *13*, 1–10.

[30]   F. Puza, Y. Zheng, L. Han, L. Xue, J. Cui, *Polym Chem* **2020**, *11*, 2339–2345.

[31]   Y. Huang, P. G. Lawrence, Y. Lapitsky, *Langmuir* **2014**, *30*, 7771–7777.

[32]   F. Luo, T. L. Sun, T. Nakajima, T. Kurokawa, Y. Zhao, K. Sato, A. bin Ihsan, X. Li, H. Guo, J. P. Gong, *Advanced Materials* **2015**, *27*, 2722–2727.

[33]   S. Ma, S. Wang, Q. Li, Y. Leng, L. Wang, G. H. Hu, *Ind Eng Chem Res* **2017**, *56*, 7971–7976.

[34]   G. Li, Q. Yan, H. Xia, Y. Zhao, *ACS Appl Mater Interfaces* **2015**, *7*, 12067–12073.

[35]   Z. Rao, M. Inoue, M. Matsuda, T. Taguchi, *Colloids Surf B Biointerfaces* **2011**, *82*, 196–202.

[36]   M. Mihajlovic, M. Staropoli, M. S. Appavou, H. M. Wyss, W. Pyckhout-Hintzen, R. P. Sijbesma, *Macromolecules* **2017**, *50*, 3333–3346.

[37]   A. Michael, *Journal für Praktische Chemie* **1894**, *49*, 20–25.

[38]   R. Randriantsilefisoa, Y. Hou, Y. Pan, J. L. C. Camacho, M. W. Kulka, J. Zhang, R. Haag, *Adv Funct Mater* **2020**, *30*, 1905200.

[39]   A. Herrmann, L. Kaufmann, P. Dey, R. Haag, U. Schedler, *ACS Appl Mater Interfaces* **2018**, *10*, 11382–11390.

[40]   B. D. Prof Rolf Huisgen, *Angewandte Chemie International Edition in English* **1963**, *2*, 565–598.

[41]   C. E. Hoyle, C. N. Bowman, C. N. Bowman, C. E. Hoyle, *Angewandte Chemie International Edition* **2010**, *49*, 1540–1573.

[42]   L. E. Jansen, L. J. Negrón-Piñeiro, S. Galarza, S. R. Peyton, *Acta Biomater* **2018**, *70*, 120–128.

[43]   T. Göckler, S. Haase, X. Kempter, R. Pfister, B. R. Maciel, A. Grimm, T. Molitor, N. Willenbacher, U. Schepers, T. Göckler, S. Haase, X. Kempter, R. Pfister, A. Grimm, T. Molitor, U. Schepers, B. R. Maciel, N. Willenbacher, *Adv Healthc Mater* **2021**, *10*, 2100206.

[44] O. Diels, K. Alder, *Justus Liebigs Ann Chem* **1928**, *460*, 98–122.

[45] M. Gregoritza, F. P. Brandl, *European Journal of Pharmaceutics and Biopharmaceutics* **2015**, *97*, 438–453.

[46] J. Yan, B. Gundsambuu, M. Krasowska, K. Platts, P. Facal Marina, C. Gerber, S. C. Barry, A. Blencowe, *J Mater Chem B* **2022**, *10*, 3329–3343.

[47] L. J. Smith, S. M. Taimoory, R. Y. Tam, A. E. G. Baker, N. Binth Mohammad, J. F. Trant, M. S. Shoichet, *Biomacromolecules* **2018**, *19*, 926–935.

[48] A. Wurtz vo, *Journal für Praktische Chemie* **1872**, *5*, 457–464.

[49] V. Delplace, P. E. B Nickerson, A. Ortin-Martinez, A. E. G Baker, V. A. Wallace, M. S. Shoichet, V. Delplace, A. E. G Baker, M. S. Shoichet, P. E. B Nickerson, A. Ortin-Martinez, V. A. Wallace Donald K Johnson, V. A. Wallace, *Adv Funct Mater* **2020**, *30*, 1903978.

[50] A. C. Knall, M. Hollauf, C. Slugovc, *Tetrahedron Lett* **2014**, *55*, 4763–4766.

[51] D. L. Boger, *Chem Rev* **1986**, *86*, 781–793.

[52] P. K. Sharma, Y. Singh, *Biomacromolecules* **2019**, *20*, 2174–2184.

[53] Y. Zhang, C. Y. Pham, R. Yu, E. Petit, S. Li, M. Barboiu, *Front Chem* **2020**, *8*, 739.

[54] E. D. Hughes, C. K. Ingold, *Journal of the Chemical Society (Resumed)* **1935**, 244–255.

[55] V. X. Truong, I. Donderwinkel, J. E. Frith, *J Polym Sci A Polym Chem* **2019**, *57*, 1872–1876.

[56] J. I. Paez, A. de Miguel-Jiménez, R. Valbuena-Mendoza, A. Rathore, M. Jin, A. Gläser, S. Pearson, A. del Campo, *Biomacromolecules* **2021**, *22*, 2874–2886.

[57] B. Fu, X. Wang, Z. Chen, N. Jiang, Z. Guo, Y. Zhang, S. Zhang, X. Liu, L. Liu, *J Mater Chem B* **2022**, *10*, 656–665.

[58] L. Arens, D. Barther, J. Landsgesell, C. Holm, M. Wilhelm, *Soft Matter* **2019**, *15*, 9949–9964.

[59] A. E. Madkour, J. M. Grolman, G. N. Tew, *Polym Chem* **2010**, *2*, 114–119.

[60] A. Cavallo, M. Madaghiele, U. Masullo, M. G. Lionetto, A. Sannino, *J Appl Polym Sci* **2017**, *134*, 44380.

[61] P. J. Flory, *J Am Chem Soc* **1940**, *62*, 1561–1565.

[62] J. Herzberger, K. Niederer, H. Pohlit, J. Seiwert, M. Worm, F. R. Wurm, H. Frey, *Chem Rev* **2016**, *116*, 2170–2243.

[63] N. Yamaguchi, M. Sato, *Polymer Journal* **2009**, *41*, 588–594.

[64] T. Uchida, Y. Kurita, N. Koizumi, M. Kubo, *Journal of Polymer Science* **1956**, *21*, 313–322.

[65] M. Winger, A. H. de Vries, W. F. van Gunsteren, *Mol Phys* **2009**, *107*, 1313–1321.

[66] G. Liu, Y. Li, L. Yang, Y. Wei, X. Wang, Z. Wang, L. Tao, *RSC Adv* **2017**, *7*, 18252–18259.

[67] C. Fruijtier-Pölloth, *Toxicology* **2005**, *214*, 1–38.

[68] A. S. Hoffman, *Acta Biomater* **2016**, *40*, 1–5.

[69] H. P. le Khanh, D. Nemes, Á. Rusznyák, Z. Ujhelyi, P. Fehér, F. Fenyvesi, J. Váradi, M. Vecsernyés, I. Bácskay, *Polymers* **2022**, *14*, 279.

[70] A. A. D'souza, R. Shegokar, *Expert Opin Drug Deliv* **2016**, *13*, 1257–1275.

[71] D. Hutanu, *Modern Chemistry & Applications* **2014**, *02*, 1000132.

[72] S. Liu, T. Jiang, R. Guo, C. Li, C. Lu, G. Yang, J. Nie, F. Wang, X. Yang, Z. Chen, *ACS Appl Bio Mater* **2021**, *4*, 2769–2780.

[73] H. Frey, R. Haag, *Reviews in Molecular Biotechnology* **2002**, *90*, 257–267.

[74] W. Daniel, S. E. Stiriba, F. Holger, *Acc Chem Res* **2010**, *43*, 129–141.

[75] A. Sunder, R. Hanselmann, H. Frey, R. Mülhaupt, *Macromolecules* **1999**, *32*, 4240–4246.

[76] E. J. Vandenberg, *Journal of Polymer Science: Polymer Chemistry Edition* **1985**, *23*, 915–949.

[77] A. Dworak, W. Walach, B. Trzebicka, *Macromol Chem Phys* **1995**, *196*, 1963–1970.

[78] S. R. Sandler, F. R. Berg, *J Polym Sci A1* **1966**, *4*, 1253–1259.

[79] S. Abbina, S. Vappala, P. Kumar, E. M. J. Siren, C. C. La, U. Abbasi, D. E. Brooks, J. N. Kizhakkedathu, *J Mater Chem B* **2017**, *5*, 9249–9277.

[80] M. Wallert, J. Plaschke, M. Dimde, V. Ahmadi, S. Block, R. Haag, *Macromol Mater Eng* **2021**, *306*, 2000688.

[81] M. Kumari, S. Prasad, L. Fruk, B. Parshad, *Future Med Chem* **2021**, *13*, 419–438.

[82] S. Schötz, F. Reisbeck, A. C. Schmitt, M. Dimde, E. Quaas, K. Achazi, R. Haag, *Pharmaceutics* **2021**, *13*, 1276.

[83] C. Wu, C. Strehmel, K. Achazi, L. Chiappisi, J. Dernedde, M. C. Lensen, M. Gradzielski, M. B. Ansorge-Schumacher, R. Haag, *Biomacromolecules* **2014**, *15*, 3881–3890.

[84] A. R. Otrelo-Cardoso, M. A. da Silva Correia, V. Schwuchow, D. I. Svergun, M. J. Romão, S. Leimkühler, T. Santos-Silva, *Int J Mol Sci* **2014**, *15*, 2223–2236.

[85] P. Dey, M. Adamovski, S. Friebe, A. Badalyan, R. C. Mutihac, F. Paulus, S. Leimkühler, U. Wollenberger, R. Haag, *ACS Appl Mater Interfaces* **2014**, *6*, 8937–8941.

[86] N. K. Devaraj, M. G. Finn, *Chem Rev* **2021**, *121*, 6697–6698.

[87] K. Nwe, M. W. Brechbiel, *Cancer Biother Radiopharm* **2009**, *24*, 289–302.

[88] P. Thirumurugan, D. Matosiuk, K. Jozwiak, *Chem Rev* **2013**, *113*, 4905–4979.

[89] Y. Jiang, J. Chen, C. Deng, E. J. Suuronen, Z. Zhong, *Biomaterials* **2014**, *35*, 4969–4985.

[90] C. W. Tornøe, C. Christensen, M. Meldal, *Journal of Organic Chemistry* **2002**, *67*, 3057–3064.

[91] J. E. Hein, V. v. Fokin, *Chem Soc Rev* **2010**, *39*, 1302–1315.

[92] T. Deb, J. Tu, R. M. Franzini, *Chem Rev* **2021**, *121*, 6850–6914.

[93] M. Martínek, L. Filipová, J. Galeta, L. Ludvíková, P. Klán, *Org Lett* **2016**, *18*, 4892–4895.

[94] V. X. Truong, K. Zhou, G. P. Simon, J. S. Forsythe, V. X. Truong, K. Zhou, G. P. Simon, S. Forsythe, *Macromol Rapid Commun* **2015**, *36*, 1729–1734.

[95] W. Song, Y. Wang, J. Qu, Q. Lin, *J Am Chem Soc* **2008**, *130*, 9654–9655.

[96] J. Chen, K. Huang, Q. Chen, C. Deng, J. Zhang, Z. Zhong, *ACS Appl Mater Interfaces* **2018**, *10*, 3929–3937.

[97] C. M. Madl, L. M. Katz, S. C. Heilshorn, *Adv Funct Mater* **2016**, *26*, 3612–3620.

[98] D. H. Reid, D. T. Clark, *Royal Society of Chemistry* **1970**, 1–48.

[99] A. K. Chandra, P. C. Nam, M. T. Nguyen, *Journal of Physical Chemistry A* **2003**, *107*, 9182–9188.

[100] Lamar Field, *Synthesis (Stuttg)* **1972**, *3*, 101–133.

[101] T. Posner, *Berichte der deutschen chemischen Gesellschaft* **1905**, *38*, 646–657.

[102] M. D. Nolan, E. M. Scanlan, *Front Chem* **2020**, *8*, 583272.

[103] Y. Sun, H. Liu, L. Cheng, S. Zhu, C. Cai, T. Yang, L. Yang, P. Ding, *Polym Int* **2018**, *67*, 25–31.

[104] A. W. Snow, E. E. Foos, *Synthesis (Stuttg)* **2003**, *2003*, 0509–0512.

[105] R. Mahou, C. Wandrey, *Polymers* **2012**, *4*, 561–589.

[106] J. van Hoorick, A. Dobos, M. Markovic, T. Gheysens, L. van Damme, P. Gruber, L. Tytgat, J. van Erps, H. Thienpont, P. Dubruel, A. Ovsianikov, S. van Vlierberghe, *Biofabrication* **2020**, *13*, 015017.

[107] R. Holmes, X. bin Yang, A. Dunne, L. Florea, D. Wood, G. Tronci, *Polymers* **2017**, *9*, 226.

[108] X. Tong, J. Lai, B. H. Guo, Y. Huang, *J Polym Sci A Polym Chem* **2011**, *49*, 1513–1516.

[109] J. Liang, B. B. Karakoçak, J. J. Struckhoff, N. Ravi, *Biomacromolecules* **2016**, *17*, 4064–4074.

[110] Q. Wang, W. Xu, R. Koppolu, B. van Bochove, J. Seppälä, L. Hupa, S. Willför, C. Xu, X. Wang, *Carbohydr Polym* **2022**, *276*, 118780.

[111] M. M. Pérez-Madrigal, J. E. Shaw, M. C. Arno, J. A. Hoyland, S. M. Richardson, A. P. Dove, *Biomater Sci* **2019**, *8*, 405–412.

[112] K. M. Yoo, S. v. Murphy, A. Skarda, *Gels* **2021**, *7*, 1–17.

[113] S. A. Stewart, M. B. Coulson, C. Zhou, N. A. D. Burke, H. D. H. Stöver, *Soft Matter* **2018**, *14*, 8317–8324.

[114] T. M. FitzSimons, E. v. Anslyn, A. M. Rosales, *ACS Polymers Au* **2021**, *2*, 129–136.

[115] D. T. N. Chen, Q. Wen, P. A. Janmey, J. C. Crocker, A. G. Yodh, *Annu. Rev. Condens. Matter Phys.* **2010**, *1*, 301–322.

[116] T. Miri, *Practical Food Rheology: An Interpretive Approach* **2010**, 7–28.

[117] C. Yan, D. J. Pochan, *Chem Soc Rev* **2010**, *39*, 3528–3540.

[118] B. von Lospichl, S. Hemmati-Sadeghi, P. Dey, T. Dehne, R. Haag, M. Sittinger, J. Ringe, M. Gradzielski, *Colloids Surf B Biointerfaces* **2017**, *159*, 477–483.

[119] J. M. Zuidema, C. J. Rivet, R. J. Gilbert, F. A. Morrison, *J Biomed Mater Res B Appl Biomater* **2014**, *102*, 1063–1073.

[120] P. A. Janmey, M. Schliwa, *Curr Biol* **2008**, *18*, R639–R641.

[121] S. G. Marapureddy, P. Thareja, S. G. Marapureddy, · P Thareja, *Biointerface Engineering: Prospects in Medical Diagnostics and Drug Delivery* **2020**, 75–99.

[122] M. Dabbaghi, S. Namjoshi, B. Panchal, J. E. Grice, S. Prakash, M. S. Roberts, Y. Mohammed, *Pharmaceutics* **2021**, *13*, 1351.

[123] G. Stojkov, Z. Niyazov, F. Picchioni, R. K. Bose, *Gels* **2021**, *7*, 255.

[124] A. J. Kuijpers, G. H. M. Engbers, J. Feijen, S. C. de Smedt, T. K. L. Meyvis, J. Demeester, J. Krijgsveld, S. A. J. Zaat, J. Dankert, *Macromolecules* **1999**, *32*, 3325–3333.

[125] D. M. Roquero, E. Katz, *Sensors and Actuators Reports* **2022**, *4*, 100095.

[126] U. B. Gunatilake, S. Garcia-Rey, E. Ojeda, L. Basabe-Desmonts, F. Benito-Lopez, *ACS Appl Mater Interfaces* **2021**, *13*, 37734–37745.

[127] G. Yang, K. Zhu, W. Guo, D. Wu, X. Quan, X. Huang, S. Liu, Y. Li, H. Fang, Y. Qiu, Q. Zheng, M. Zhu, J. Huang, Z. Zeng, Z. Yin, H. Wu, *Adv Funct Mater* **2022**, *32*, 2200457.

[128] C. A. Hong, J. C. Park, H. Na, H. Jeon, Y. S. Nam, *Biosens Bioelectron* **2021**, *182*, 113110.

[129] B. Ray, I. Ali, S. Jana, S. Mukherjee, S. Pal, S. Ray, M. Schütz, M. Marschall, *Viruses* **2022**, *14*, 35.

[130] M. Hoffmann, N. L. Snyder, L. Hartmann, *Macromolecules* **2022**, *55*, 7957–7973.

[131] A. Akbari, A. Bigham, V. Rahimkhoei, S. Sharifi, E. Jabbari, *Polymers (Basel)* **2022**, *14*, 1634.

[132] P. Pouyan, C. Nie, S. Bhatia, S. Wedepohl, K. Achazi, N. Osterrieder, R. Haag, *Biomacromolecules* **2021**, *22*, 1545–1554.

[133] R. S. L. Tan, P. Hassandarvish, C. F. Chee, L. W. Chan, T. W. Wong, *Carbohydr Polym* **2022**, *290*, 119500.

[134] L. Soria-Martinez, S. Bauer, M. Giesler, S. Schelhaas, J. Materlik, K. Janus, P. Pierzyna, M. Becker, N. L. Snyder, L. Hartmann, M. Schelhaas, *J Am Chem Soc* **2020**, *142*, 5252–5265.

[135] F. Fan, C. Cai, W. Wang, L. Gao, J. Li, J. Li, F. Gu, T. Sun, J. Li, C. Li, G. Yu, *ACS Macro Lett* **2018**, *7*, 330–335.

[136] N. Modhiran, N. S. Gandhi, N. Wimmer, S. Cheung, K. Stacey, P. R. Young, V. Ferro, D. Watterson, *Antiviral Res* **2019**, *168*, 121–127.

[137] B. Thongrom, M. Dimde, U. Schedler, R. Haag, *Macromol Chem Phys* **2022**, 2200271.

[138] B. Thongrom, A. Sharma, C. Nie, E. Quaas, M. Raue, S. Bhatia, R. Haag, *Macromol Biosci* **2022**, *22*, 2100507.

8. List of abbreviations

PEG   Polyethylene glycol

GelMa   Gelatin Methacrylate

PAA   Polyacrylic acid

3D   3 Dimensional

kDa   Kilo Dalton (kilogram/mol)

MDa   Mega Dalton

PVA   Polyvinyl alcohol

SPAAC   Strain promoted alkyne-azide cycloaddition

UV/Vis   Ultraviolet/Visible light

LAP   Lithium phenyl-2,4,6-trimethylbenzoylphosphinate

HA   Hyaluronic acid

IEDDA   Inverse electron-demand Diels–Alder

LUMO   Lowest unoccupied molecular orbital

HOMO   Highest occupied molecular orbital

BSA   Bovine serum albumin

PEO   Polyethylene oxide

DCM   Dichloromethane

Ref   Reference

T-cells   Thymus-cells

dPG   Dendritic polyglycerol

hPG   hyperbranched polyglycerol

PDI   Polydispersity index

DMF   *N,N*-Dimethyl formamide

DMSO	Dimethylsulfoxide
hMSCs	Human mesenchymal stem cells
PaoABC	Periplasmatic aldehyde oxidoreductase
CuAAC	Copper-catalyzed azide-alkyne cycloaddition
DA	Diels-Alder
2D	2 Dimensional
G´	Elastic or storage modulus
G´´	Loss modulus
LVR	Linear viscoelastic region
LOX	Lactate oxidase
GOX	Glucose oxidase
HRP	Horseradish peroxidase
TMB	Tetramethylbenzidine
DNA	Deoxyribonucleic Acid
FRET	Föster resonance energy transfer
HS	Heparan sulfate
HIV	Human immunodeficiency virus
HSV	Herpes simplex virus
HPV	Human papillomavirus
RSV	Respiratory syncytial virus
SARS-CoV	Severe acute respiratory syndrome-associated coronavirus

9. List of Publications and Patents

[1] B. Thongrom, P. Amornpitoksuk, S. Suwanboon, J. Baltrusaitis, *Korean Journal of Chemical Engineering* **2014**, 31, 587-592.

[2] A. Sharma, B. Thongrom, S. Bhatia, B. v. Lospichl, A. Addante, S. Y. Graeber, D. Lauster, M. A. Mall, M. Gradzielski, R. Haag *Macromolecular Rapid Communications* **2021**, *42*, 2100303.

[3] B. Thongrom, A. Sharma, C. Nie, E. Quaas, M. Raue, S. Bhatia, R. Haag, *Macromolecular Bioscience* **2022**, *22*, 2100507.

[4] B. Thongrom, M. Dimde, U. Schedler, R. Haag, *Macromolecular Chemistry and Physics* **2022**, 2200271.

[5] European Patent Nr. 22 152 754.2-1109
Boonya Thongrom, Rainer Haag
"*Hydrogel comprising dendritic polyglycerol units and polyether units*"

10. Curriculum Vitae

For reasons of data protection, the curriculum vitae is not included in the online version.